



2018/2019

## FINAL YEAR PROJECT

Submitted in fulfillment of the requirements for the

ENGINEERING DEGREE FROM THE LEBANESE UNIVERSITY  
FACULTY OF ENGINEERING- BRANCH I

Major: Electrical engineering

By:

Sahar ALLOUCH

---

### GRAPH THEORY-BASED METHOD TO IDENTIFY PATHOLOGICAL NETWORKS INVOLVED IN ALZHEIMER'S DISEASE

Supervised by:  
Dr. Aya KABBARA  
Prof. Mohamad KHALIL

Defended on June 2019 in front of the jury:

Dr. Wassim EL FALOU	Member
Dr. Nada CHENDEB	Member
Dr. Amani RAAD	Member

# Abstract

Alzheimer's disease (AD) is a neurodegenerative brain disorder characterized by progressive memory impairment and cognitive deficits. Accurate diagnosis of AD at an early stage has become a topic of increasing interest. Understanding the pathophysiology of AD is the first step toward the conception of novel neuro-markers able to identify and predict the disease. In this context, due to its non-invasiveness, its ease of use, its availability and low cost, in addition to its excellent temporal resolution, electroencephalography (EEG) represent an excellent candidate to adopt for the conception of the desired neuro-markers. Therefore, the main objective of this project is to identify, using EEG, differences between brain activity between AD patients and healthy controls that correlate with the cognitive impairment level of each group. Two complementary studies were conducted. First, differences in scalp voltage topographies between AD patients and healthy controls were investigated during a motor task, with both static and dynamic approaches. The dynamic analysis showed significant differences between the two groups. These results highlighted the advantages of dynamic analysis over static analysis. Second, alterations in dynamic functional brain networks were investigated during a picture naming and button press tasks. An increased averaged strength variability of the network nodes in AD patients was reported in both tasks. In addition, a negative correlation was found between the averaged strength variability and cognitive clinical score. These findings may open perspectives towards designing novel neuro-marker of cognitive impairment in AD.

**Keywords:** Alzheimer's disease, electroencephalography, voltage topography, dynamic functional brain networks.

**Allouch, S., Tabbal, J., Nasser, A., Hassan, M., Khalil, M., & Kabbara, A. (2019). Altered motor performance in Alzheimer ' s disease : a dynamic analysis using EEG. *Fifth International Conference on Advances in BioMedical Engineering IEEE, Lebanon.* (Submitted)**

# Résumé

La maladie d'Alzheimer (MA) est un trouble neurodégénératif du cerveau caractérisé par une altération progressive de la mémoire et des déficits cognitifs. Un diagnostic précis de la MA à un stade précoce demeure un sujet assez intéressant. Comprendre la physiopathologie de la MA constitue une première étape vers la conception de nouveaux neuro-marqueurs capables d'identifier et de prédire la maladie. Dans ce contexte, en raison de son caractère non invasif, de sa facilité d'utilisation, de sa disponibilité et de son faible coût, ainsi que de son excellente résolution temporelle, l'électroencéphalographie (EEG) représente un excellent candidat à adopter pour la conception des neuro-marqueurs désirés. Par conséquent, l'objectif principal de ce projet est d'identifier, à l'aide de l'EEG, les différences entre les activités cérébrales chez les patients de la MA et les contrôles sains, corrélées avec le niveau de déficience cognitive de chaque groupe. Deux études complémentaires ont été menées. Premièrement, les différences de topographies de voltage du cuir chevelu entre les patients atteints de MA et les témoins sains ont été étudiées au cours d'une tâche motrice, avec des approches statiques et dynamiques. L'analyse dynamique a montré des différences significatives entre les deux groupes. Ces résultats ont mis en évidence les avantages de l'analyse dynamique par rapport à l'analyse statique. Deuxièmement, des altérations dans les réseaux cérébraux fonctionnels dynamiques ont été étudiées au cours d'une tâche de nommage d'image et de pression de bouton. Une accroissement variabilité de la force moyenne des nœuds du réseau chez les patients AD a été rapportée dans les deux tâches. De plus, une corrélation négative a été trouvée entre la variabilité de la force moyenne et le score clinique cognitif. Ces résultats pourraient ouvrir des perspectives pour la conception de nouveaux neuro-marqueurs de la déficience cognitive dans la MA.

**Mots clés:** Maladie d'Alzheimer, électroencéphalographie, topographie de voltage, réseaux cérébraux fonctionnels dynamiques

# Table of Contents

<b>Abstract .....</b>	<b>2</b>
<b>Résumé .....</b>	<b>3</b>
<b>List of Tables.....</b>	<b>7</b>
<b>List of Figures.....</b>	<b>8</b>
<b>List of Abbreviations.....</b>	<b>10</b>
<b>INTRODUCTION.....</b>	<b>12</b>
<b>Chapter 1. ALZHEIMER'S DISEASE .....</b>	<b>14</b>
1.1    Introduction .....	14
1.2    Prevalence .....	14
1.3    Signs and Symptoms.....	14
1.4    Pathophysiology of AD.....	16
1.5    The genetic basis of AD .....	18
1.6    Diagnosis .....	18
1.7    Treatment.....	19
1.8    Conclusion.....	19
<b>Chapter 2. NEUROIMAGING TECHNIQUES .....</b>	<b>21</b>
2.1    Introduction .....	21
2.2    Functional neuroimaging overview .....	21
2.2.1    Positron Emission Tomography .....	21
2.2.2    Single Photon Emission Computed Tomography.....	21
2.2.3    Functional Magnetic Resonance Imaging .....	22
2.2.4    Magnetoencephalography .....	23
2.2.5    Electroencephalography .....	23
2.3    Electroencephalography and Alzheimer's disease .....	26
2.3.1    Past studies .....	26
2.3.2    Limitations of past studies.....	27
2.4    Conclusion.....	27
<b>Chapter 3. EXPERIMENTAL DESIGN.....</b>	<b>28</b>
3.1    Introduction .....	28
3.2    Project goals and innovations .....	28
3.3    Experimental setup.....	29

3.3.1	Neuropsychological test.....	29
3.3.2	EEG acquisition .....	29
3.3.3	Demographic characteristics and clinical scores.....	34
3.4	EEG Pre-processing .....	36
3.4.1	EEG artifacts overview .....	36
3.4.2	Signal pre-processing.....	42
3.4.3	Pre-processing results .....	48
3.5	Conclusion.....	48
<b>Chapter 4. A COMPARATIVE STUDY: STATIC VS DYNAMIC ANALYSIS.....</b>	<b>49</b>	
4.1	Introduction .....	49
4.2	Normality test .....	49
4.3	Statistical test.....	50
4.4	Results.....	50
4.5	Discussion .....	51
4.6	Limitations.....	52
4.7	Conclusion.....	52
<b>Chapter 5. BRAIN NETWORK ANALYSIS.....</b>	<b>53</b>	
5.1	Introduction .....	53
5.2	The human brain: a complex network.....	53
5.3	Network diseases .....	54
5.4	EEG scalp connectivity .....	55
5.5	Volume conduction and field spread .....	56
5.6	EEG source connectivity .....	56
5.6.1	Source reconstruction.....	57
5.6.2	Dynamic functional connectivity.....	58
5.7	Network analysis.....	59
5.7.1	Group-level analysis: .....	60
5.7.2	Individual-level analysis: .....	60
5.8	Results .....	60
5.8.1	Group-level analysis .....	60
5.8.2	Individual-level analysis .....	61
5.9	Discussion: .....	65
5.10	Limitations .....	67

5.11	Conclusion .....	67
<b>CONCLUSION</b>	.....	<b>68</b>
<b>References</b> .....	.....	<b>69</b>
<b>Appendix A</b> .....	.....	<b>83</b>
<b>Appendix B</b> .....	.....	<b>86</b>
<b>Appendix C</b> .....	.....	<b>93</b>

# List of Tables

<b>Table 3.1.</b> Demographic characteristics and clinical score.....	35
<b>Table 3.2.</b> The number of subjects in each group and the average number of trials per subjects following the pre-processing procedure. *Number: nb., average: avg., subject: subj. ....	48
<b>Table 5.1.</b> List of brain network diseases (Crossley et al., 2014) .....	55

# List of Figures

<b>Figure 1.1.</b> Prevalence of neuropsychiatric symptoms in AD patients. The figure was reproduced based on data published in (Zhao et al., 2016).....	16
<b>Figure 1.2.</b> A) Amyloid plaque. B) Neurofibrillary tangles. (Masters et al., 2015). .....	17
<b>Figure 1.3.</b> a) In Healthy neuron, microtubules are stabilized by tau protein. b) In diseased neuron, microtubules lose their stability, and neurofibrillary tangles are formed. Picture reproduced from (Chen et al., 2013). ....	17
<b>Figure 2.1.</b> A) PET scanner ( <a href="https://www.iibi.uiowa.edu/pet-center">https://www.iibi.uiowa.edu/pet-center</a> ). B) PET scans examples (Rowe et al., 2008).....	21
<b>Figure 2.2.</b> A) SPECT scanner ( <a href="https://www.uofmhealth.org/health-library/acc4790">https://www.uofmhealth.org/health-library/acc4790</a> ). B) SPECT scans examples (O'Brien et al., 2014).....	22
<b>Figure 2.3.</b> A) MRI machine (used for both MRI and fMRI scans). B) fMRI scan during task performance (Hafkemeijer et al., 2012). ....	22
<b>Figure 2.4.</b> A) MEG scanner ( <a href="https://www.admin.ox.ac.uk/estates/aboutus/sp_oltight/cases_studies/capitalprojects/megscanner/">https://www.admin.ox.ac.uk/estates/aboutus/sp_oltight/cases_studies/capitalprojects/megscanner/</a> ). B) MEG data. ....	23
<b>Figure 2.5.</b> A) EEG acquisition ( <a href="https://www.vice.com/en_us/article/43844m/researchers-mind-melded-three-people-to-collaboratively-play-tetris">https://www.vice.com/en_us/article/43844m/researchers-mind-melded-three-people-to-collaboratively-play-tetris</a> ). B) 32-channel EED data. ....	24
<b>Figure 2.6.</b> Approximation of the resolution in time and space of the most commonly employed functional neuroimaging techniques based on measurements of hemodynamic (fMRI, PET, SPECT) and electrical (EEG, MEG) activity of the brain (Laureys et al., 2002). ....	24
<b>Figure 2.7.</b> The 10-20 international system is used for electrodes placement.....	25
<b>Figure 2.8.</b> EEG rhythms (Jacobs, 2015). ....	26
<b>Figure 3.1.</b> A) EEG acquisition was done at Vita Nova polyclinic. B) Twente Medical Systems International -TMSi-, Porti system, (32 electrode system). ....	30
<b>Figure 3.2.</b> Resting state paradigm.....	30
<b>Figure 3.3.</b> Picture naming task. ....	31
<b>Figure 3.4.</b> One-back task.....	31
<b>Figure 3.5.</b> Button press task. ....	32
<b>Figure 3.6.</b> E-studio application (E-prime 2.0 software) used for the experiments design....	32
Figure 3.7. E-DataAid application (E-prime 2.0 software) used for data management .....	33
<b>Figure 3.8.</b> Digital triggers are sent between E-prime software and the EEG acquisition system in order to mark stimulus onset and response events.....	34
<b>Figure 3.9.</b> The clinical scores of AD patients and healthy controls. Wilcoxon test was used to examine whether there is a statistical difference between the two groups.....	35
<b>Figure 3.10.</b> Eye Blink artifacts (Marella, 2012). ....	36
<b>Figure 3.11.</b> Eye flutter artifacts (Marella, 2012). ....	37
<b>Figure 3.12.</b> Lateral eye movements (Marella, 2012). ....	37
<b>Figure 3.13.</b> Muscle artifacts due to facial muscle contraction (Marella, 2012). ....	38
<b>Figure 3.14.</b> Chewing artifacts ( <a href="https://learningcentral.health.unm.edu/learning/user/onlineaces/CE/eeg/artifacts/index.html">https://learningcentral.health.unm.edu/learning/user/onlineaces/CE/eeg/artifacts/index.html</a> ). ....	38
<b>Figure 3.15.</b> Cardiac activity artifacts (Marella, 2012). ....	39
<b>Figure 3.16.</b> Pulse artifact (Marella, 2012).....	39
<b>Figure 3.17.</b> Line power artifact (Marella, 2012). ....	40

<b>Figure</b>	<b>3.18.</b>	Cellphone https://learningcentral.health.unm.edu/learning/user/onlin CE/eeg/artifacts/index.html).....	charger	artifact eaccess/ 40
<b>Figure 3.19.</b>	<b>Electrode pop artifact</b> (Marella, 2012).....			41
<b>Figure 3.20.</b>	<b>Electrode movement artifact</b> (Marella, 2012).....			41
<b>Figure 3.21.</b>	<b>Lead movement artifact</b> (Marella, 2012).....			41
<b>Figure 3.22.</b>	<b>Band-pass filtering of raw signals</b> .....			43
<b>Figure 3.23.</b>	<b>Eye-blink removal via ICA</b> .....			45
<b>Figure 3.24.</b>	<b>Epochs extraction</b> .....			46
<b>Figure 3.25.</b>	<b>Bad channels interpolation</b> .....			47
<b>Figure 4.1.</b>	<b>Shapiro-Wilk test results</b> .....			50
<b>Figure 4.2.</b>	<b>2D topography showing significant t-values resulting from the Student t-test</b> (Bonferroni corrected, $p<0.05$ ) applied on EEG data recorded from AD and healthy controls.			
	.....			51
<b>Figure 5.1.</b>	<b>The human brain can be visualized as a network</b> .....			53
<b>Figure 5.2.</b>	<b>Structural brain network (connectome)</b> (Park & Friston, 2013). B) <b>Functional brain network</b> (Hong et al., 2013). C) <b>Effective brain network</b> (Wu et al., 2014). .....			54
<b>Figure 5.3.</b>	<b>Functional alterations characterizing brain diseases</b> (Bassett & Sporns, 2017). .			55
<b>Figure 5.4.</b>	<b>EEG scalp connectivity</b> (Tsiaras et al., 2011). ....			56
<b>Figure 5.5.</b>	<b>Field spread effect</b> (Oostenveld et al., 2011). ....			56
<b>Figure 5.6.</b>	<b>Mean (<math>\pm</math>std) strength variability</b> in AD patients and healthy controls, in the two tasks-related paradigms. Wilcoxon test was used to assess the statistical difference between the two groups. ....			61
<b>Figure 5.7.</b>	<b>Seven nodes showing a significant difference in strength variability</b> between AD patients and healthy controls. Wilcoxon test was performed, Bonferroni corrected ( $p_{\text{Bonferroni adjusted}} < 0.0568$ ).....			61
<b>Figure 5.8.</b>	<b>Correlation between cognitive scores and strength variability relative to the motor task paradigm.</b> Red dots refer to AD patients, and black dots refer to healthy controls.....			63
<b>Figure 5.9.</b>	<b>Correlation between cognitive scores and strength variability relative to the picture naming paradigm.</b> Red dots refer to AD patients, and black dots refer to healthy controls. ..			64
<b>Figure 5.10.</b>	<b>Seven nodes showing significant correlation between cognitive scores and strength variability</b> in the button press task. Bonferroni correction ( $p_{\text{Bonferroni adjusted}} < 0.0568$ ) was applied. ....			65
<b>Figure 5.11.</b>	<b>Seven nodes showing significant correlation between cognitive scores and strength variability</b> in the button press task. Bonferroni correction ( $p_{\text{Bonferroni adjusted}} < 0.0568$ ) was applied. ....			65

# List of Abbreviations

ACE-R - Addenbrooke's Cognitive Examination – Revised.

AD - Alzheimer's disease.

ADRDA - Alzheimer's Disease and related Disorders Association.

APP - Amyloid Precursor Protein.

A $\beta$  - Beta-Amyloid.

A $\beta$ 40 - Beta-Amyloid 40.

A $\beta$ 42 - Beta-Amyloid 42.

BOLD - Blood Oxygenation Level-Dependent.

BSS - Blind Source Separation.

CAA - Cerebral Amyloid Angiopathy.

CASI - Cognitive Abilities Screening Instrument.

CSF - Low Cerebrospinal Fluid.

EEG – Electroencephalography.

EOAD - Early-Onset Alzheimer's Disease.

ERP - Event-Related Potential.

FDG – fluorodeoxyglucose.

fMRI - Functional magnetic resonance imaging.

HEOG - Horizontal Electrooculogram.

ICA - Independent Component Analysis.

LOAD – Late-Onset Alzheimer's Disease.

MEG – Magnetoencephalography.

MMSE - Mini-Mental State Examination.

MRI - Magnetic Resonance Imaging.

NCSE - Neurobehavioral Cognitive Status Examination.

NFTs neurofibrillary tangles.

NINCDS - National Institute of Neurological and Communicative Disorders and Stroke.

NPS - Neuropsychiatric symptoms.

PCA - Principal Component Analysis.

PET - Positron emission tomography.

qEEG - Quantitative EEG.

rIFC - Right Inferior Frontal Cortex.

SPECT - Single-Photon Emission Computed Tomography.

VEOG – Vertical Electrooculogram.

# INTRODUCTION

Alzheimer's disease (AD), named after the German neurologist Alois Alzheimer who first identified it, is a neurodegenerative brain disorder affecting 30 to 35 million people worldwide ([WHO, 2019](#)). It is characterized by an irreversible progressive memory loss and cognitive deficits.

Accurate diagnosis of AD at an early stage has become a topic of increasing interest. In fact, we believe that early detection and intervention could represent a key factor in AD treatment. Currently adopted diagnosis approach is based on the evaluation of clinical symptoms and cognitive screening tests. However, this approach may be insensitive to the disease early stages. In addition, its performance is highly affected by sociodemographic variables and mood disorders ([Anderson et al., 2007](#); [Scazufca et al., 2009](#)). Therefore, the need is high for objective neuro-markers to support the results obtained from currently used clinical tests.

Advances in neuroimaging techniques have led to numerous researches tackling changes in brain activity in AD patients. In this context, electroencephalography (EEG) provides a non-invasive, easy-to-use, and low-cost method tracking brain activity at a sub-second timescale. It represents, therefore, an excellent candidate to adopt for the conception of novel neuro-markers for AD diagnosis and prognosis.

The general objective of this project is to identify, using EEG, differences in brain activity, between AD patients and healthy controls. In order to achieve our goal, two main studies were conducted. We have first investigated differences in scalp voltage topographies between AD and healthy controls during a motor task. The feasibility of both static and dynamic analysis was compared in this study.

On the other side, it became evident that the human brain is conceptualized as a complex network ([Medaglia et al., 2015](#); [Sporns, 2014](#)). Brain disorders are, consequently, considered as network diseases ([Crossley et al., 2014](#); [Fornito et al., 2015](#)). Emerging evidence shows that functional connectivity, derived from EEG recordings, is disrupted in AD brain networks. Thus, in a second study, we investigated the functional alterations in AD brain networks and their correlation with the level of cognitive impairment.

This project is done in collaboration between the Lebanese University and Université de Rennes1. Experimental design and methodological techniques were discussed and approved by the two teams.

This report is organized as follows: The first chapter offers a general presentation of AD. The second provides an overview of different neuroimaging techniques. As our focus is mainly on EEG, a literature review about previous studies characterizing AD using EEG, and a discussion about their main limitations were presented. In the third chapter, we clarify how our study confronts previous studies limitations, we present our experimental paradigm and the different signal processing steps we adopted. Chapter four investigate scalp voltage differences between AD and healthy controls in both static and dynamic approach. The last chapter introduces the

concept of brain networks. It details how, based on EEG signals, networks are reconstructed, and presents the results of the network analysis we have conducted.

# **Chapter 1.**

## **ALZHEIMER'S DISEASE**

### **1.1 Introduction**

Alzheimer's disease (AD) is a neurodegenerative disease characterized by progressive memory impairment and cognitive deficits. Accounting for 60-70% of dementia cases ([WHO, 2019](#)), AD is considered among the greatest global challenges for health and social care in the 21st century. AD was first introduced in 1901, by German neurologist Alois Alzheimer's, when he identified an "unusual disease of the cerebral cortex" which affected a woman in her fifties, and resulted in memory loss, disorientation, hallucinations and ultimately her death at the age of 55 ([World Alzheimer Report, 2018](#)). Thus far, neuroscientists attempt to more understand the disease pathology and to propose valuable methods able to predict, diagnose or treat AD.

We will present in this chapter an overview of Alzheimer's disease, its prevalence (Sec. 1.2), and its clinical symptoms (Sec. 1.3). We will then explain the pathological (Sec. 1.4) and genetic (Sec 1.5) basis of the disease. Finally, diagnosis criteria (Sec. 1.6) and treatments approaches (Sec. 1.7) are reviewed.

### **1.2 Prevalence**

Worldwide, around 50 million people are affected by dementia in 2019. As the world's older population continues to grow, this number is projected to reach 82 million in 2030 and 152 million in 2050 ([WHO, 2019](#)). Among more than 70 recognized causes of dementia ([Karantzoulis & Galvin, 2014](#)), Alzheimer's disease, Cerebrovascular disease, Lewy body disease, mixed dementia, Fronto-temporal lobar degeneration, and Parkinson's disease are the most common ([Alzheimer's Association, 2019](#)). The 2018 global cost of dementia was estimated to be US\$ 1 trillion; this figure will rise to US\$ 2 trillion by 2030 ([World Alzheimer Report, 2018](#)).

Accounting for 60-70% of diagnosis cases, Alzheimer's disease (AD) is considered the most common cause of dementia ([WHO, 2019](#)). According to ([Alzheimer's Association, 2019](#)), AD is listed the sixth-leading cause of death in the United States, the fifth for those age 65 and older. AD is typically a disease of old age. Early-onset (i.e. before 65 years of age) is unusual and seen in less than 10% of AD patients ([Kumar & Taso, 2018](#)).

### **1.3 Signs and Symptoms**

Clinical symptoms of AD start usually with memory complaints affecting episodic memory, speech production, naming, semantic problems, and visual orientation ([Jahn, 2013](#)). However, AD is a progressive disease, its symptoms are stage-specific and worsen over time ([Alzheimer's Association, 2019](#)). The clinical symptoms relative to each stage are detailed below.

- **Preclinical Alzheimer's disease**

Changes in the brain begin at this stage, although no symptoms are yet noticed ([Alzheimer's Association, 2019](#)).

- **Mild Alzheimer's disease (early-stage)**

At this stage, the patient may feel as if he is having memory lapses. However, he is still able to manage his life independently. Symptoms include problems coming up with finding the right word or name, remembering names when introduced to new people, performing tasks in social or work settings, forgetting the material that one has just read, losing or misplacing a valuable object, increasing troubles with planning or organizing ([Alzheimer's Association, 2019](#)).

- **Moderate Alzheimer's disease (middle-stage)**

At this stage, considered the longest stage of the disease, symptoms are more noticeable. The patient starts to forget the events of his life. He may feel moody or withdrawn, especially in socially or mentally challenging situations. In addition, he becomes unable to recall his own address or telephone number or the high school or college from which he graduated. He is often confused about where he is or what day it is. He also needs help in choosing proper clothing for the season or the occasion. Changes in sleep patterns, such as sleeping during the day and becoming restless at night start to appear. Some individuals develop troubles controlling bladder and bowels. An increased risk of wandering and becoming lost emerges. Moreover, this stage is marked by personality and behavioral changes, including suspiciousness and delusions or compulsive, repetitive behavior like hand-wringing or tissue shredding ([Alzheimer's Association, 2019](#)).

- **Severe Alzheimer's disease (late-stage)**

At this stage, the patient loses the ability to respond to his environment and needs round-the-clock assistance with daily activities and personal care. He suffers from increased difficulties in communication, loses awareness of recent experiences as well as of their surroundings. In addition, changes in his physical abilities occur, including the ability to walk, sit and, eventually, swallow. Moreover, he becomes vulnerable to infections, especially pneumonia ([Alzheimer's Association, 2019](#)).

Beside cognitive symptoms, neuropsychiatric symptoms (NPS), previously denominated as behavioral and psychological symptoms of dementia, are recognized in AD patients ([Petrovic et al., 2007](#)). In a meta-analysis published in 2016, ([Zhao et al., 2016](#)) reported the prevalence of 12 NPS in AD patients (Fig. 1.1). Symptoms can be classified into four sub-syndromes as follow: hyperactivity (aggression, disinhibition, irritability, aberrant motor behavior, euphoria), psychosis (delusion, hallucination, sleep disorder), affective behavior (depression, anxiety), and apathy (apathy, appetite disorder) ([Aalten et al., 2007](#)).

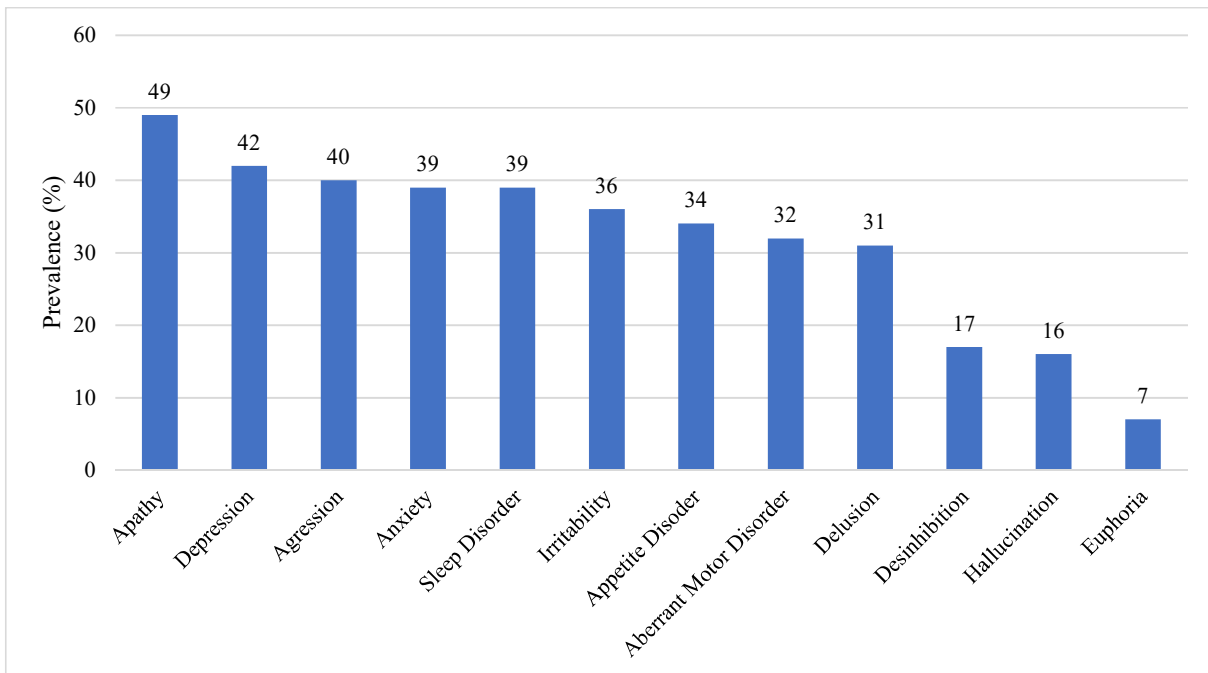


**Figure 0.1.** Prevalence of neuropsychiatric symptoms in AD patients. The figure was reproduced based on data published in ([Zhao et al., 2016](#)).

## 1.4 Pathophysiology of AD

Alzheimer's disease is pathologically defined by an excessive accumulation of Amyloid plaques and neurofibrillary tangles (NFTs) in the brain ([Crous-bou et al., 2017](#); [Karch & Goate, 2015](#)).

Plaques are microscopic, spherical, lesions that have an extracellular amyloid beta-peptide core surrounded by enlarged axonal terminations (Fig. 1.2.A). Beta-amyloid (A $\beta$ ) peptide is derived from the amyloid precursor protein (APP) (a transmembrane protein) and is cleaved from APP by the action of the alpha, beta, gamma-secretase proteases. Usually, APP divided by alpha or beta-secretase results in non-toxic fragments. However, when the sequential cleavage is performed by beta and then gamma-secretase, amino acid peptides 40 and 42 are formed (beta-amyloid 40 (A $\beta$ 40) and beta-amyloid 42 (A $\beta$ 42)). Increased levels of A $\beta$ 42 causes amyloid aggregation responsible for neuronal toxicity. Beta-amyloid 42 favors the formation of aggregated fibrillary amyloid protein over normal APP degradation ([Kumar & Taso, 2018](#)). The amyloid-beta peptide does not only accumulate in the brain parenchyma but also in the vessel walls in the form of cerebral amyloid angiopathy (CAA). Indeed, the more insoluble and aggregation-prone A $\beta$ 42 peptide tends to accumulate in the core of senile plaques, while the more soluble A $\beta$ 40 peptide is the major constituent of CAA ([Serrano-pozo et al., 2011](#)).

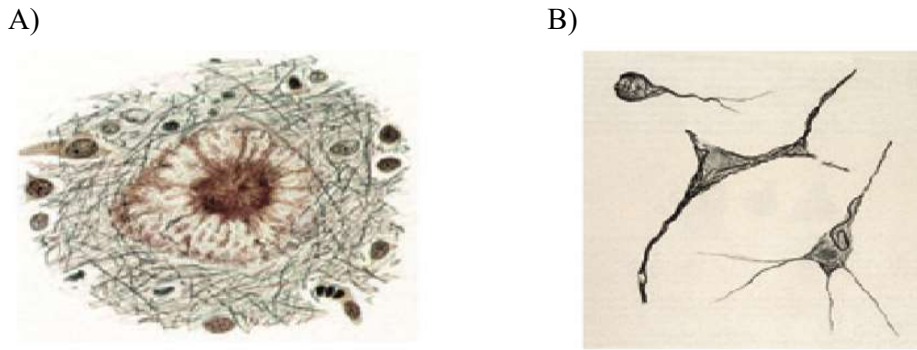


**Figure 0.2.** A) Amyloid plaque. B) Neurofibrillary tangles. ([Masters et al., 2015](#)).

On the other hand, the neurofibrillary tangles (Fig. 1.2.B), formed by a protein called tau, are intracellular fibrillary structures accumulated in neurons cytoplasm. Tau protein is responsible of the stabilization of axonal microtubules providing intra-cellular transport. In AD, the aggregation of extracellular beta-amyloid causes hyperphosphorylation of tau leading to the formation of tau aggregates. Tau aggregates form twisted paired helical filaments known as neurofibrillary tangles (Fig. 1.3). They occur first in the hippocampus and then they may be seen throughout the cerebral cortex ([Kumar & Taso, 2018](#)).

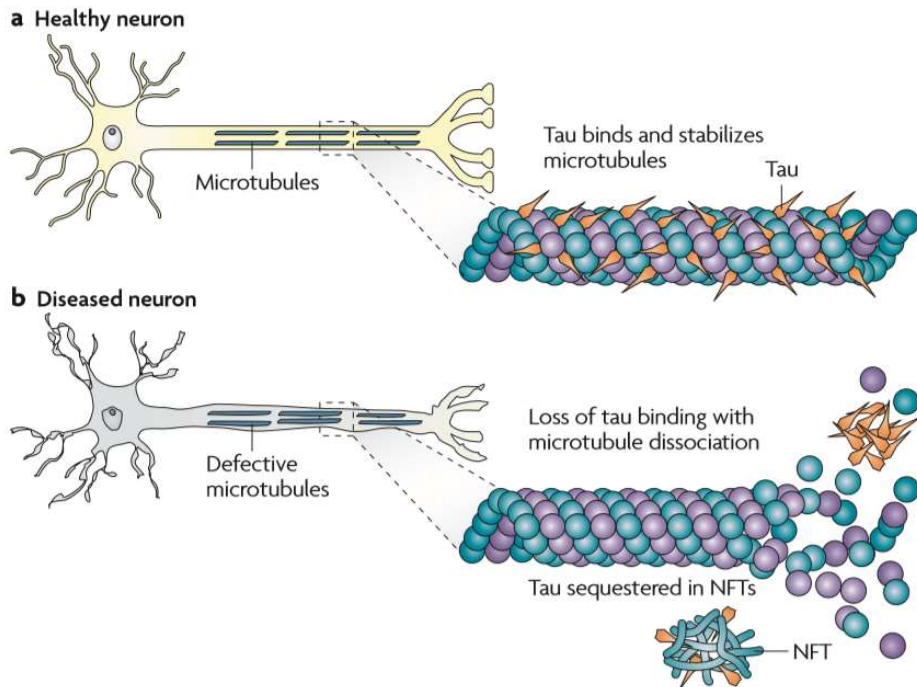


**Figure 0.3.** a) In Healthy neuron, microtubules are stabilized by tau protein. b) In diseased neuron, microtubules lose their stability, and neurofibrillary tangles are formed. Picture reproduced from ([Chen et al., 2013](#)).

Another feature of AD is granulovacuolar degeneration of hippocampal pyramidal cells by amyloid angiopathy. Many studies indicate that cognitive decline correlates more with a

decrease in density of presynaptic boutons from pyramidal neurons in laminae<sup>1</sup> III and IV, rather than an increase in the number of plaques ([Kumar & Taso, 2018](#)).

Vascular contribution to the neurodegenerative process of Alzheimer disease is not fully determined. Risk of dementia is increased fourfold with subcortical infarcts. The cerebrovascular disease also exaggerates the degree of dementia and its rate of progression ([Verma et al., 2018](#); [Wallace et al., 2018](#)).

## 1.5 The genetic basis of AD

Genetic variants may have an important role in the development of the disease ([Seshadri et al., 2010](#)). Having a first-degree relative with late-onset AD (LOAD, onset  $\geq$  65 years, accounting for 1-5% of all cases) doubles the expected life-time risk ([Reitz & Mayeux, 2014](#)). The principle genetic factor is allele  $\epsilon 4$  of the APOE gene. In fact, APEO, a lipid-binding protein, presents three allele APEO $\epsilon 2$ ,  $\epsilon 3$ , and  $\epsilon 4$ . The more common APEO $\epsilon 3$  and the rare APEO $\epsilon 2$  forms of are relatively protective against AD ([Mucke, 2009](#); [Reitz & Mayeux, 2014](#)). However, the presence of APEO $\epsilon 4$  is neither necessary nor sufficient for developing the disease ([Myers et al., 1996](#)). In contrast, for early-onset AD (EOAD, onset  $< 65$  years, accounting for  $> 95\%$  of cases), three genes encoding proteins involved in A $\beta$  production (APP, PSEN1, PSEN2) are considered to be involved in EOAD pathophysiology ([Reitz & Mayeux, 2014](#)).

PSEN1 is the most commonly involved gene, with 221 pathogenic mutations. The second most commonly involved gene is APP, with 32 pathogenic mutations described, while 19 different PSEN2 pathogenic mutations have been reported ([Lanoiselée et al., 2017](#)).

APP encodes the amyloid- $\beta$  precursor protein which, processed by the  $\beta$ -secretase and the  $\gamma$ -secretase complex leads to the production of the A $\beta$  peptide. PSEN1 and PSEN2 encode the presenilins, which constitutes the catalytic subunit of the  $\gamma$ -secretase complex (for a review, see ([Campion et al., 2016](#); [Haass et al., 2012](#))). EOAD causative mutations are thought to be responsible of the increased aggregation of the A $\beta$  peptide in the brain's parenchyma through one of the two following mechanisms: increased overall production of all A $\beta$  species (e.g., APP duplications or APP mutations located around the  $\beta$  cleavage site) or production of a more aggregation-prone form of the A $\beta$  peptide ([Lanoiselée et al., 2017](#)).

## 1.6 Diagnosis

To date, the diagnosis of AD is based on a set of clinical symptoms. The National Institute of Neurological and Communicative Disorders and Stroke (NINCDS) and Alzheimer's Disease and Related Disorders Association (ADRDA) defined the NINCDS-ADRDA criteria to describe the clinical diagnosis of AD ([McKhann et al., 2011](#)). First published in 1984, the criteria were used for 27 years. Lately revised in 2010-2011, the criteria assessed the cognitive and behavioral symptoms for AD diagnosis. Described symptoms are basically related to remembering abilities, reasoning capability, visuospatial abilities, language functions, and changes in personality (see ([McKhann et al., 2011](#)) for details). Cognitive impairment is

---

<sup>1</sup> Most of the cortex that covers the cerebral hemispheres is neocortex, defined as cortex that has six cellular layers, or laminae. Each layer comprises more or less distinctive populations of cells based on their different densities, sizes, shapes, inputs, and outputs.

diagnosed by either a history-taking from the patient or an objective cognitive assessment which may be a “bedside” mental status examination. When the routine history and bedside mental status examination cannot provide a confident diagnosis, neuropsychological testing should be performed (McKhann et al., 2011), and the cognitive impairment level is determined based on the obtained test scores (Cullen et al., 2007)

39 cognitive screening tests were reviewed in (Cullen et al., 2007) including the Mini-Mental State Examination (MMSE), the Addenbrooke’s Cognitive Examination—Revised (ACE-R), the Neurobehavioral Cognitive Status Examination (also known as Cognistat, NCSE), the Cognitive Abilities Screening Instrument (CASI). However, the performance of neuropsychological tests is highly affected by sociodemographic variables, mainly age and education (Anderson et al., 2007; Cullen et al., 2007; Scazufca et al., 2009).

New findings about AD pathophysiology have led to the development of several biomarkers for disease diagnosis and prognosis, derived from the recording of brain activity. However, only five biomarkers were formally incorporated into the diagnostic criteria. The amyloid Positron emission tomography<sup>2</sup> (PET) and low cerebrospinal fluid (CSF) Aβ42 are two biomarkers of Aβ accumulation. On the other hand, biomarkers of neuronal degeneration or injury include elevated CSF tau, decreased fluorodeoxyglucose uptake on PET, and atrophy visualized on magnetic resonance imaging<sup>3</sup> (MRI) (Jack et al., 2011).

## 1.7 Treatment

Since 1998, there have been more than 100 attempts to develop an effective drug to treat the disease but only four have been approved (World Alzheimer Report, 2018): Cholinesterase inhibitors (donepezil, rivastigmine, galantamine) recommended for all AD stages, and memantine approved for moderate-to-severe AD (Weller & Budson, 2018). However, current treatment tends to manage the disease manifestations, but it is actually unable to cure dementia or modify its time course (Livingston et al., 2017). New therapeutic approaches are targeting the pathological features associated with AD, Aβ and p-tau trying to reduce their burden in the brain (Weller & Budson, 2018).

Although no disease-modifying treatment for AD is available yet, a delay in the disease onset would be beneficial. Higher education levels, physical exercising, no smoking, no depression, and improved social contact were reported in (Livingston et al., 2017) as modifiable risk factors that may help in the disease prevention.

## 1.8 Conclusion

Alzheimer’s disease is a progressive and irreversible, brain disorder. AD pathophysiological processes are thought to begin 20 years before the first symptoms can be detected (Bateman et al., 2012; Perl, 2010). Thus, accurate diagnosis of AD in its early stage is a true challenge. In fact, we believe that early detection and intervention could represent a key factor in the disease treatment. The conception of novel “neuro-makers” would reply on investigating the functional

---

<sup>2,3</sup> Principles of neuroimaging techniques will be discussed in the next chapter

changes in the brain activity of AD patients. The brain activity can be derived from different neuroimaging techniques.

Therefore, in the next chapter, we will present a detailed review of the neuroimaging techniques, and focus on the electroencephalography (EEG) as a promising tool in elucidating brain changes in AD.

# Chapter 2.

## NEUROIMAGING TECHNIQUES

### 2.1 Introduction

Advances in neuroimaging techniques have provided the possibility not only to capture structural images of the brain (i.e. anatomical imaging) but also to track mental processes as they occur (i.e. functional imaging) (Laureys et al., 2002). An increasing interest in neuroimaging technique is to detect *in vivo* brain changes associated with neurodegeneration and cognitive decline in brain disorders (Ewers et al., 2011).

In this chapter, we will present an overview of the most used functional neuroimaging techniques. Mostly interested in Electroencephalography, we will detail some of this technique principles. We will then report the most interesting results achieved in electroencephalography-based AD diagnosis field, and determine the main limitations of those existing studies.

### 2.2 Functional neuroimaging overview

#### 2.2.1 Positron Emission Tomography

Positron emission tomography (PET) is a type of nuclear medicine imaging (Fig. 2.1). It is used to measure physiological function by looking at blood flow, metabolism, neurotransmitters, and radiolabeled drugs. Radioactively labeled organic molecules or probes, named radiotracers, are injected into veins, and then detected by a PET scanner as they are absorbed by tissues. The most commonly used PET tracers in brain scans are [<sup>18</sup>F]-fluorodeoxyglucose (FDG) used to assess the amount of glucose absorbed by living cells, and [<sup>15</sup>O]-labeled water used to measure cerebral blood flow. Neural activity is reflected by either the amount of glucose or the blood flow (Valk et al., 2006). The main disadvantage of PET scans is its poor temporal resolution limited by the speed of metabolic and hemodynamic processes (Baillet et al., 2001) to 45 sec, in addition to a spatial resolution of about 6 mm (Laureys et al., 2002).

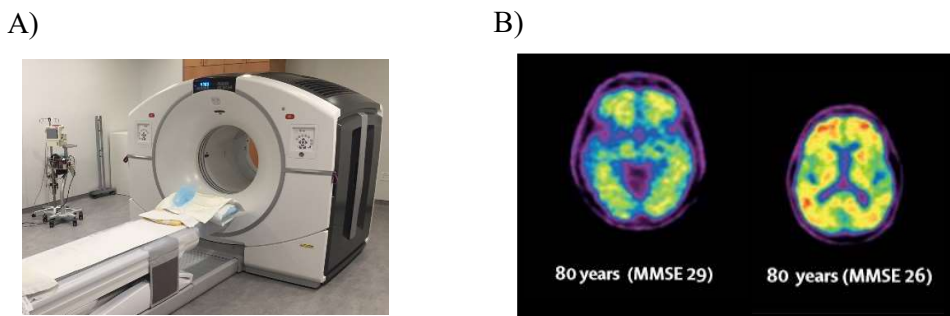
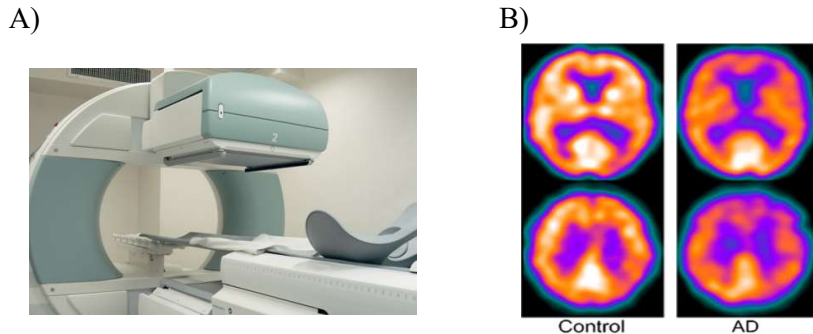


Figure 0.1. A) PET scanner (<https://www.iibi.uiowa.edu/pet-center>). B) PET scans examples (Rowe et al., 2008).

#### 2.2.2 Single Photon Emission Computed Tomography

Similar to PET, single-photon emission computed tomography (SPECT) is a nuclear imaging technique that uses radioactive tracers but involves the detection of individual photon rather than positrons emitted from the radionuclide to be imaged (Fig. 2.2). In addition, SPECT

tracers offer the opportunity to inject the tracer at a time when scanning is impossible (e.g. during an epileptic crisis) and to scan (post-event) the associated distribution of activated brain regions. SPECT scans are less expensive and more widely available than PET scans. However, they are more limited in the kind of brain activity they measure and has a poorer spatial resolution (Laureys et al., 2002).



**Figure 0.2.** A) SPECT scanner (<https://www.uofmhealth.org/health-library/acc4790>). B) SPECT scans examples (O'Brien et al., 2014).

### 2.2.3 Functional Magnetic Resonance Imaging

Functional magnetic resonance imaging (fMRI) is a non-invasive neuroimaging technique that measures the blood oxygenation level-dependent (BOLD) signal (Fig. 2.3). In fact, the amount of oxygen carried by hemoglobin affects its magnetic properties, resulting in small fluctuations that can be detected by magnetic resonance imaging (MRI) (Laureys et al., 2002). Changes in blood flow and oxygenation level are noticed when neurons become active. Hence, the BOLD signal can be considered as a correlate of the underlying neural activity (Baillet et al., 2001). However, the exact relation through which BOLD signal models the neural activity remains unknown (Singh, 2012).

Although they both measure the hemodynamic response, fMRI presents many advantages over PET scanning since it doesn't require an injection of radioactive tracers, being hence totally non-invasive. In addition, spatial resolution and temporal resolution are both better in fMRI compared to PET (Laureys et al., 2002).

The limitation of fMRI resides in its inability to match the speed of the electrical neural activity. While electrical signal propagates in the brain in 10 ms or less, the rate of blood oxygenation level ranges from hundreds of milliseconds to several seconds (Laureys et al., 2002).

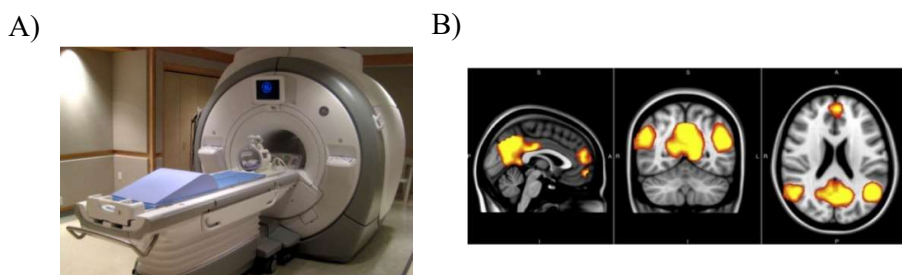


**Figure 0.3.** A) MRI machine (used for both MRI and fMRI scans). B) fMRI scan during task performance (Hafkemeijer et al., 2012).

## 2.2.4 Magnetoencephalography

Magnetoencephalography (MEG) is a direct measure of brain activity (Fig. 2.4). It measures the extra-cranial magnetic field generated by neuronal electric current. A major advantage of MEG is its excellent temporal resolution allowing to track brain dynamics at a millisecond timescale. Compared to PET and fMRI, MEG suffers from a reduced spatial resolution. The number of spatial measurements is about a few hundred versus tens of thousands in PET and fMRI (Baillet et al., 2001). Noise is a major concern in MEG, thus the need for superconducting materials for instrumental noises, gradiometers as sensing units for low frequency artifacts, and shielded rooms made of successive layers of mu-metal, copper, and aluminum for high frequency perturbations (Baillet et al., 2001), all leading to a high cost technology (Baillet, 2017).

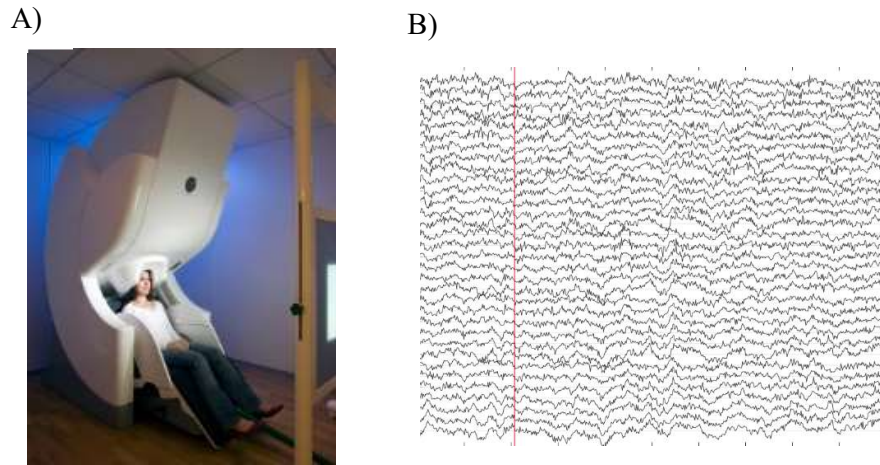


**Figure 0.4.** A) MEG scanner  
(<https://www.admin.ox.ac.uk/estates/aboutus/spotlight/casestudies/capitalprojects/megscanner/>). B) MEG data.

## 2.2.5 Electroencephalography

Similar to MEG, electroencephalography (EEG) presents a non-invasive direct neuroimaging technique that measures scalp electric potentials. Electrical currents generated by active neuronal assemblies -mainly in cortical regions - propagate through different layers (cortex, skull, and skin). Weak signals detected by scalp electrodes are then massively amplified (Laureys et al., 2002).

The main advantage of EEG, just as MEG, is its high temporal resolution, allowing to capture neural activity at a millisecond timescale (Baillet et al., 2001). However, spatial resolution is lower in EEG than in MEG (Laureys et al., 2002). What may let EEG overcome MEG in several applications is mainly the relatively low operating cost, its ease of use, and its portability compared to MEG devices.

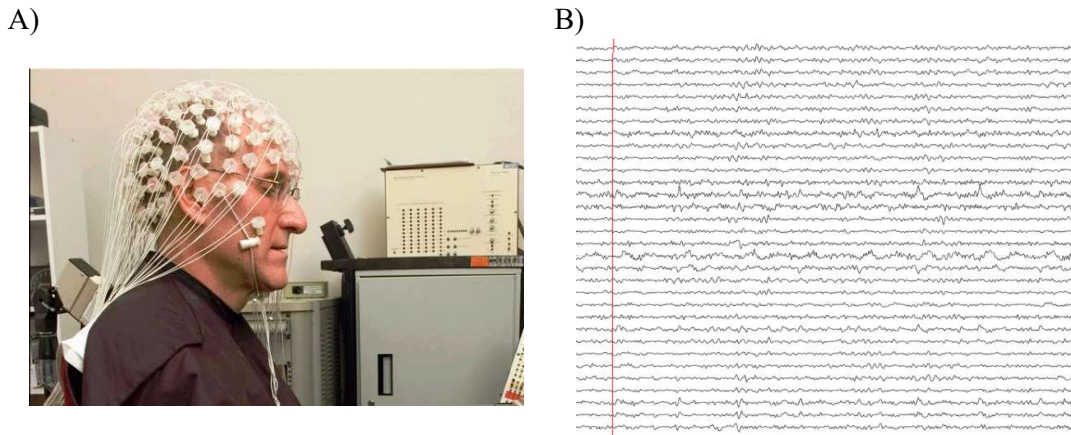


**Figure 0.5.** A) EEG acquisition ([https://www.vice.com/en\\_us/article/43844m/researchers-mind-melded-three-people-to-collaboratively-play-tetris](https://www.vice.com/en_us/article/43844m/researchers-mind-melded-three-people-to-collaboratively-play-tetris)). B) 32-channel EED data.

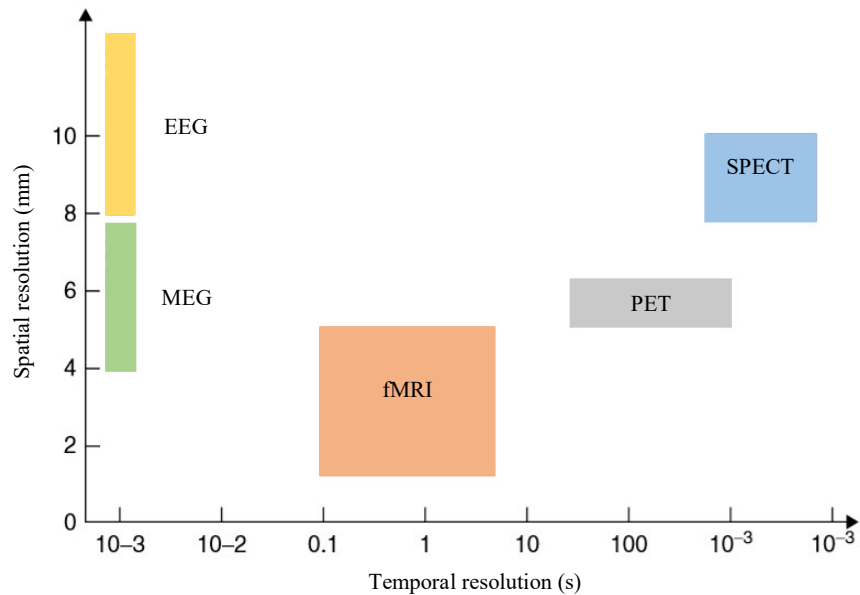


**Figure 0.6.** Approximation of the resolution in time and space of the most commonly employed functional neuroimaging techniques based on measurements of hemodynamic (fMRI, PET, SPECT) and electrical (EEG, MEG) activity of the brain (Laureys et al., 2002).

### 2.2.5.1 EEG basics

EEG signals can be recorded using Ag/AgCl, water-based, or dry contact electrodes. The 10-20 international system is used for electrodes placement (Fig. 2.7). It ensures that inter-electrode spacing is equal, and that electrode placement is proportional to skull size and shape. Each electrode site is labeled with a letter and a number. The letter refers to the area of the brain underlying the electrode: Pre-Frontal (Fp) – Frontal (F) – Central (C) – Temporal (T) – Parietal (P) – Occipital (O) – Auricular or earlobe (A). Odd numbers refer to the left-sided electrodes and even numbers to the right. The numbers increase from anterior to posterior of the head. The letter “z” designates midline.

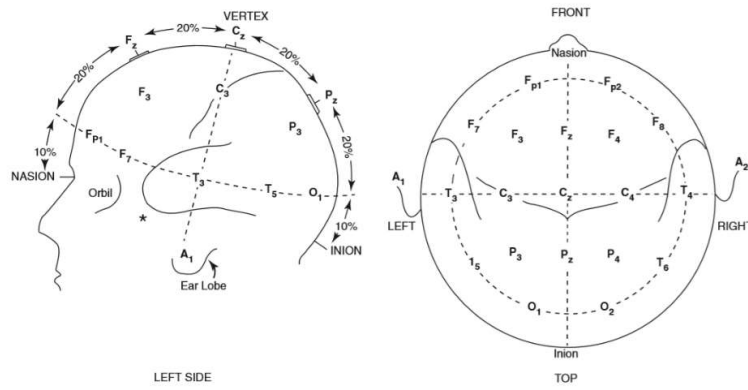


**Figure 0.7.** The 10-20 international system is used for electrodes placement.

### 2.2.5.2 EEG Montages

EEG machines use a differential amplifier that amplifies the voltage difference between the two signals at each of its inputs. The manner in which pairs of electrodes are connected to the amplifier inputs is called a montage:

- Bipolar Montage: Every channel represents the difference between two adjacent electrodes.
- Laplacian Montage: Every channel represents the difference between the corresponding electrode and the weighted average of the surrounding electrodes.
- Common Referential Montage: Each channel represents the difference between the corresponding electrode and a designed reference electrode (usually earlobes or mastoids).
- Average Reference Montage: Outputs of all channels are averaged, and the resulting signal is used as a common reference for each channel.

A detailed description of the EEG neurophysiologic basis can be found in ([Olejniczak, 2006](#)).

### 2.2.5.3 EEG Rhythms

Brain oscillations are characterized by their frequency, amplitude, and source. Although many types of waves may be coursing through the brain at any given time, certain types dominate during particular behaviors, suggesting some mechanistic links ([Thomson, 2018](#)).

- Delta [0.5 – 4 Hz]: The slowest brainwaves, called delta waves, are associated with deep, often dreamless sleep.
- Theta [4 – 8 Hz]: Theta rhythms are seen in young children and adults in a drowsy, meditative or pathological state.
- Alpha [8 – 13 Hz]: Arising in the occipital lobe, alpha waves are associated with wakeful rest with eyes closed.
- Beta [13 – 32 Hz]: Beta waves are associated with normal wakeful consciousness and concentration, and are suppressed during movements.
- Gamma [25 – 140 Hz]: Gamma waves are linked to normal visual consciousness and rapid-eye-movement sleep, these might help decipher multiple sensory signals.

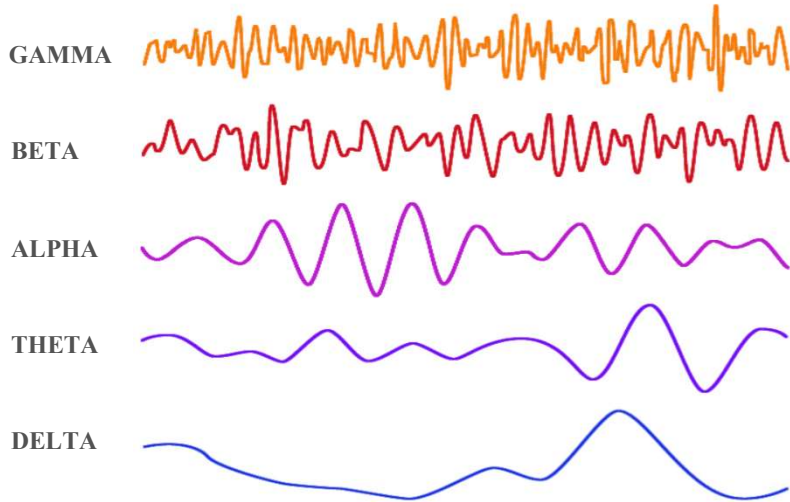


**Figure 0.8.** EEG rhythms (Jacobs, 2015).

## 2.3 Electroencephalography and Alzheimer's disease

### 2.3.1 Past studies

Since Hans Berger discovered the electroencephalography, studies aiming at revealing EEG abnormalities in AD brains are being performed. A large number of studies investigated quantitative EEG (qEEG) measures in order to discriminate AD EEG patterns (Brenner et al., 1986; Coben et al., 1983; Czigler et al., 2008; Hogan et al., 2003; Jelic et al., 2000; Penttila et al., 1985; Schreiter-gasser et al., 1994). Spectral analysis of EEG signals by Fourier or wavelet transformation has been widely used (Horvath et al., 2018). An increase in low frequency (theta and delta) activities and a decrease in high frequency (alpha and beta) activities have been repeatedly reported (Bennys, Rondouin, Vergnes, & Touchon, 2001; Coben et al., 1983; Coben, Danziger, & Storandt, 1985; Guiaquito & Nolfe, 1986; Kwak, 2006; Lindau et al., 2003). This shifting of EEGs to lower frequencies is correlated with the disease clinical severity and stages (Coben et al., 1983; Kwak, 2006). In (Petit et al., 1992), EEG slowing was reported to be more marked during sleep than during awakening. Other studies based on the non-linearity of brain activity, questioned the complexity of brain dynamics. They assume that the loss of neurons and synapses in AD brains results in less complex dynamics of neural networks which were assessed by complexity measures such as correlation dimension (Jeong et al., 2001), Lempel-Ziv complexity (Abásolo et al., 2006), multiscale entropy (Mizuno et al., 2010). Moreover, a decrease in information transmission was reported in (Jeong et al., 2001) using mutual information analysis.

Event-related potentials (ERPs) are electrical potential generated by the brain time-locked to a sensory, cognitive, or motor event (Luck, 2014). Different ERP components were investigated to assess cognitive processes in AD patients. P300, an ERP component that reflects attention and memory processing, has shown delayed latency and reduced amplitude in AD patients (Gironell et al., 2005; Pokryszko-dragan et al., 2003; van Deursen et al., 2009). (Olichney et al., 2002; Olichney et al., 2006) showed a decreased amplitude in the N400 ERP component

reflecting semantic comprehension, with a less well-defined peak at posterior electrode sites. In addition, longer olfactory ERPs were observed in AD patients ([Morgan & Murphy, 2002](#)).

### 2.3.2 Limitations of past studies

Past researches investigating EEG abnormalities in AD patients suffer from three main limitations:

- First, most of the previous studies were performed in a resting state paradigm. However, it will be interesting to investigate brain activity during the performance of cognitive tasks targeting the cognitive decline aspect in AD patients.
- Second, the majority of the previous EEG studies assumed stationarity of EEG recordings, and static analysis was usually performed, ignoring the dynamic changes of brain activity throughout the measurement period. However, the brain is a dynamic system ([Cohen & D'Esposito, 2016](#)), in which cognitive processes may occur on a timescale of hundreds of milliseconds ([Bullmore & Sporns, 2009](#)).
- Third, EEG studies in AD were performed on small datasets where the number of subjects in each group does not exceed usually 20 participants.

## 2.4 Conclusion

Due to its excellent temporal resolution, non-invasiveness, ease of use, availability and low cost, EEG represents a powerful neuroimaging tool allowing to track brain dynamics at a sub-second timescale. Studies assessing brain activity in AD patients using EEG are numerous. However, they usually suffer from different limitations. In the next chapter, we will clarify how our study confronts previous studies limitations before getting into the details of the experiment design.

# **Chapter 3.**

## **EXPERIMENTAL DESIGN**

### **3.1 Introduction**

Understanding the pathophysiology of AD using EEG is a promising research topic. It is the first step toward the conception of novel neuro-markers able to identify and even predict the disease (Bateman et al., 2012; Perl, 2010). Such neuro-markers are increasingly needed for an accurate objective diagnosis of the disease. The non-invasiveness of EEG, its ease of use, its availability and low cost, in addition to its excellent temporal resolution make EEG an excellent candidate to adopt for the conception of the desired neuro-markers.

Thus, the general objective of this study is to identify, using EEG as a neuroimaging technique, differences between AD and healthy controls brain activities that correlate with the cognitive impairment level of each group.

In this chapter, we will first pinpoint the objectives intended by this study and the innovations differentiating it from previous researches (Sec. 3.2). Second, we will then detail the experimental setup of the data acquisition process (Sec. 3.3). We will then present the pre-processing procedure we have performed (Sec. 3.4).

### **3.2 Project goals and innovations**

AD is characterized by a clinical heterogeneity (Cummings, 2000). As we reviewed in chapter 1 (Sec. 1.3), cognitive deficits in AD are very diverse. Anomia, for example, is a well remarked impaired function in AD (Appell et al., 1982). Patients encounter difficulties in naming objects due to semantic abilities degradation (Huff et al., 1986). Another aspect of cognitive decline in AD appears in the working memory (i.e. temporary storage), specifically in attentional control required during tasks execution (Baddeley, 1992). Besides the cognitive decline, a decline of motor performance is noticed in AD patients (Pettersson, Olsson, & Wahlund, 2005). A loss of motor function is reported to occur in AD patients even prior to the clinical diagnosis (Buchman & Bennett, 2011).

Therefore, in this study, we are trying to tackle this symptoms diversity by the conception of different paradigms. Our EEG acquisition scenario consists of one task-free (“resting state”), and three task-related paradigms. Semantic memory was targeted by a picture naming task. The one-back task stimulated the participant working memory. A button press task was designed for triggering motor networks.

As we mentioned in chap 2 (Sec. 1.3.2), in most of the EEG-based studies investigating AD abnormalities, datasets sizes are limited to less than twenty subjects. However, the current study is a part of a Ph.D. project<sup>4</sup> in which one of the main contributions is to collect a large dataset. A total number of 50 AD patients and 50 healthy controls is targeted, in addition to 50

---

<sup>4</sup> Judie Tabbal is working on the project in a collaboration between the Lebanese University and Université de Rennes1

subjects at risk of developing the disease based on the familial medical history. Furthermore, the project aims at conducting a longitudinal study: each subject is supposed to perform 3 sessions during 3 years in order to examine the disease progression.

In this project, we aim to conduct a group-level comparison in order to investigate the brain activity differences between the three groups. An individual-level analysis will be also performed in order to test the ability of EEG to predict AD. A dynamic analysis is also targeted in this study rather than a static analysis benefiting from EEG's excellent temporal resolution. A comparative study between static and dynamic approach will be presented.

### **3.3 Experimental setup**

Data acquisition took place at Vita Nova polyclinic (Fig. 3.1.A). AD Patients and subjects at risk were recruited by neurologists Assef Nasser and Rashid Al Mohamad, whereas healthy controls were selected from the local community. Data were acquired from 11 AD patients, 13 healthy controls, and 2 subjects at risk between April 2019 and June 2019. All participants gave their informed consent to participate in the study (see Appendix A). A complete session lasts between one and two hours according to the level of cognitive decline of the participant.

#### **3.3.1 Neuropsychological test**

In order to assess the level of cognitive impairment, all subjects underwent the Addenbrooke's cognitive examination – Revised (ACE-R) ([Mioshi et al., 2006](#)), which assess five cognitive domains: attention/orientation (18 points), memory (26 points), fluency (14 points), language (26 points), and visuospatial abilities (16 points). Attention is tested by asking the patient for the date, season, current location, etc... in addition to repeating back three simple words, and performing a serial subtraction. In the memory questions section, the patient is asked to recall the three words previously repeated, memorize and recall a fictional name and address; and recall widely-known historical facts. The participant fluency is assessed by asking to recall as many words as they can think of starting with a specified letter within one minute, and naming as many animals as they can think of in one minute. Language is tested by asking the patient to complete a set of sequenced physical commands, to write one grammatically-complete sentences, to repeat several polysyllabic words and two short proverbs; to name the objects shown in 12 line drawings, and answer contextual questions about some of the objects; and to read aloud five commonly-mispronounced words. Visuospatial abilities are determined by asking the patient to copy two diagrams, to draw a clock face with the hands set at a specified time, to count sets of dots, and to recognize four letters which are partially obscured. ACE-R maximum score is 100, composed by the addition of all sub-domains scores. A translated validated Arabic version of ACE-R was adopted ([Al Salman, 2013](#)). (see Appendix B).

#### **3.3.2 EEG acquisition**

EEG data were recorded using the water-based 32 electrode EEG system (Twente Medical Systems International -TMSi-, Porti system) available at Azm Research center (Fig. 3.1.B), and OpenVibe software platform.

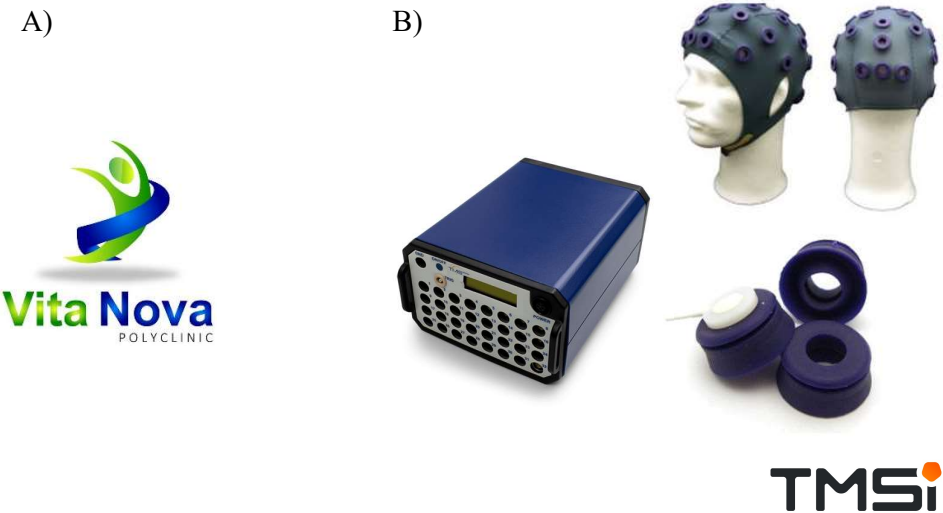


**Figure 0.1.** A) EEG acquisition was done at Vita Nova polyclinic. B) Twente Medical Systems International -TMSi-, Porti system, (32 electrode system).

A complete acquisition session consisted of one task-free (“resting state”), and three task-related paradigms, and the effective recording duration is about 30 minutes.

All four paradigms are detailed below.

### 3.3.2.1 Task-free paradigm (5 minutes)

Subjects underwent 5 minutes resting state EEG recordings, in which they were asked to relax and close their eyes, without falling asleep. (Fig. 3.2).

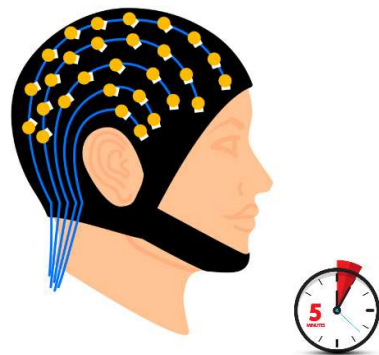


**Figure 0.2.** Resting state paradigm

### 3.3.2.2 Task-related paradigms (25 minutes)

#### 3.3.2.2.1 Picture naming task (10 minutes)

A set of 100 pictures selected from a database of 400 pictures standardized for French ([Alario & Ferrand, 1999](#)) were displayed on a screen. All pictures were in black and white. Order of presentation was randomized across subjects. The first 4 trials were for practice. A typical trial lasted 6 sec: a central fixation cross appears first for 3 sec, followed by the picture onset. Participants were asked to name the picture while it was displayed (during 3 sec). Their answers were recorded and then analyzed using Praat software to set the voice onset time ([Boersma](#),

2002). Task performance was measured by both accuracy (defined as the percentage of correct answers) and response time (defined as the latency between picture onset and the beginning of vocalization). (Fig. 3.3).

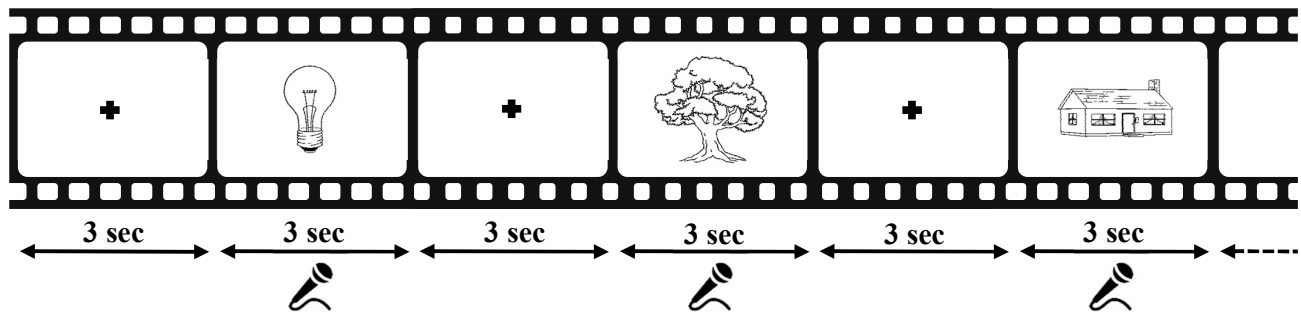


Figure 0.3. Picture naming task.

### 3.3.2.2.2 One-Back test (7 minutes)

Numbers from 1 to 4 were displayed, in diamond shapes, successively, in random order on the screen. A single trial consists of 500 ms stimulus display and 2500 ms interstimulus fixation. In each trial, participants were asked to type on the keyboard Numpad, using their dominant hand, the number that appeared in the previous trial. A total of 10 to 15 trials were set for practice followed by 120 non-practice trials. (Fig. 3.4).

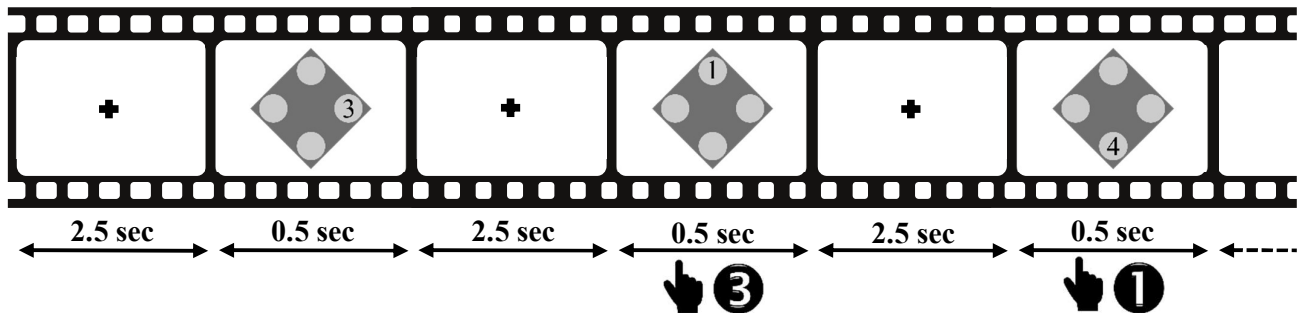


Figure 0.4. One-back task.

### 3.3.2.2.3 Button Press test (4 min)

Participants were asked to press, with their dominant hand, the keyboard “space button” whenever a stimulus picture appears. The picture was displayed, in black and white, on the screen. The experiment consisted of 44 trials, among which 4 were for practice. Each trial consists of a central fixation cross (3 sec), followed by the stimulus picture appearing (for a maximum 3 seconds interval), and vanishing at the button press. (Fig. 3.5).

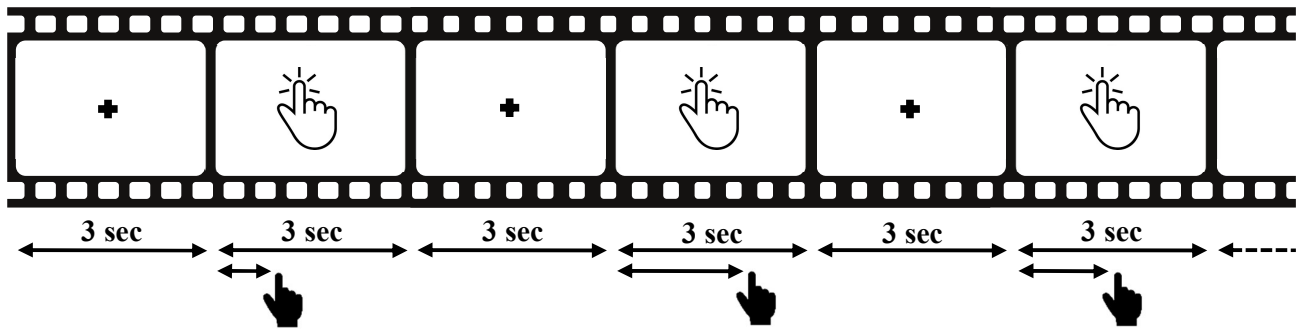


Figure 0.5. Button press task.

### 3.3.2.3 E-prime software

All three task-related experiments were designed using E-prime 2.0 software (Psychology Software Tools, Pittsburg, PA (Schneider et al., 2002). It is considered the world-leading behavioral experiment software providing an environment for computerized experiment design, data collection, and analysis at a millisecond precision timing to ensure the accuracy of the data. It comes with a bunch of applications. We mainly used the E-Studio application for creating the experiments (Fig. 3.6), and the E-dataAid application for data management (filtering, editing, analyzing experimental data) (Fig. 3.7).

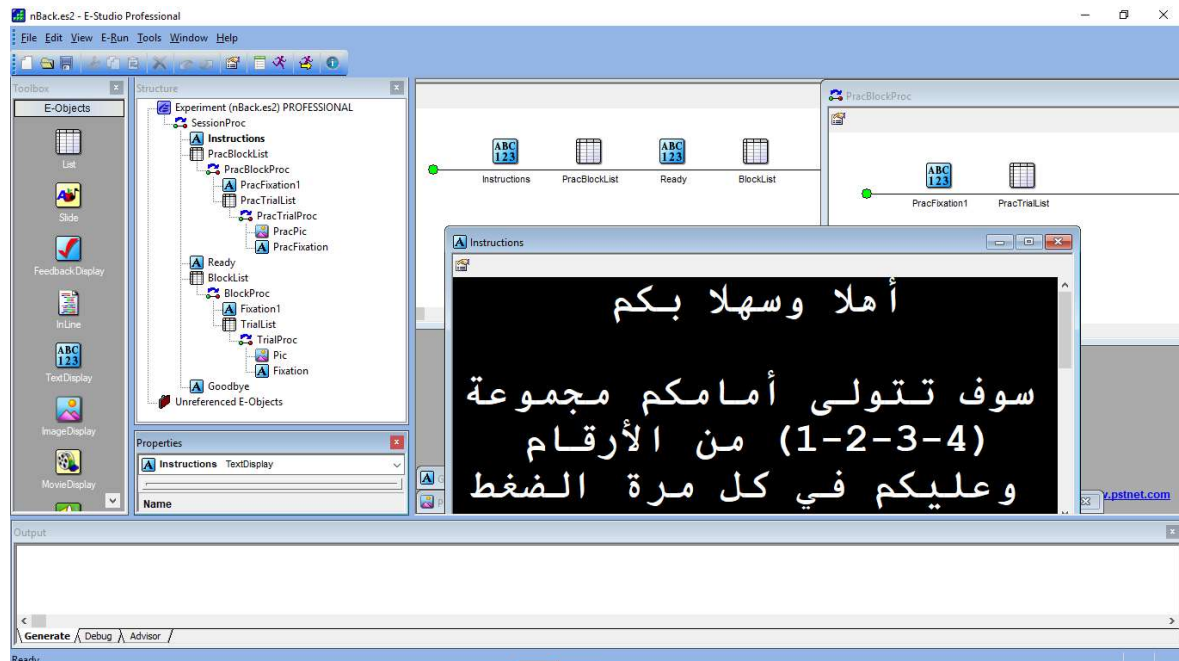


Figure 0.6. E-studio application (E-prime 2.0 software) used for the experiments design.

The screenshot shows a data management interface for E-prime 2.0 software. The main window displays a table with three columns: Trial, Stimulus, and PicSoundIn1.filename. The 'Trial' column contains integers from 1 to 26. The 'Stimulus' column contains file names for Arabic pictures, such as 'Pics\_arabic\_الفيلق.bmp' and 'Pics\_arabic\_العنقرة.bmp'. The 'PicSoundIn1.filename' column contains corresponding audio file names, such as 'Picture\_neuro\_final-28-3Pic-5.wav' and 'Picture\_neuro\_final-28-3Pic-6.wav'. A red box highlights the 'Stimulus' column, and a yellow box highlights the 'PicSoundIn1.filename' column. Below the table, there is a 'Filters' section and two arrows pointing downwards: one red arrow labeled 'Stimulus' pointing to the 'Stimulus' column, and one yellow arrow labeled 'Recorded answers' pointing to the 'PicSoundIn1.filename' column.

Trial	Stimulus	PicSoundIn1.filename
1	Pics_arabic_الفيلق.bmp	NULL
2	Pics_arabic_العنقرة.bmp	NULL
3	Pics_arabic_العنقرة.bmp	NULL
4	Pics_arabic_العنقرة.bmp	NULL
5	Pics_arabic_العنقرة.bmp	Picture_neuro_final-28-3Pic-5.wav
6	Pics_arabic_العنقرة.bmp	Picture_neuro_final-28-3Pic-6.wav
7	Pics_arabic_العنقرة.bmp	Picture_neuro_final-28-3Pic-7.wav
8	Pics_arabic_العنقرة.bmp	Picture_neuro_final-28-3Pic-8.wav
9	Pics_arabic_العنقرة.bmp	Picture_neuro_final-28-3Pic-9.wav
10	Pics_arabic_العنقرة.bmp	Picture_neuro_final-28-3Pic-10.wav
11	Pics_arabic_العنقرة.bmp	Picture_neuro_final-28-3Pic-11.wav
12	Pics_arabic_العنقرة.bmp	Picture_neuro_final-28-3Pic-12.wav
13	Pics_arabic_العنقرة.bmp	Picture_neuro_final-28-3Pic-13.wav
14	Pics_arabic_العنقرة.bmp	Picture_neuro_final-28-3Pic-14.wav
15	Pics_arabic_العنقرة.bmp	Picture_neuro_final-28-3Pic-15.wav
16	Pics_arabic_العنقرة.bmp	Picture_neuro_final-28-3Pic-16.wav
17	Pics_arabic_العنقرة.bmp	Picture_neuro_final-28-3Pic-17.wav
18	Pics_arabic_العنقرة.bmp	Picture_neuro_final-28-3Pic-18.wav
19	Pics_arabic_العنقرة.bmp	Picture_neuro_final-28-3Pic-19.wav
20	Pics_arabic_العنقرة.bmp	Picture_neuro_final-28-3Pic-20.wav
21	Pics_arabic_العنقرة.bmp	Picture_neuro_final-28-3Pic-21.wav
22	Pics_arabic_العنقرة.bmp	Picture_neuro_final-28-3Pic-22.wav
23	Pics_arabic_العنقرة.bmp	Picture_neuro_final-28-3Pic-23.wav
24	Pics_arabic_العنقرة.bmp	Picture_neuro_final-28-3Pic-24.wav
25	Pics_arabic_العنقرة.bmp	Picture_neuro_final-28-3Pic-25.wav
26	Pics_arabic_العنقرة.bmp	Picture_neuro_final-28-3Pic-26.wav

Figure 0.7. E-DataAid application (E-prime 2.0 software) used for data management

Particularly, E-DataAid was used to assess the accuracy of each participant in the picture naming task. Recorded answers can be compared to the corresponding stimulus in one single environment (Fig. 3.7).

For data analysis purposes, the exact time of the stimulus onset and the participant response must be marked in the EEG signals. In other words, synchronization between E-prime software and the acquisition system is needed. Thus, triggers and markers are sent through a parallel port from the software to the digital trigger isolated input of the Porti amplifier (Fig. 3.8).

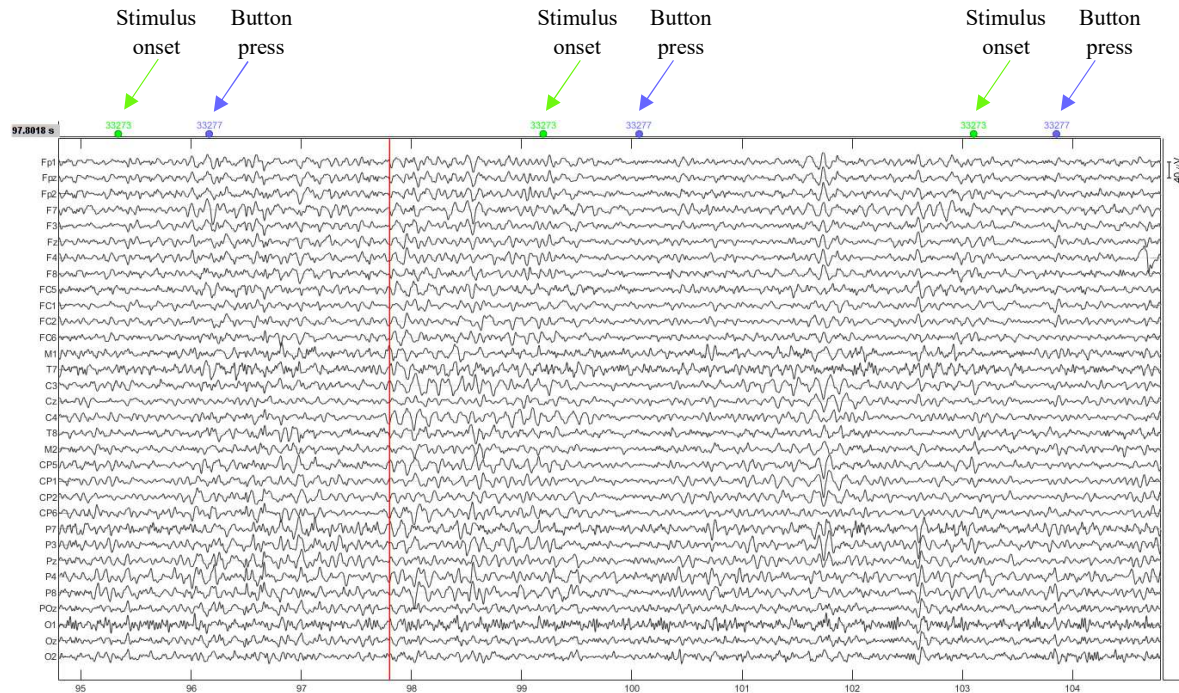


**Figure 0.8.** Digital triggers are sent between E-prime software and the EEG acquisition system in order to mark stimulus onset and response events

### 3.3.3 Demographic characteristics and clinical scores

26 subjects participated in the study. Their demographical characteristics and cognitive scores are shown in (table 3.1). As the two groups have a different sample size, we used the Wilcoxon test to examine whether there is a statistical difference between the two groups. Results show that AD group differs significantly from the control group, in terms of ACE-R score ( $p=0.001$ ), attention score ( $p=0.004$ ), memory score ( $p=0.001$ ), MMSE score ( $p=0.0007$ ), language ( $p=0.004$ ), visuospatial ( $p=0.008$ ) and fluency ( $p=0.001$ ). The neuropsychological scores of participants of both groups are illustrated in (Fig. 3.9).

N = 26	AD Mean (SD)	Control Mean (SD)	At risk Mean (SD)
<b>Demographic</b>			
n (%)	11 (42.69)	13 (50)	2 (7.69)
Age (y)	80.18 (7.26)	61.92 (5.99)	59 (0)
Sex (% male)	27.27	69.23	0
Handedness (% right)	100	100	100
<b>Cognition</b>			
ACE_R (/100)	40.64 (19.04)	88.31 (5.99)	85.5 (6.36)
MMSE (/30)	12.82 (6.60)	28.61 (1.45)	28 (1.41)
Attention/orientation (/18)	7.91 (3.88)	17.92 (0.28)	17.5 (0.71)
Memory (/26)	6.64 (5.61)	21.85 (2.58)	25 (1.41)
Fluency (/14)	3 (2.19)	9.31 (1.79)	7.5 (3.54)
Language (/26)	16.64 (5.03)	24.08 (1.32)	22.5 (2.12)
Visuospatial abilities (/16)	66.45 (4.16)	15.15 (1.41)	13 (2.83)

**Table 0.1.** Demographic characteristics and clinical score.

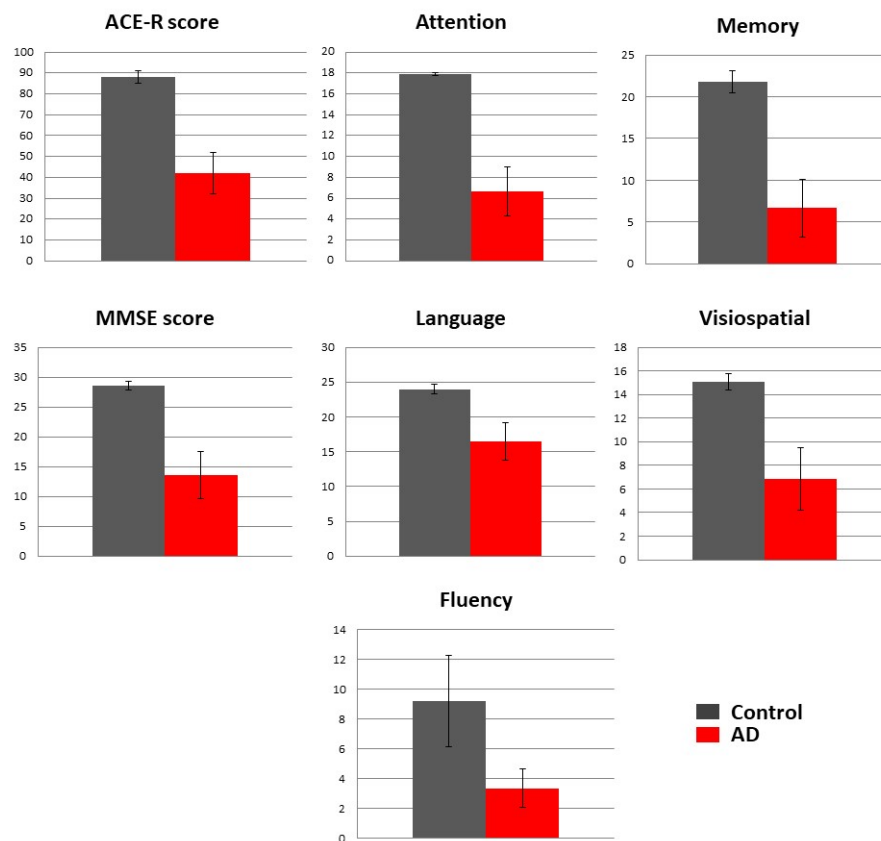


**Figure 0.9.** The clinical scores of AD patients and healthy controls. Wilcoxon test was used to examine whether there is a statistical difference between the two groups.

### 3.4 EEG Pre-processing

Once the data is collected, it must be pre-processed. EEG signals are usually contaminated by several artifacts and noise sources that may introduce undesired changes in the measurements and affect the signal of interest ([Urigüen & Garcia-Zapirain, 2015](#)). Thus, the cancellation of artifacts sources is a prerequisite for the subsequent analysis to be reliable ([Urigüen & Garcia-Zapirain, 2015](#)). While the best way of dealing with artifacts is “prevention” (i.e. avoid artifacts occurrence) ([Kirkove et al., 2014](#)), it seems to be unachievable. Therefore, pre-processing techniques and denoising methods are needed.

We will present hereafter an overview of the different artifact sources causing the deformation of the signal of interest, then, detail the pre-processing steps we have performed.

#### 3.4.1 EEG artifacts overview

EEG artifacts can be classified into two categories: physiological and non-physiological artifacts ([Kirkove et al., 2014](#); [Urigüen & Garcia-Zapirain, 2015](#)). Physiological artifacts are induced by the body of the subject body, while non-physiological artifacts originate from the recording environment and equipment.

##### 3.4.1.1 Physiological artifacts

###### 3.4.1.1.1 Ocular artifacts

Ocular artifacts are a major source of contamination in EEG signals. They are caused by eyeballs and eyelids movements ([Kirkove et al., 2014](#)). They include eye blink (Fig. 3.10), eye flutter (Fig. 3.11), lateral gaze (Fig. 3.12), slow/roving eye movements, lateral rectus spike.

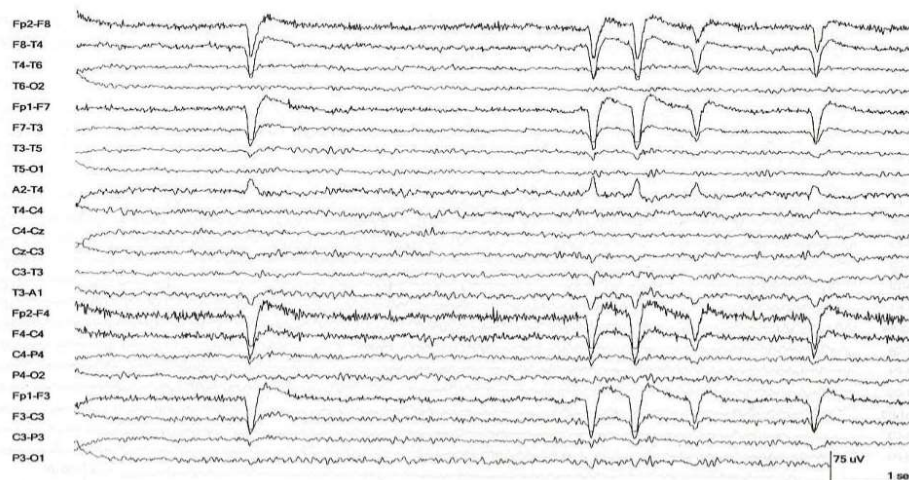
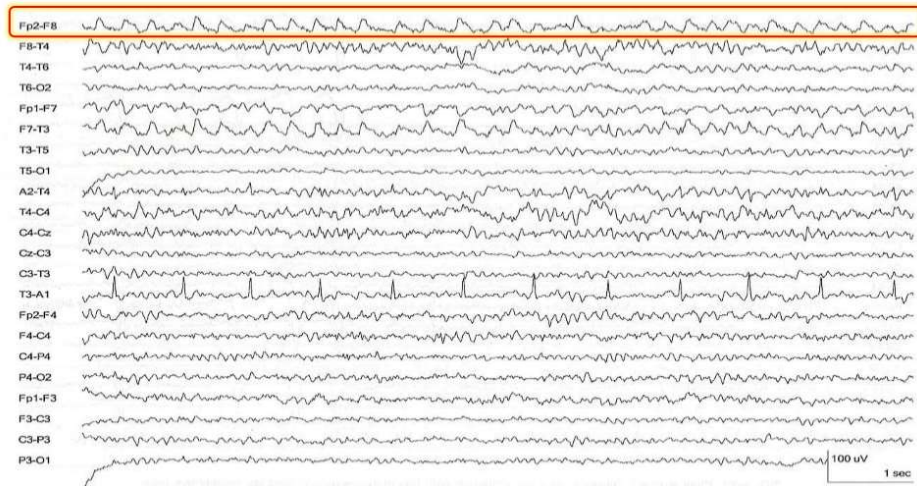
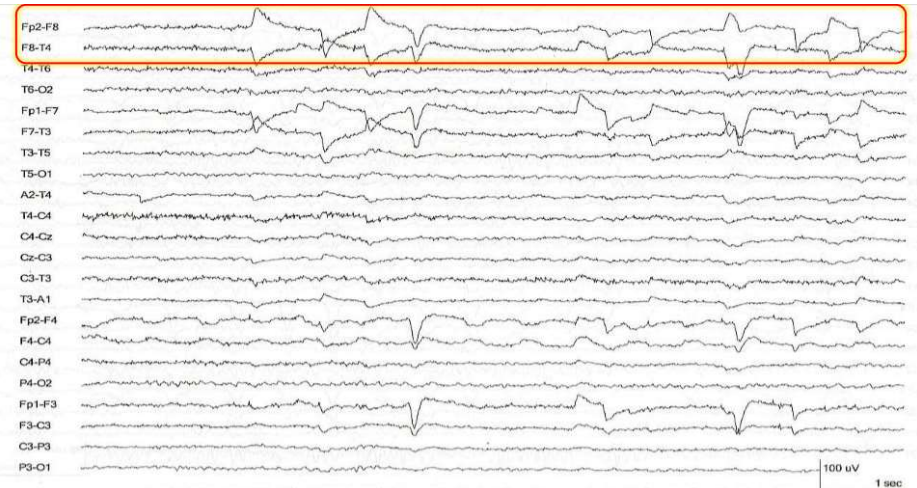


Figure 0.10. Eye Blink artifacts ([Marella, 2012](#)).



**Figure 0.11.** Eye flutter artifacts (Marella, 2012).



**Figure 0.12.** Lateral eye movements (Marella, 2012).

### 3.4.1.1.2 Muscle artifacts

Generally, the potentials generated in the muscles are of shorter duration than those generated in the brain. Thus, muscle artifacts (myogenic activity) can be identified easily on the basis of duration, morphology, and frequency. They may occur when the subject chew, swallow, talk, move, etc... (Urigüen & Garcia-Zapirain, 2015). Due to their high frequency and amplitude, they obscure EEG activity (Marella, 2012). (Fig. 3.13, Fig. 3.14).

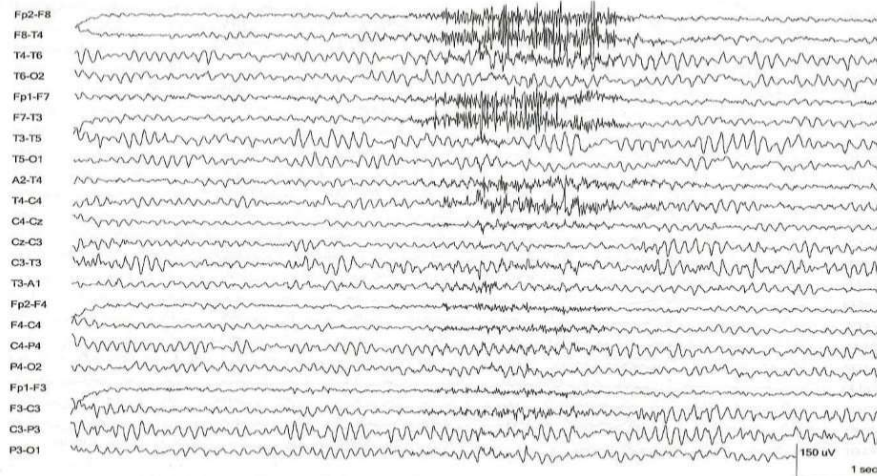


**Figure 0.13.** Muscle artifacts due to facial muscle contraction ([Marella, 2012](#)).

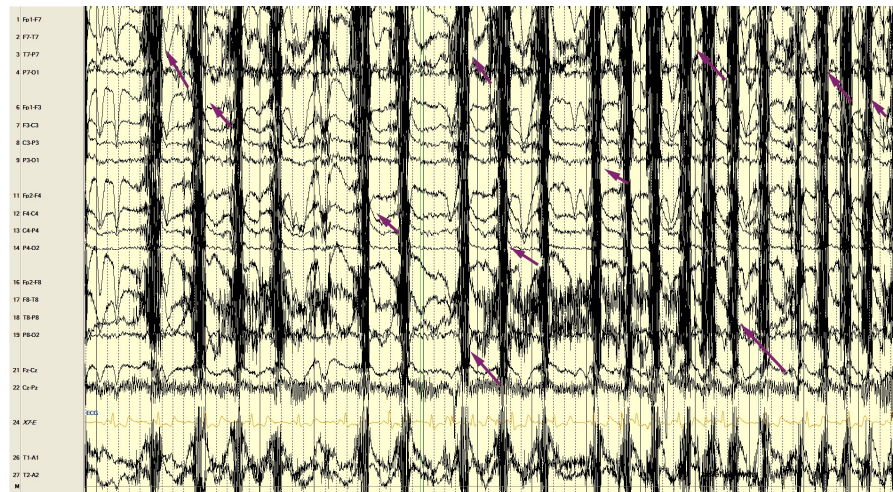


**Figure 0.14.** Chewing artifacts  
(<https://learningcentral.health.unm.edu/learning/user/onlineaccess/CE/eeg/artifacts/index.html>).

### 3.4.1.1.3 Cardiac activity

Cardiac activity may be picked up by EEG electrodes resulting in the contamination of EEG signals. Electrocardiogram (ECG) artifact is recognized easily by its rhythmicity/regularity and coincidence with the ECG tracing (Fig. 3.15). A pulse artifact appears when an electrode rests over a pulsating vessel generating slow periodic waves that may resemble EEG activity ([Urigüen & Garcia-Zapirain, 2015](#)). It occurs usually 200-300 ms following the ECG QRS complex (Fig. 3.16).

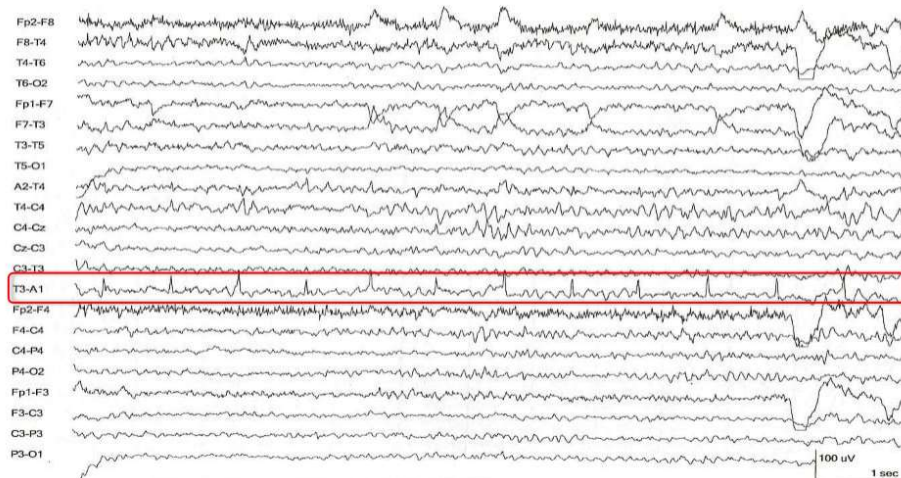


**Figure 0.15.** Cardiac activity artifacts ([Marella, 2012](#)).

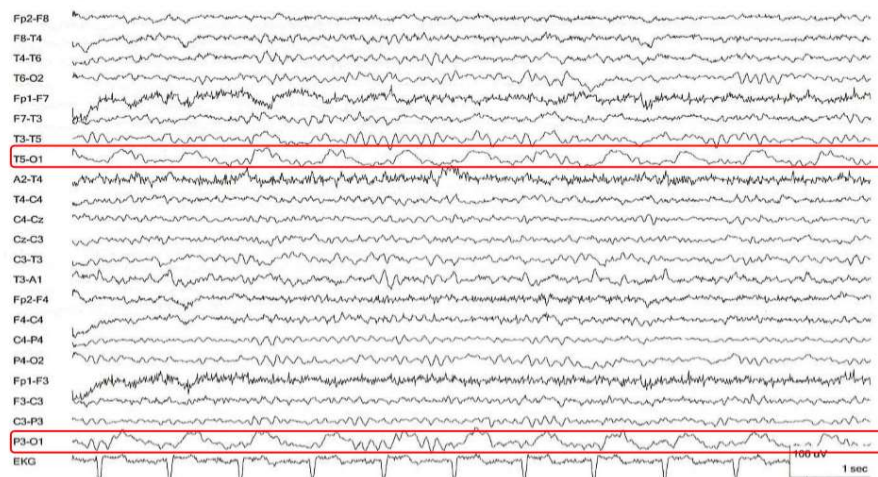


**Figure 0.16.** Pulse artifact ([Marella, 2012](#)).

#### 3.4.1.1.4 Less common physiological artifacts

Other physiological artifacts may lead to the distortion of EEG signals, including perspiration artifacts, chest movement, tongue movement, dental restorations with dissimilar metals, etc... ([Urigüen & Garcia-Zapirain, 2015](#)).

#### 3.4.1.2 Non-Physiological artifacts

##### 3.4.1.2.1 Power Line artifacts

The most common external EEG artifact is due to the interference with the 50Hz/60Hz line power, more likely to be picked up by faulty electrodes (Fig. 3.17).

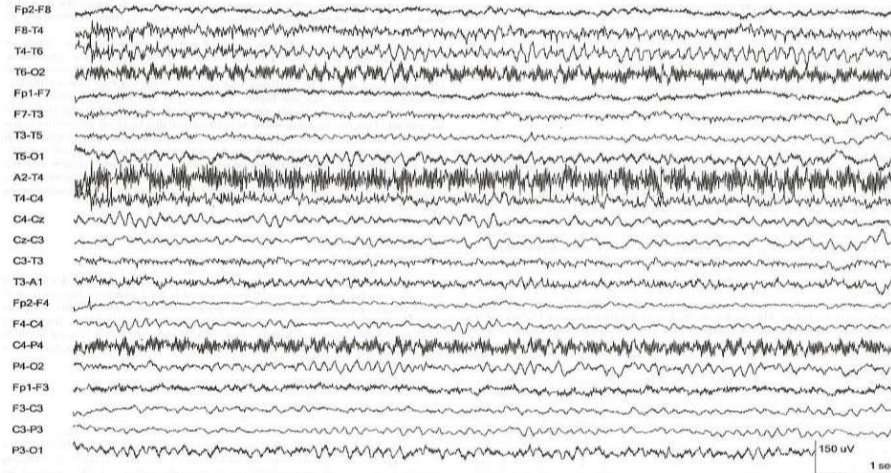


**Figure 0.17.** Line power artifact (Marella, 2012).

### 3.4.1.2.2 Electronic devices artifacts

Electrical equipment may also cause interference resulting in artifactual measurements. Interference from a laptop or cell phone charger, for example, appear as black solid lines in one or a few channels (Fig. 3.18).

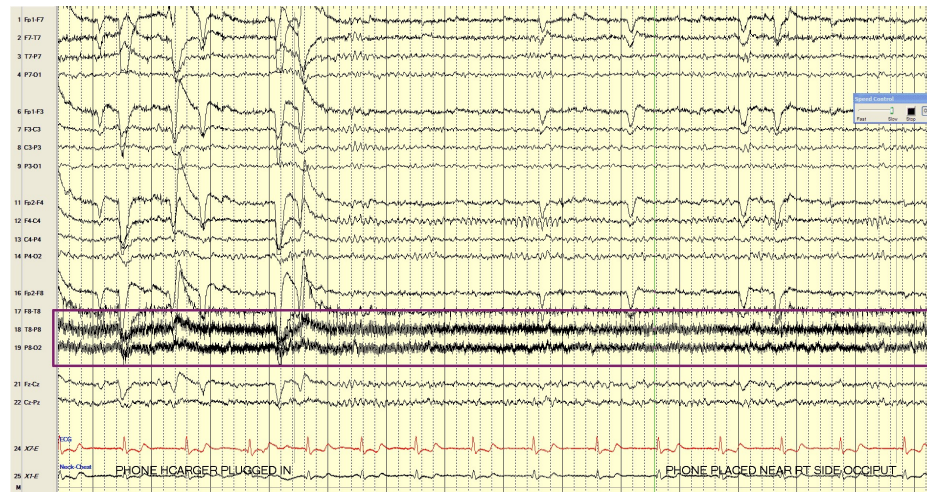


**Figure 0.18.** Cellphone charger artifact  
<https://learningcentral.health.umm.edu/learning/user/onlineaccess/CE/eeg/artifacts/index.html>

### 3.4.1.2.3 Electrodes artifacts

Electrode artifacts usually manifest either as brief transients limited to one electrode, or low-frequency rhythms across a scalp region. The most common electrode artifact is the electrode popping. It has a characteristic morphology of a nearly vertical rise followed by a slower fall (Fig. 3.19). Poor electrode contact or lead movement produces artifact with a less conserved morphology than electrode pop. Poor contact produces instability in the impedance, which leads to sharp or slow waves of varying morphology and amplitude (Fig. 3.20 – Fig. 3.21)

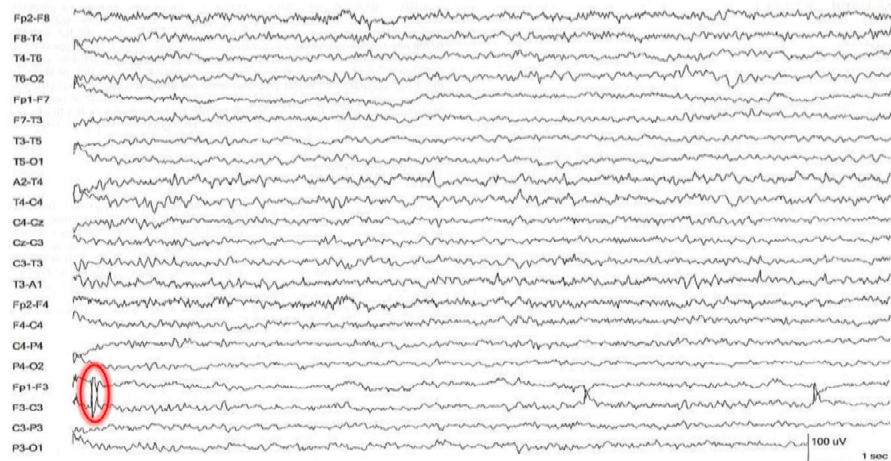


**Figure 0.19.** Electrode pop artifact (Marella, 2012).

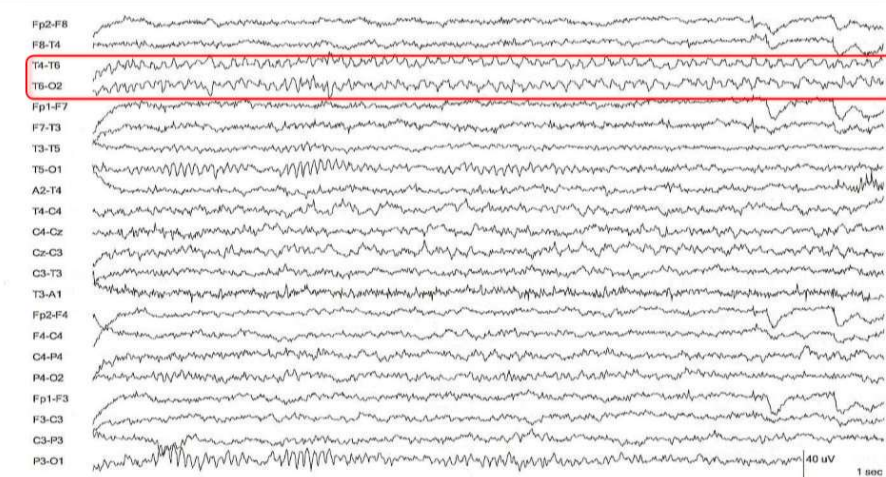


**Figure 0.20.** Electrode movement artifact (Marella, 2012).

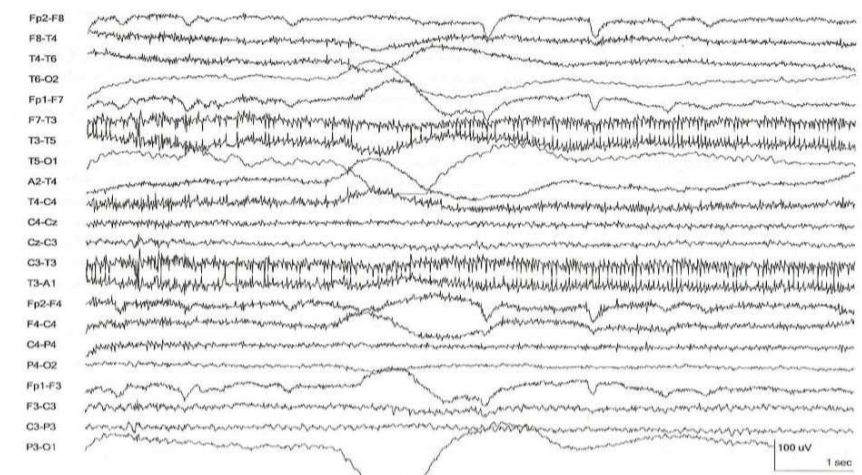


**Figure 0.21.** Lead movement artifact (Marella, 2012).

### **3.4.2 Signal pre-processing**

In order to prevent signals contamination, cell phones were turned off during acquisition session, laptop charger unplugged, air-conditioner turned off.

Data pre-processing was done using brainstorm ([Tadel et al., 2011](#)) and some written MATLAB codes. In the following, we state the different pre-processing steps we have adopted.

#### **3.4.2.1 Band-pass filtering**

Raw signals were band-pass filtered between 3 and 45 Hz (Fig. 3.22). If the frequency band of interest includes the 50 Hz frequency, a notch filter is needed to eliminate power line artifact.

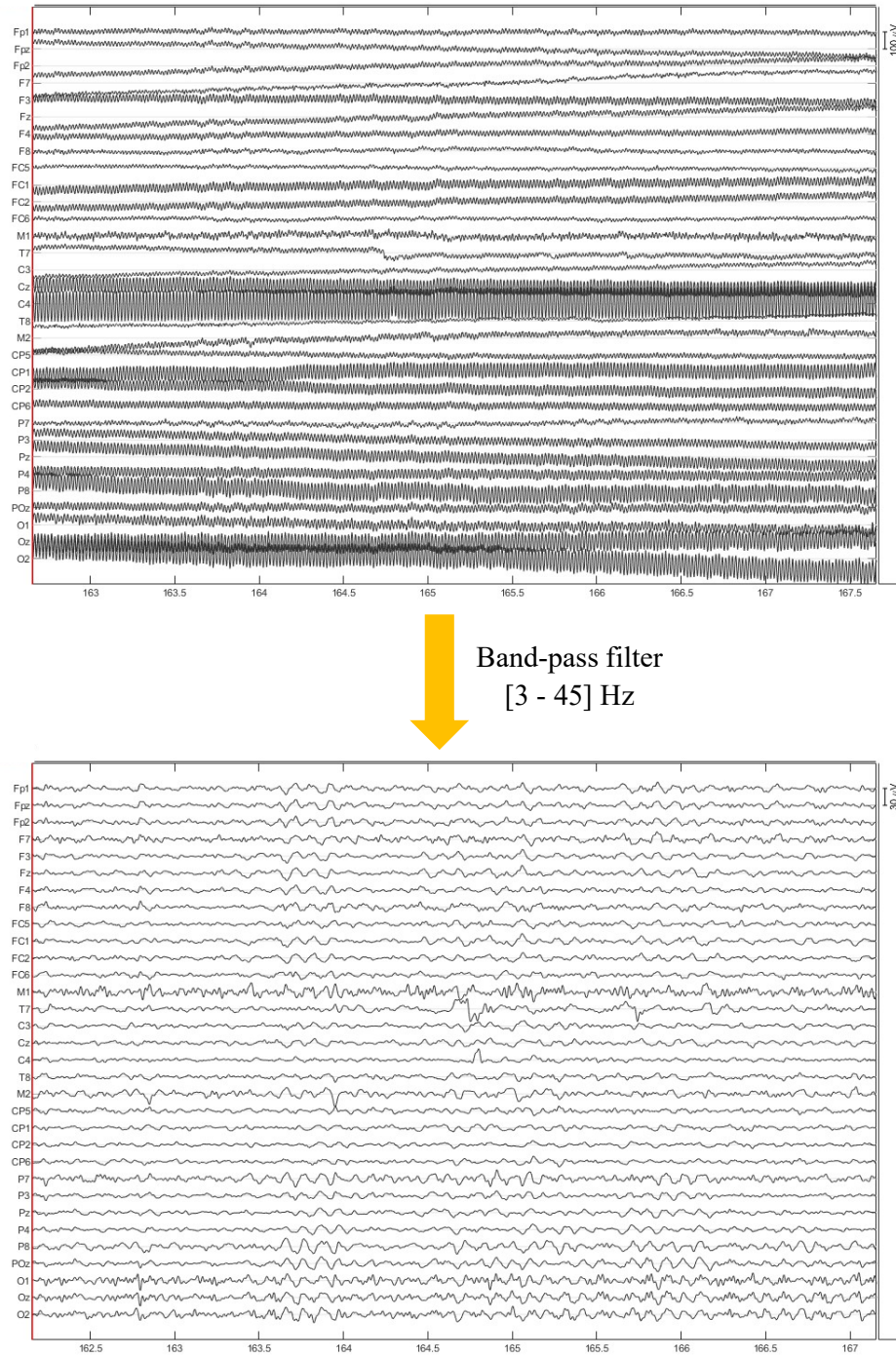


**Figure 0.22.** Band-pass filtering of raw signals.

### 3.4.2.2 Eye blinks removal

Ocular artifacts rejection methods are mainly regression- and blind source separation (BSS)-based methods ([Klados et al., 2011](#)).

Regression-based methods are characterized by their reduced computational cost and the need for one or more reference channel (horizontal and vertical electrooculogram (HEOG, VEOG) channels recording ocular activity). Assuming that recorded signals are a linear mixture of cerebral activity and noise signals, EEG denoising is done by subtracting a regressed portion of each reference channel from the contaminated EEG ([Urigüen & Garcia-Zapirain, 2015](#)). (See ([Croft & Barry, 2000](#); [Gratton et al., 1983](#)) for EEG correction methods).

Although the regression-based method for ocular artifact rejection is methodologically simple, its use is limited by the existence of EOG recording channels. Thus, alternative artifacts rejection techniques exploiting recorded EEG data only are needed. Many researchers have used the principal component analysis (PCA) ([Fitzgibbon et al., 2017](#); [Ille et al., 2002](#); [Lagerlund et al., 1997](#)). PCA, also known as the discrete Karhunen–Loëve transform, aims at de-correlating signal sources in EEG. It uses an orthogonal transformation to convert possibly correlated variables into linearly uncorrelated variables called principal components, less than or equal in number to the original variables ([Urigüen & Garcia-Zapirain, 2015](#)). However, the orthogonality assumption doesn't always hold in EEG data ([Joyce et al., 2004](#)) which is the main criticism of this method. On another hand, independent component analysis (ICA), a BSS technique that assumes statistical independence of the source signals, has gained a lot of success since artifacts and brain activity are usually sufficiently independent ([Urigüen & Garcia-Zapirain, 2015](#)). Most used ICA algorithms exploit higher-order statistics of the signals ([Bell & Sejnowski, 1995](#); [Comon, 1994](#); [Hyvärinen & Oja, 1997](#); [James & Hesse, 2005](#)).

The instantaneous mixture model of ICA procedure is shown in (eq. 4.1). Measurements at the sensors,  $x(t)$ , are assumed to be composed of a linear mixture of the independent sources,  $s(t)$ . ICA produces an unmixing matrix  $W$ , which unmixes the measurements to give estimates of the independent sources  $\hat{s}(t)$  ([James & Hesse, 2005](#)).

$$x(t) = As(t) \rightarrow \hat{s}(t) = Wx(t) , \quad W = \text{inv}(A) \quad (4.1)$$

Where  $A$  is the mixing matrix, and  $W$  its inverse.

Artifacts related components were inspected visually and removed (Fig. 3.23).

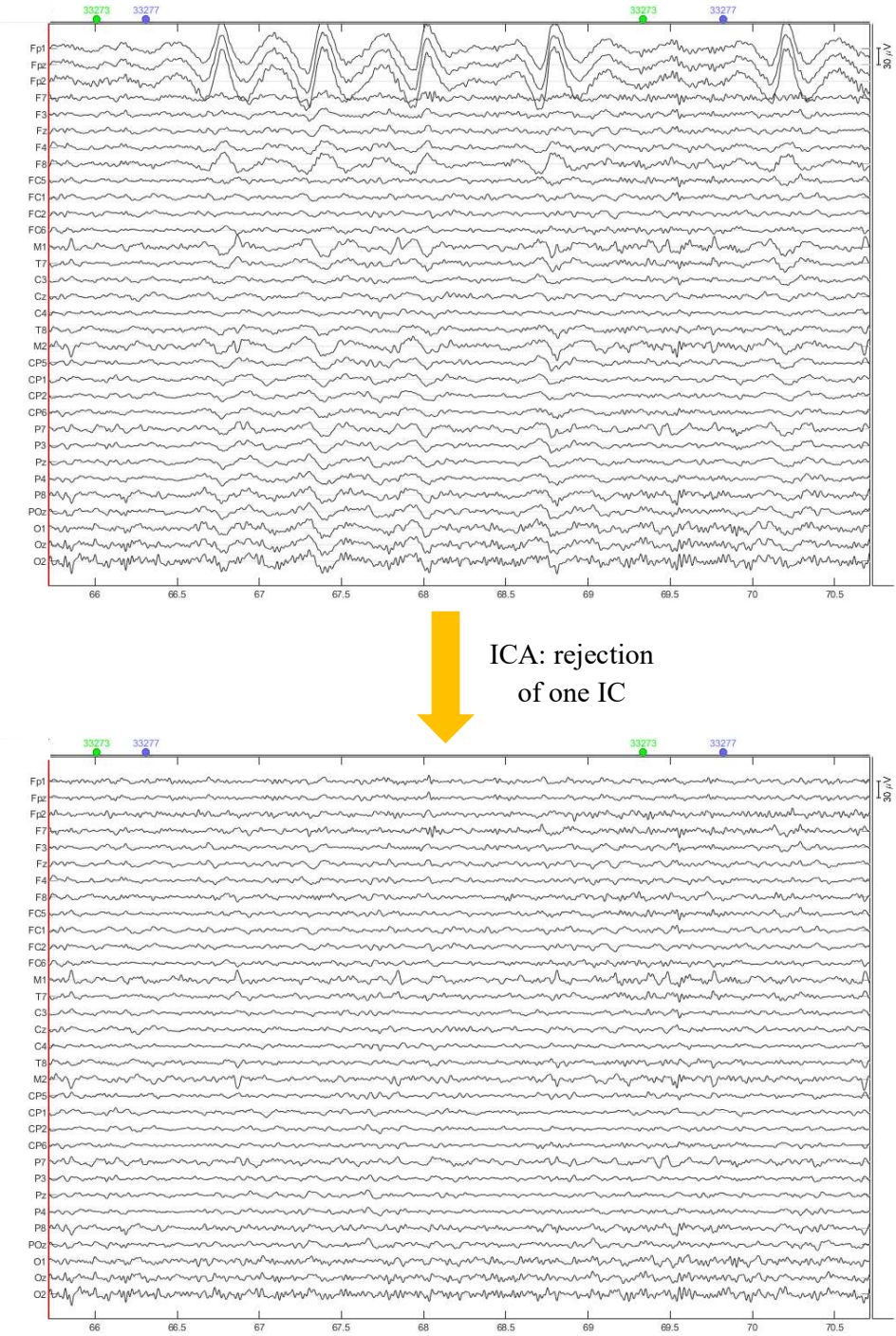


**Figure 0.23.** Eye-blink removal via ICA.

### 3.4.2.3 Epochs extraction

In the picture naming task, epochs length was 1000 ms starting 200ms before the picture onset (Fig. 3.24).

In the button press task, epochs were extracted at two different instants based on the analysis to perform later. 1000ms epochs starting 200ms before the stimulus onset (Fig. 3.24), and 1600ms epochs centered at the button press events were extracted.

In the resting state data, for each participant, three epochs of 40s lengths were selected. This epoch length is chosen based on the intended later analysis. It was largely used previously and is considered as a good compromise between the needed temporal resolution and the reproducibility of the results ([Kabbara et al., 2017](#)).

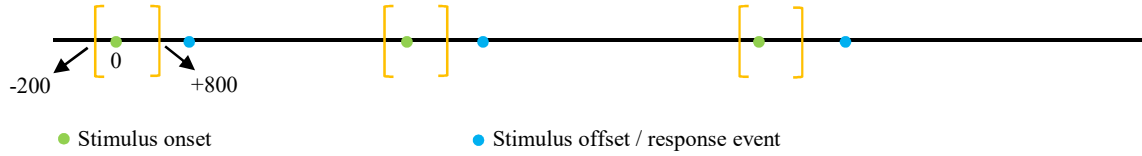


**Figure 0.24.** Epochs extraction.

#### 3.4.2.4 Bad channels interpolation

In each epoch, channels displaying signals that are completely flat, contaminated with movements artifact, or oscillating at high amplitudes were interpolated. Corrected channels were computed by averaging neighboring channels activity (Fig. 3.25). An epoch with more than 15% of its channels (i.e. more than four channels in our case) interpolated is rejected. In addition, trials corresponding to wrong answers in the picture naming task were discarded for the subsequent analysis.

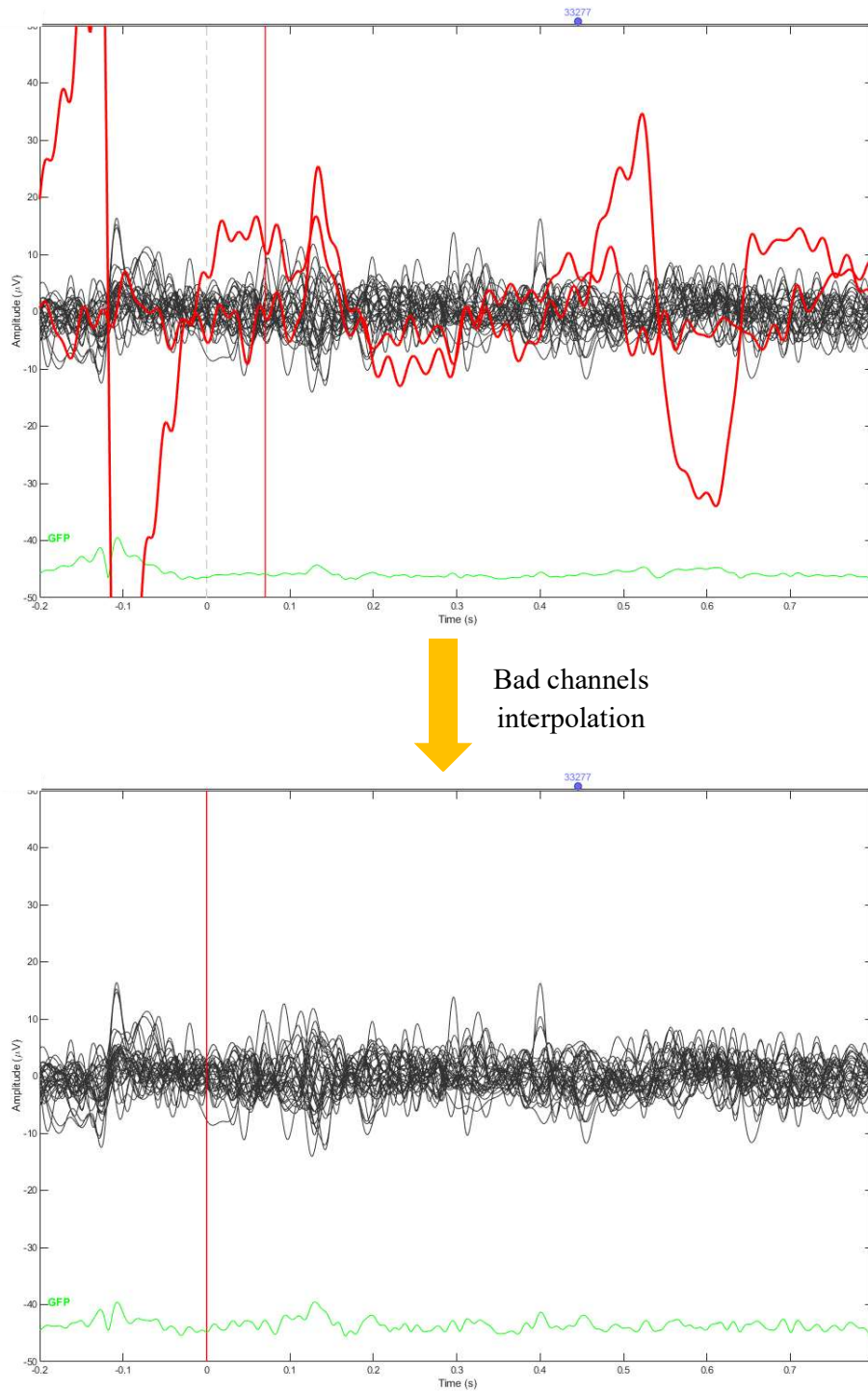


**Figure 0.25.** Bad channels interpolation.

### 3.4.3 Pre-processing results

The number of subjects in each group and the average number of trials per subjects following the pre-processing procedure are given in (table 3.2).

	nb. of AD patients (nb. of trials/subj.)	nb. of healthy controls (avg. nb. of trials/subj)	nb. of subjects at risk (avg. nb. of trials/subj)
Resting state	10 (3)	13 (3)	2 (3)
Picture naming	9 (19)	13 (56)	2 (39)
Button press	10 (20)	12 (30)	2 (32)

**Table 0.2.** The number of subjects in each group and the average number of trials per subjects following the pre-processing procedure. \*Number: nb., average: avg., subject: subj.

## 3.5 Conclusion

Once the pre-processing of data is finished, we can start analyzing it. We will present, in the next chapter, a preliminary analysis investigating the voltage topography differences between AD patients and healthy controls while performing a button press task.

# **Chapter 4.**

## **A COMPARATIVE STUDY: STATIC VS DYNAMIC ANALYSIS**

### **4.1 Introduction**

This chapter presents a comparative study of the feasibility of both static and dynamic analysis in detecting differences between AD patients (mild to moderate stage) and healthy elderly subjects using EEG. Group-level statistics were used to test for significant differences between the two groups. Data from the button press task, bandpass filtered in beta band, were used in the subsequent analysis.

The following section will test the normality of the data (Sec. 4.2) before performing the statistical testing (Sec. 4.3). Results are reported in (Sec. 4.4), then discussed in (Sec. 4.5). finally, the limitations of the present study are listed in (Sec. 4.6).

### **4.2 Normality test**

An assessment of the normality of data is a prerequisite for statistical tests. Therefore, we applied Shapiro-Wilk test. The null-hypothesis of the Shapiro–Wilk test is that the population is normally distributed. Thus, on the one hand, if the  $p$ -value is less than the chosen alpha level, then the null hypothesis is rejected and there is evidence that the data tested are not normally distributed. On the other hand, if the  $p$ -value is greater than the chosen alpha level, then the null hypothesis that the data came from a normally distributed population cannot be rejected.

Brainstorm ([Tadel et al., 2011](#)) offers the possibility of testing the normality of the data based on the Shapiro-Wilk test. Results are shown in (Fig. 5.1) The null hypothesis was rejected; the data are not normally distributed.

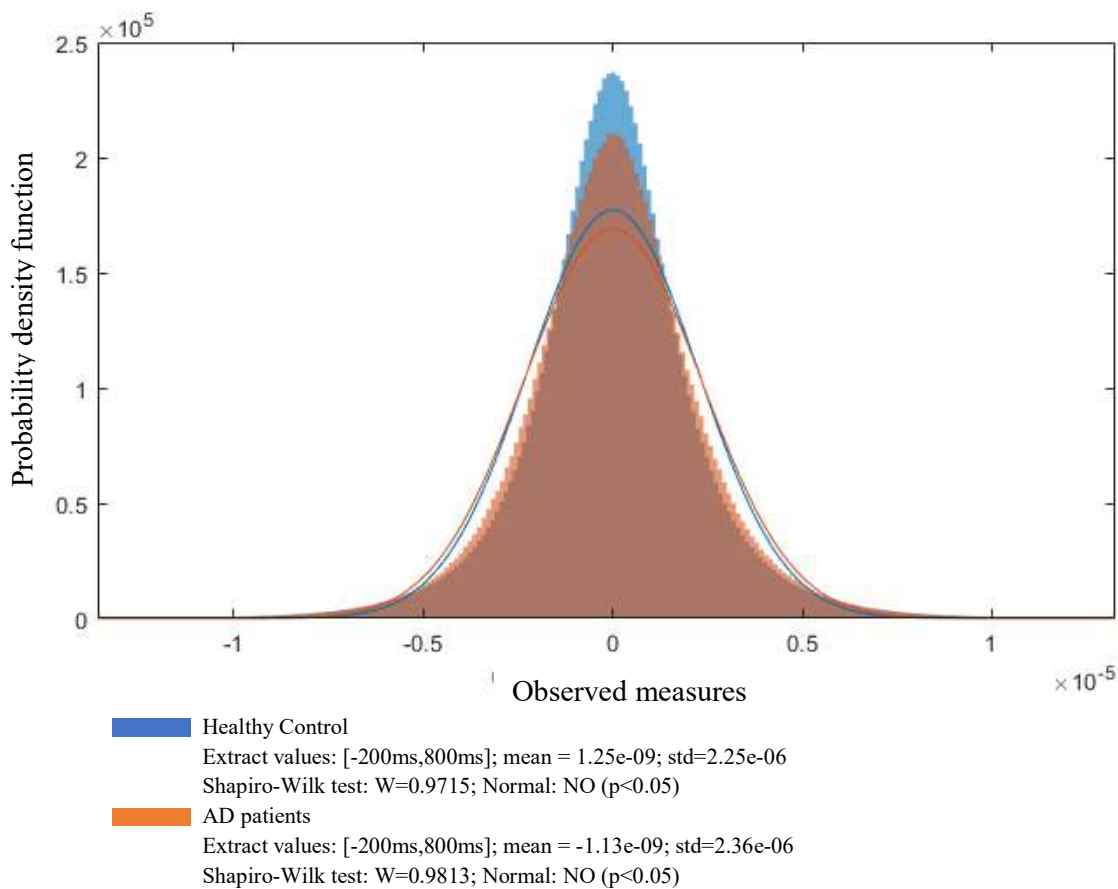


**Figure 0.1.** Shapiro-Wilk test results

### 4.3 Statistical test

As data were not normally distributed, a non-parametric equivalent of the two-tailed Student's t-test was performed in order to investigate the regional differences in voltage distribution between AD and controls. The *t*-test is used to determine whether there exists a significant difference between the means of two datasets. It is a parametric test assuming that the data follow a normal distribution. However, its equivalent non-parametric test, also called distribution-free test, doesn't assume that the data follow a specific distribution. The statistical test was corrected for multiple comparisons using Bonferroni method ( $p_{\text{Bonferroni adjusted}} < 0.05/N$ , with N (32) denotes the number of channels).

Two analysis approaches were performed. In the static analysis, we averaged the brain activity over the entire epoch length. This leads to a unique topographic map for each trial. In the dynamic analysis, the statistical test was performed at each millisecond.

### 4.4 Results

While the static analysis didn't reveal any significant difference between the AD and controls, the dynamic analysis indicated between-groups differences in 18 out of 32 channels during the first 200 ms following stimulus onset. (Fig. 4.2) shows the 2D topographical distribution of

significant t-values. The maps are based on 32 EEG electrodes placed according to the 10-20 international system. Positive t-values (red) correspond to a significantly greater mean of healthy controls group. Negative t-values (blue) correspond to a significantly greater mean of AD group. Sensors having p-values ( $p>0.05$ ) are set to zero.

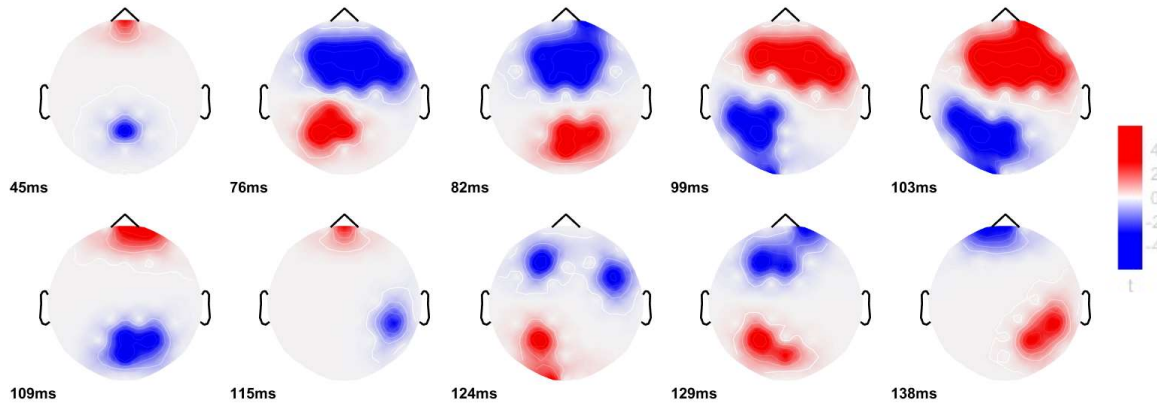


**Figure 0.2.** 2D topography showing significant t-values resulting from the Student t-test (Bonferroni corrected,  $p<0.05$ ) applied on EEG data recorded from AD and healthy controls.

(Fig. 4.2) shows that no single region maintained a constant t-value across all epoch duration. A region may show alternating, positive, negative, and null t-values at different time moments. In particular, results show higher activity of central regions in AD compared to controls at  $t = [99, 103, 115]$  ms. In contrast, healthy controls show higher activity in central regions at  $t = [76, 138]$  ms. Differences in the pre-frontal regions were observed at  $t = 45$  ms (control>AD), 82 ms (AD>control), 103 ms (control>AD), 109ms (control>AD), 115 ms (control>AD), 129 ms (AD>control), 138 ms (AD>Control). Frontal regions showed higher activity in AD at  $t = [76, 82, 124, 129]$  ms, and in healthy controls at  $t = [99, 103]$  ms. Activity in parietal regions was opposed in most cases to the frontal and pre-frontal activity. Higher parietal activity was detected at  $t = [45, 99, 103, 109]$  ms in AD, and at  $t = [76, 82, 124, 129]$  ms in healthy controls. Occipital region showed a higher activity in AD at  $t = 103$  and  $t = 109$  ms, and in Controls at  $t = 82$  ms,  $t = 109$  ms, and  $t = 124$  ms.

## 4.5 Discussion

The main objective of this preliminary study is to highlight the necessity of adopting a dynamic analysis when exploring brain activity differences between AD and controls. Static analyses, characterizing data with a single parameter over all the recording duration, may hide significant activities occurring at fast timescales. Thus, it is of great importance to track spatiotemporal brain dynamics at a millisecond timescale. Using non-parametric t-test analyses, we were able to detect significant differences between EEG signals recorded from AD subjects and healthy controls while performing a button pressing motor task. Differences in beta band appeared in different brain areas, at distinct time instants during the first 200 ms following stimulus onset. On the other hand, static analysis showed no difference between the means of the two groups, stating a similar response from AD and healthy controls while performing the motor task. Importantly, several studies demonstrated the existence of motor dysfunction in AD ([Albers et al., 2015](#); [Vidoni et al., 2012](#)). ([Vidoni et al., 2012](#)) showed greater activation in supplementary

motor area, and premotor cortex, commonly associated with motor preparation and motor planning in healthy elderly controls. Other studies investigating motor cortex function using transcranial magnetic stimulation, revealed early loss of intracortical inhibition of the motor cortex and increased motor cortex excitability (Ferreri et al., 2003; Lipert et al., 2001; Pepin et al., 1999). Therefore, assuming no differences between AD and healthy controls voltage topologies while performing a motor task, based on the results of the static analysis is to be criticized. In our study, the dynamic analysis showed that differences obtained between AD and control groups were not limited to the central regions, but were also observed in occipital regions (linked mainly to the visual processing) and the frontal regions (linked to the decision making). These observations may be explained by the fact that in the paradigm performed, the participant should visually process the stimulus picture, and then take a decision to press the button. Overall, our findings demonstrate the advantage of dynamic analysis compared to static analysis while investigating electrical potential differences between AD and controls.

## 4.6 Limitations

In the above study, we only performed a group-level analysis. While this type of analysis provides an overall understanding of the difference between AD and control groups, a subject-level analysis may afford additional information.

One of the main limitations of this study is that it is performed at the sensor level. In fact, scalp EEG signals are usually corrupted by the volume conduction problem (Hassan & Wendling, 2018; Schoffelen & Gross, 2009). In addition, as AD is now considered as network disease (Canuet et al., 2012; Crossley et al., 2014; Fornito et al., 2015; Kabbara et al., 2018), it is not sufficient to investigate regional alterations associated with the disease. It will be interesting to investigate the functional alterations in the brain networks of AD patients.

## 4.7 Conclusion

We reported in this study differences in scalp voltage topographies between AD and healthy controls during a motor task. We demonstrated that static analysis does not provide a reliable representation of underlying neuronal activity. In contrast, the dynamic analysis succeeded to track temporal dynamics of brain activity occurring at fast timescales. This work was submitted to the fifth International Conference on Advances in Biomedical Engineering (ICABME19).

In the next chapter, we will introduce the notion of brain networks and proceed into a more sophisticated characterization of the differences between the two groups of the study.

# Chapter 5.

## BRAIN NETWORK ANALYSIS

### 5.1 Introduction

Emerging evidence shows that the human brain can be conceptualized as a highly complex, yet highly organized network (Bassett & Sporns, 2017; Fornito et al., 2016; Sporns, 2014). Importantly, brain disorders are thought to alter the organization of brain networks, disrupting communication between distributed brain regions (Crossley et al., 2014; Fornito et al., 2015; Sporns et al., 2005).

In this chapter, we will present an overview of network neuroscience (Sec. 5.2, 5.3). We will then proceed into the mathematical details of brain network reconstruction, and functional connectivity assessment (Sec. 5.4 to 5.6). Finally, a network analysis is conducted in the aim to characterize AD brain networks (Sec. 5.7 to 5.10).

### 5.2 The human brain: a complex network

With more than 100 billion ( $10^{11}$ ) neurons and 100 trillion ( $10^{14}$ ) synapses, the human brain is considered the most complex system in the known universe (Fornito et al., 2016). It represents a puzzling and challenging paradox that can be summarized in the many-to-one function-structure relationship: Despite a fixed anatomy, the brain is capable of reconfiguring connections between distributed neuronal assemblies enabling action, perception, and cognition (Park & Friston, 2013). Brain functions depend on the extraordinary complex, yet highly organized communication between different brain regions (Braun et al., 2018; Medaglia et al., 2015; Sporns, 2014).

Mathematically, complex systems can be studied through network science concepts (Avena-Koenigsberger et al., 2018; Bullmore & Sporns, 2009). The human brain, thus, can be modeled by a complex graph or network (Bassett & Sporns, 2017; Fornito et al., 2016; Sporns, 2014). A graph is composed by: 1) a set of nodes (vertices) representing neural elements ranging from a single synapse, a neuron, a neuronal population or an entire brain region, and 2) a set of edges representing the nodes pairwise connections (Avena-Koenigsberger et al., 2018) (Fig. 5.1).

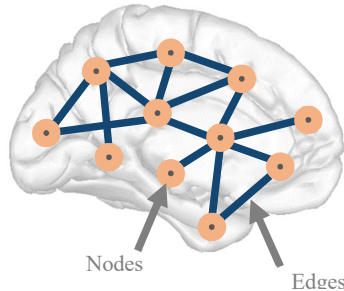


**Figure 0.1.** The human brain can be visualized as a network.

A brain network edge can be defined by either structural, functional, or effective connectivity (Park & Friston, 2013). Structural connectivity represents anatomical links (Park & Friston, 2013), that is, the set of physical or structural (synaptic) connections linking neuronal units at a given time (Sporns et al., 2004). It can be assessed using diffusion MRI (Basser et al., 1994)(Basser 1994) (Fig. 5.2.A). On another hand, functional connectivity does not necessarily coincide with direct neuronal communication. It expresses the statistical dependencies between neuronal units, without explicit reference to causal effects (Sporns et al., 2004). It can be inferred from BOLD signal, or MEG/EEG data, and results in undirected networks (Park & Friston, 2013) (Fig. 5.2.B). Effective connectivity describes the causal effects between neuronal assemblies (Sporns et al., 2004). It refers to the influence that one neural system exerts over another, either at a synaptic or population level (Friston, 2011). It is inferred by using a model of neuronal integration and estimating the model parameters (effective connectivity) that best explain observed BOLD or EEG/MEG signals (Park & Friston, 2013). (See (Friston, 2011) for a review of functional and effective connectivity) (Fig. 5.2.C).

Our study investigates functional brain networks inferred from EEG data.

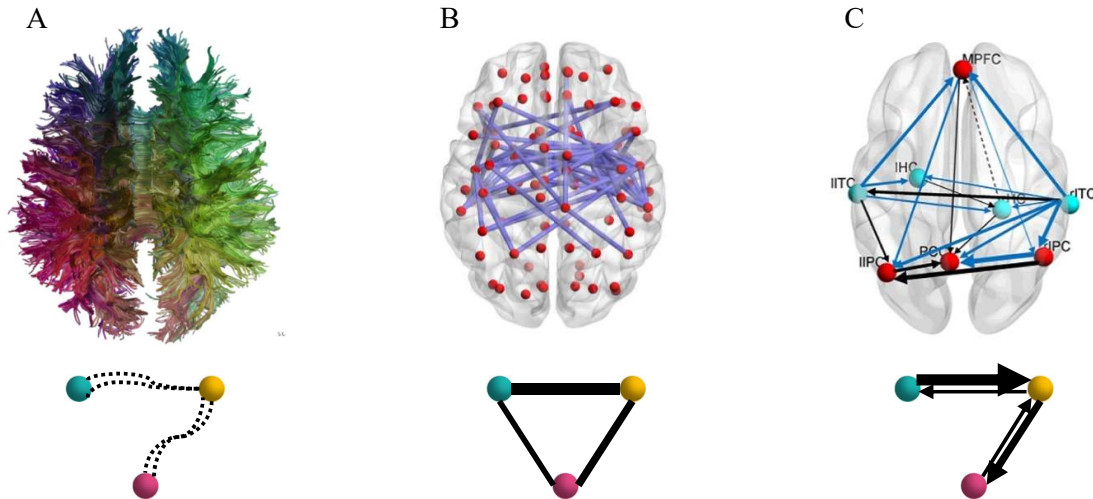


**Figure 0.2.** Structural brain network (connectome) (Park & Friston, 2013). B) Functional brain network(Hong et al., 2013). C) Effective brain network (Wu et al., 2014).

### 5.3 Network diseases

The concept of brain network has led to a new understanding of clinical brain disorders (Crossley et al., 2014). Brain diseases are now seen as network diseases suggesting disrupted communication (i.e. functional connectivity) between distributed brain regions (Crossley et al., 2014; Fornito et al., 2015; Sporns et al., 2005) (Fig. 5.3). In (Crossley et al., 2014), 26 brain disorders, including AD, are reported as network diseases (table 5.1). Therefore, since cognitive deficits in AD are associated with disruptions in brain functional connectivity, the identification of those alterations has become a topic of increasing interest.

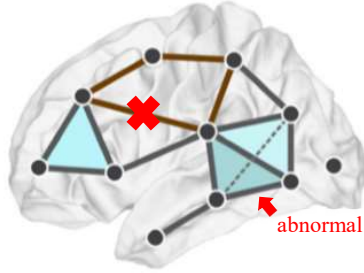


**Figure 0.3.** Functional alterations characterizing brain diseases (([Bassett & Sporns, 2017](#)), edited).

<b>Brain Disorders</b>
Amyotrophic lateral sclerosis
Dystonia
Developmental dyslexia
Anorexia nervosa
Obsessive-compulsive disorder
Parkinson's disease
Hereditary ataxia
Dementia in Parkinson's
Chronic pain
Panic disorder
Attention deficit hyperactivity disorder
Bipolar affective disorder
Multiple sclerosis
Frontotemporal dementia
Obstructive sleep apnea
Autism
Schizophrenia
Alzheimer's disease
Asperger syndrome
Huntington's disease
Depressive disorder
Right temporal lobe epilepsy
Post-traumatic stress disorder
Progressive supranuclear palsy
Left temporal lobe epilepsy
Juvenile myoclonic epilepsy

**Table 0.1.** List of brain network diseases ([Crossley et al., 2014](#)).

## 5.4 EEG scalp connectivity

Scalp connectivity refers to the assessment of statistical dependencies directly between recorded brain activity (i.e. at sensor level) (Fig. 5.4). It has been widely used to analyze brain networks ([Fraschini et al., 2015](#); [González et al., 2016](#); [Gupta et al., 2011](#); [Ponten et al., 2009](#); [Tsiaras et al., 2011](#); [Uhlhaas & Singer, 2006](#); [Vourkas et al., 2014](#)). However, its utility is limited due to field spread and volume conduction problem ([Brunner et al., 2016](#); [Schoffelen & Gross, 2009](#); [van de Steen et al., 2016](#)).

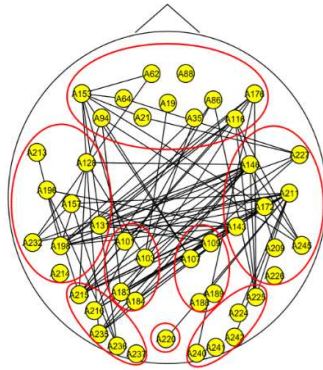


**Figure 0.4.** EEG scalp connectivity (Tsiaras et al., 2011).

## 5.5 Volume conduction and field spread

Due to the volume conduction properties of the head, the activity of a brain source is picked up by more than one sensor, resulting in a wide-representation of any source at the sensor level (Schoffelen & Gross, 2009) (Fig. 5.5). Each channel is reflecting a superposition of different activities arising from distinct cortical sources (Hassan & Wendling, 2018). This leads to spurious connectivity estimates, that is, statistical coupling computed at the sensor level does not reflect the actual connectivity between distributed brain regions (Hassan & Wendling, 2018; Nunez et al., 1997; Schoffelen & Gross, 2009).

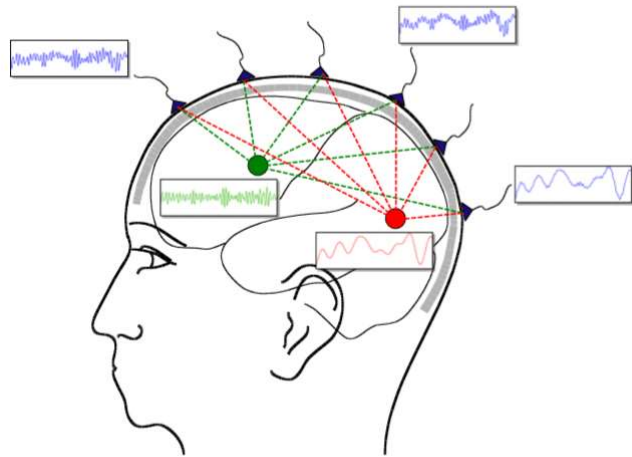


**Figure 0.5.** Field spread effect (Oostenveld et al., 2011).

## 5.6 EEG source connectivity

In order to reduce the volume conductor effects, an emerging method called “EEG source connectivity” has arisen (Hassan et al., 2015; Hassan et al., 2014; Hipp et al., 2012; Kabbara et al., 2017; Mehrkanoon et al., 2014; Pasquale et al., 2010). It consists of assessing connectivity between cortical sources rather than between recorded EEG channels.

It includes two main steps: 1) reconstructing the temporal dynamics of cortical sources by solving an inverse problem, 2) assessment of functional connectivity between reconstructed sources (Hassan & Wendling, 2018; A. Kabbara et al., 2017).

### 5.6.1 Source reconstruction

The reconstruction of regional time sources from scalp EEG signals was described in (Hassan et al., 2015, 2014; Hassan & Wendling, 2018; Kabbara et al., 2017).

According to the linear discrete equivalent dipole model, EEG signals  $X(t)$  recorded from Q channels ( $Q = 32$  in our case) can be expressed as a linear combination of P time-varying current dipole sources  $S(t)$ :

$$X(t) = G \cdot S(t) + N(t) \quad (5.1)$$

where  $G$  ( $Q \times P$ ) is the lead field matrix and  $N(t)$  is the additive noise.  $G$  reflects the contribution of each brain source to the sensors (Baillet et al., 2001). It is computed from a multiple layer head model (volume conduction) and from the position of the  $Q$  electrodes. Here we used the Boundary Element Method (BEM) as a numerical method to compute realistic head models. We computed the lead field matrix using OpenMEEG (Gramfort, Papadopoulou, Olivi, & Clerc, 2010).

The inverse problem consists of estimating the parameters of the dipolar sources  $\hat{S}(t)$  (notably the position, orientation, and magnitude). As this problem is ill-posed ( $P \gg Q$ ), physical and mathematical constraints have to be added to find a single solution among the many solutions that minimize the residual term in the fitting of measured EEG signals.

The source model, which provides information about the location and orientation of the dipole sources to be estimated, is computed from the segmentation of the anatomical MRI (template or subject-specific). Usually, the white/gray matter interface is chosen as the source space for the neocortical sources that mostly contribute to EEG. The MRI anatomy (the ICBM152 template in our case) and channel locations are co-registered using the same anatomical landmarks (the left and right preauricular points and the nasion) using Brainstorm (Tadel et al., 2011).

Using segmented MRI data, the source distributions can be constrained to a field of current dipoles homogeneously dispersed over the cortex and normal to the cortical surface. Precisely, in the source model, the electrical contribution of each macro-column to scalp electrodes can be represented by a current dipole located at the center of gravity of each triangle of the 3D mesh and oriented normally to the triangle surface. The EEG inverse problem is, therefore, reduced to the estimation of the source magnitude of:

$$\hat{S}(t) = W \cdot X(t) \quad (5.2)$$

Several algorithms have been proposed to solve this problem and estimate  $W$  based on different assumptions related to the spatiotemporal properties of the sources and regularization constraints (see (Baillet et al., 2001) for a review). Weighted Minimum Norm Estimate (wMNE) is one of the most popular approaches. Here,  $W$  is estimated in such a way as to produce the source distributions with the minimum power that fits the measurements in a least-square error:

$$W_{wmne} = BG^T(GBG^T + \lambda C)^{-1} \quad (5.3)$$

Where  $\lambda$  is the regularization parameter and  $C$  represents the noise covariance matrix. The wMNE algorithm compensates for the tendency of MNE to favor weak and surface sources (Hämäläinen & Ilmoniemi, 1994; Lin et al., 2006). Matrix  $B$  adjusts the properties of the solution by reducing the bias inherent to the standard MNE solution. Classically,  $B$  is a diagonal matrix built from matrix  $G$  with nonzero terms inversely proportional to the norm of the lead field vectors. Note that  $B = I$  in the case where the weighting is null. Practically,  $\lambda$  is computed based on the signal-to-noise ratio ( $SNR$ ):  $\lambda = 1/SNR$ .

The  $SNR$  depends on the data type. For instance, in the task-related paradigm, the pre-stimuli are usually used to estimate the noise and the post-stimuli is considered the useful signal. The  $SNR$  can be computed using the ratio of the signal variance over these two periods. In addition, the pre-stimuli period can also be used to compute the noise covariance matrix  $C$ . In resting-state data, the computation is more difficult, as the difference between the signal and baseline is very small. A long EEG segment is traditionally used to estimate the  $C$  matrix. When the noise can be assumed as spatially uniform across all channel sites, then  $C = I$ .

The estimation of matrix  $W$ , from which the dynamics of the brain sources can be reconstructed using (eq. 5.2), is usually done on high-resolution surface mesh (in our case 15,000 vertex). However, the number of reconstructed sources is too great to perform the connectivity analysis (the second step). Therefore, in practice, spatially closed brain sources are clustered based on a set of  $R$  predefined regions of interest (ROIs), with  $R$  chosen as small with respect to the number of estimated sources. To define ROIs, many anatomical and/or functional atlases are available. We used the Desikan–Killiany atlas, with 68 ROIs (Desikan et al., 2006) (see Annex C for more details about the names and abbreviations of these regions). This procedure leads to  $R$  regional time series  $R(t)$ , each one representing the average brain activity generated by one of the  $R$  predefined brain regions.

### 5.6.2 Dynamic functional connectivity

Once regional time series  $R(t)$  are reconstructed, functional connectivity may be assessed by studying either phase or amplitude coupling (Bruns, 2004; Mehrkanoon et al., 2014). Both approaches were widely adopted (see (M. Brookes et al., 2011; Hipp et al., 2012; Pasquale et al., 2010) for amplitude coupling, and (Engel et al., 2001; Lutz et al., 2004; Uhlhaas & Singer, 2006; Varela et al., 2001) for phase coupling).

In this study, functional connectivity is computed between EEG sources using phase synchronization (PS) method. The instantaneous phase must be, first, extracted using Hilbert transform, then, a measure of the synchronization degree between the estimated phases is defined.

We used the phase-locking value to measure the PS between two signals  $x$  and  $y$ :

$$PLV_t = \frac{1}{N} \left| \sum_{n=1}^N \exp(j(\varphi_y(t) - \varphi_x(t))) \right| \quad (5.4)$$

where  $\varphi_y(t)$  and  $\varphi_x(t)$  are the instantaneous phases of signals  $x$  and  $y$ , and  $N$  denotes the number of trials (Lachaux et al., 1999). The PLV ranges between zero (no synchronization) and one (full synchronization).

PLV may be computed in both ‘static’ and ‘dynamic’ ways. For the static way, the functional connectivity is computed over the entire epoch duration. However, since we were interested in assessing the dynamic functional connectivity, we used a sliding window in which PLV was calculated over its datapoints (Kabbara et al., 2018; Kabbara et al., 2017). As recommended by (Lachaux et al., 2000) the smallest window length is equal to  $\frac{6}{\text{central frequency}}$  where 6 is the number of ‘cycles’ at the given frequency band.

Prior to PLV computation, data were filtered in the frequency bands of interest: beta band in the motor task, and gamma band in the picture naming task. Thus, the window lengths used in the button press and picture naming task are 291.7 ms and 164.4 ms respectively. A 90% overlapping between consecutive time windows was considered. This results in 27 and 54 time windows per each trial in the button press and picture naming tasks respectively, that is, 27 and 54 fully connected, weighted, and undirected networks, respectively. Each network is mathematically represented by an adjacency matrix ( $68 \times 68$ ) showing all pairwise connectivity values between the 68 nodes of the Desikan-Killiany atlas.

## 5.7 Network analysis

Many functional studies based on EEG questioned the AD abnormalities in brain connectivity during a task-free (“resting state”) paradigm. As an example, (Canuet et al., 2012) showed functional connectivity alterations in alpha2 and theta band when comparing AD patients to controls. Changes in brain AD brain network topology were demonstrated in (Vecchio et al., 2014), by mean of clustering coefficient, and path length measures. (Stam et al., 2006) and (Supekar et al., 2008) investigated the small-world organization of brain networks in AD. In (Kabbara et al., 2018), improved segregation and reduced integration were found in AD patients compared to healthy controls.

Many graph measures can be extracted from networks to characterize static and dynamic network properties (degree, clustering coefficient, path length, modularity, hubness, flexibility, recruitment, vulnerability, (Bassett et al., 2011; Bullmore & Sporns, 2009; Hassan & Wendling, 2018; Kabbara et al., 2018)). Here, we focused on a measure that quantifies the dynamic aspect of each brain regions and its reconfiguration from the stimulus onset onto the reaction time. The measure used is recently proposed in (Kabbara et al., 2019) and is called “the strength variability”. It measures how much a node (i.e. brain region) changes its strength during time. Importantly, the node’s strength is defined as the sum of all edges weights connected to a node (Barat et al., 2004). It indicates how influential the node is with respect to other nodes. Strength variability is defined by:

$$V(str_i) = \sum_{tw=1}^{L-1} |Str_{i,tw} - Str_{i,tw+1}| \quad (5.5)$$

where  $i$  is the considered node,  $str$  is the strength measure,  $L$  denotes the number of time windows and  $tw$  and  $tw + 1$  refer to two consecutive time windows.

Strength variability was calculated at each node, for all subjects. We also calculated the average strength variability, that is computed simply by averaging the strength variability across all nodes.

Using this parameter, we conducted two analysis: 1) group-level analysis, 2) an individual-level analysis.

### 5.7.1 Group-level analysis:

Here, the objective is to detect whether a statistical difference can be found between healthy controls and AD groups.

On the network level, a Wilcoxon test was performed to assess the statistical difference between AD and control groups in terms of the average strength variability, for both picture naming and button press tasks.

In order to determine the nodes showing significant strength variability differences between the two groups, Wilcoxon test was performed for each of the 68 nodes of the atlas. For multiple comparisons across regions ( $p_{\text{Bonferroni adjusted}} < \frac{0.05}{N}$ ), we used Bonferroni correction.  $N$  denotes the number of brain regions (68)).

### 5.7.2 Individual-level analysis:

The individual-level analysis aims at detecting whether there is a significant correlation between the clinical scores and the characteristics of the brain networks of the subjects.

In order to investigate the associations between the strength variability and the cognitive impairment in AD, Pearson's correlation was estimated first between the strength variability and seven clinical scores (ACE-R, MMSE, and the five sub-scores of the ACE-R). In a first approach, strength variability was averaged across all the subject's nodes (network-level). In a second approach, Pearson's correlation was computed between strength variability and the clinical scores, at each node, in order to assess the nodes showing significant correlations. In order to deal with the family-wise error rate, a Bonferroni correction was applied for multiple comparisons across regions ( $p_{\text{Bonferroni adjusted}} < \frac{0.05}{N}$ ,  $N$  denotes the number of brain regions (68)).

## 5.8 Results

### 5.8.1 Group-level analysis

In both tasks, AD patients are showing greater average strength variability ( $2.91 \pm 0.411$  in the button press task, and  $7.81 \pm 1.26$  in the picture naming paradigm) compared to healthy controls ( $2.34 \pm 0.45$  in the button press task, and  $5.39 \pm 0.75$  in the picture naming task). The Wilcoxon test shows a significant difference between the two groups in the motor task ( $p=0.006$ ) and the picture naming task ( $p=3E-4$ ). (Fig. 5.7) also shows that the average strength variability is higher in the case of the picture naming task in both AD and control group.

None of the 68 nodes shows a significant difference in the strength variability in the motor task. However, in the picture naming task, three nodes located in the temporal lobe (right entorhinal, right and left parahippocampal), three in the frontal lobe (right caudalanteriorcingulate, left and right frontal pole), and one (right lingual) in the occipital lobe are have significant difference in their network measure (Fig. 5.8).

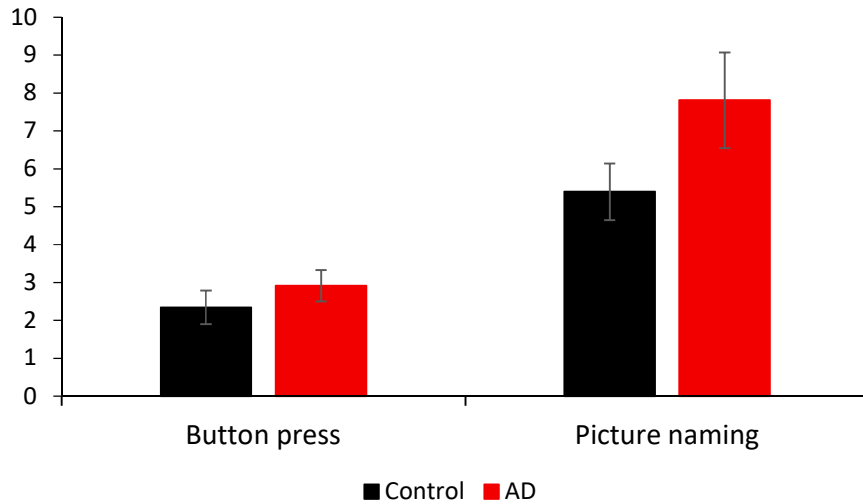


**Figure 0.6.** Mean ( $\pm$ std) strength variability in AD patients and healthy controls, in the two tasks-related paradigms.  
Wilcoxon test was used to assess the statistical difference between the two groups.

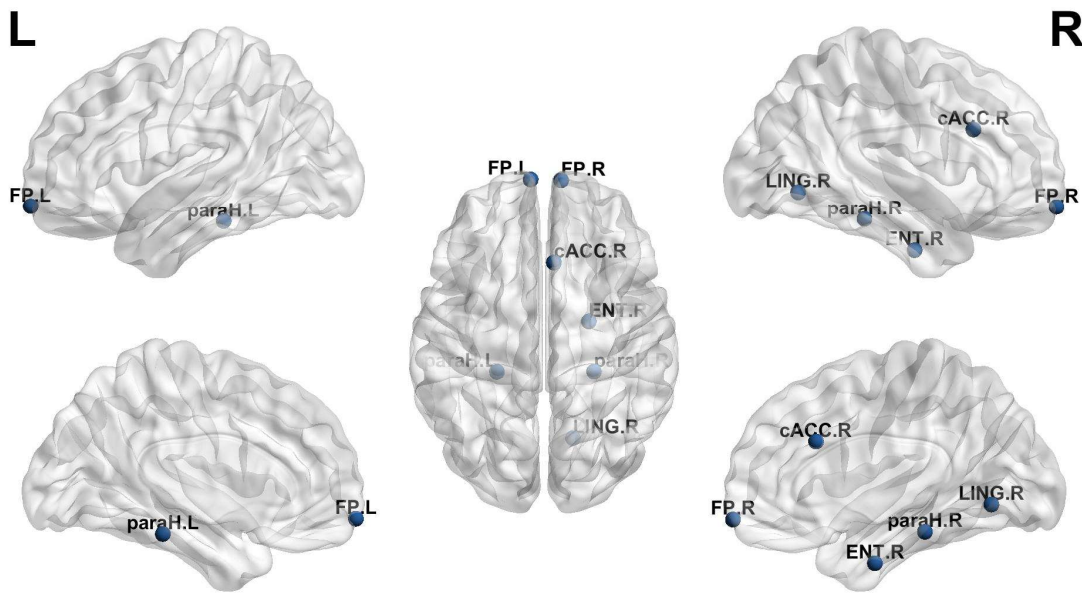


**Figure 0.7.** Seven nodes showing a significant difference in strength variability between AD patients and healthy controls.  
Wilcoxon test was performed, Bonferroni corrected ( $p_{\text{Bonferroni adjusted}} < \frac{0.05}{68}$ ).

### 5.8.2 Individual-level analysis

Results show a negative correlation between the strength variability and the clinical scores in both tasks. However, the picture naming task presented a stronger negative correlation than the motor task.

### **5.8.2.1 Motor task**

The highest correlation was found between strength variability and verbal fluency score ( $\rho = -0.60858, p = 0.002651$ ). Correlation values between other scores and the strength variability were similar ( $\rho = -0.57404, p = 0.005211$ ) for the ACE-R score, ( $\rho = -0.50679, p = 0.016082$ ) for the MMSE score, ( $\rho = -0.55667, p = 0.007128$ ) for the attention/orientation sub-score, ( $\rho = -0.55502, p = 0.007337$ ) for the memory sub-score, ( $\rho = -0.5147, p = 0.014247$ ) for the language sub-score, and ( $\rho = -0.54776, p = 0.008316$ ) for the visuospatial abilities sub-score (Fig. 5.9).

A significant difference in strength variability was found in the left bankssts located in the temporal lobe and the right parsorbitalis located in the frontal lobe (Fig. 5.11).

### **5.8.2.2 Picture naming**

Similar to the motor task, the highest correlation was found with the verbal fluency score ( $\rho = -0.81948, p = 3.08 \times 10^{-6}$ ). The correlation between the strength variability and the ACE\_R score was also high ( $\rho = -0.80367, p = 6.64 \times 10^{-6}$ ). Remaining scores showed a similar correlation with the network measure while being always higher than the correlation values obtained in the motor task (( $\rho = -0.76379, p = 3.53 \times 10^{-5}$ ) for the MMSE score, ( $\rho = -0.78532, p = 1.49 \times 10^{-5}$ ) for the attention/orientation sub-score, ( $\rho = -0.7619, p = 3.79 \times 10^{-5}$ ) for the memory sub-score, ( $\rho = -0.75807, p = 4.36 \times 10^{-5}$ ) for the language sub-score, and ( $\rho = -0.74374, p = 7.27 \times 10^{-5}$ ) for the visuospatial abilities sub-score) (Fig. 5.10).

19 nodes were found significantly correlated with the clinical scores. The majority (nine) of them are located in the temporal lobe (left bankssts, left and right entorhinal, left inferiortemporal, right insula, left and right parahippocampal, and left and right temporalpole). Six nodes (right frontalpole, right parsorbitalis, left parstriangularis, left precentral, left and right rostralanteriorcingulate) are located in the frontal lobe, two (left and right lingual) in the occipital lobe, and one node in the parietal lobe (left postcentral) (Fig. 5.12).

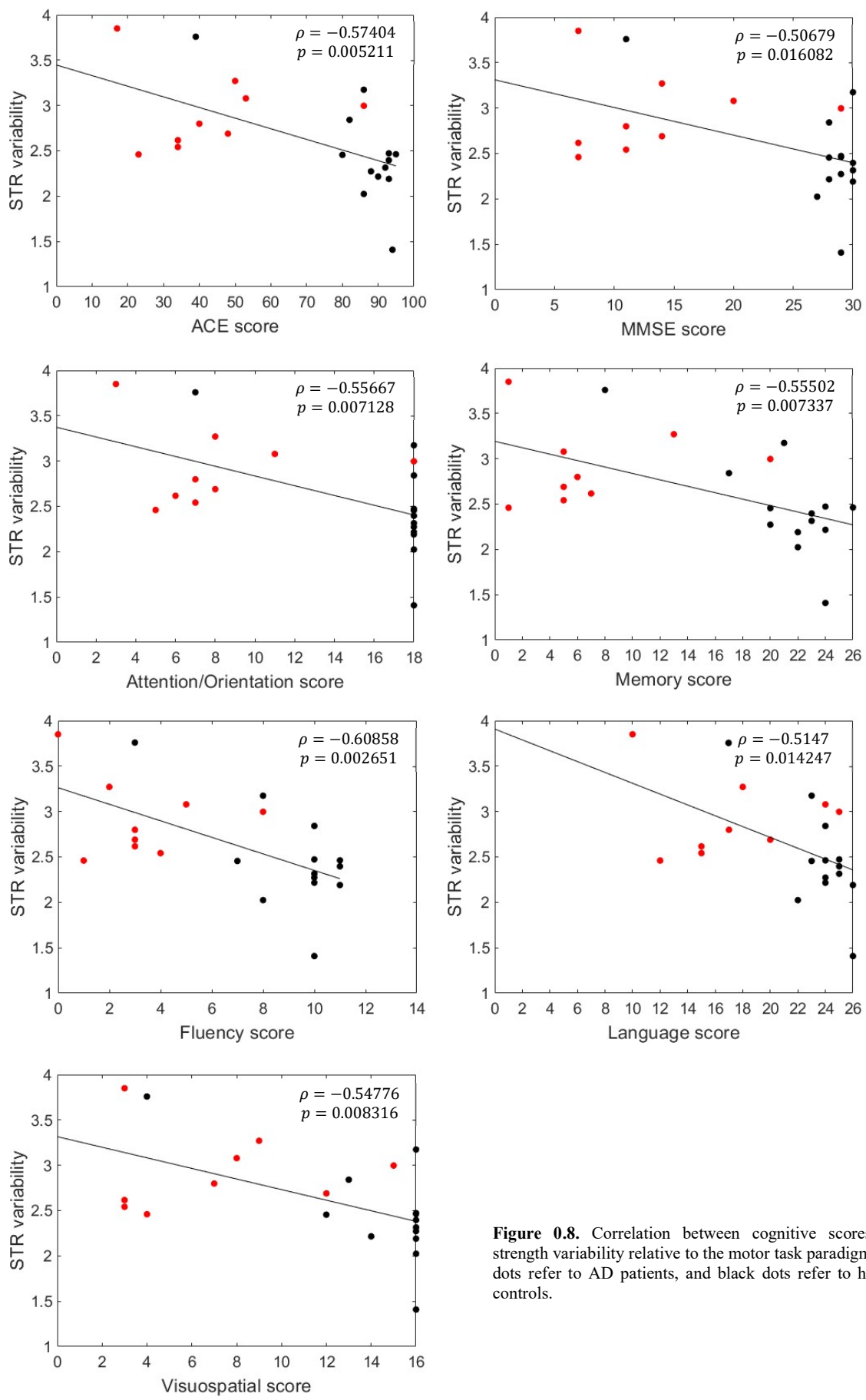


**Figure 0.8.** Correlation between cognitive scores and strength variability relative to the motor task paradigm. Red dots refer to AD patients, and black dots refer to healthy controls.

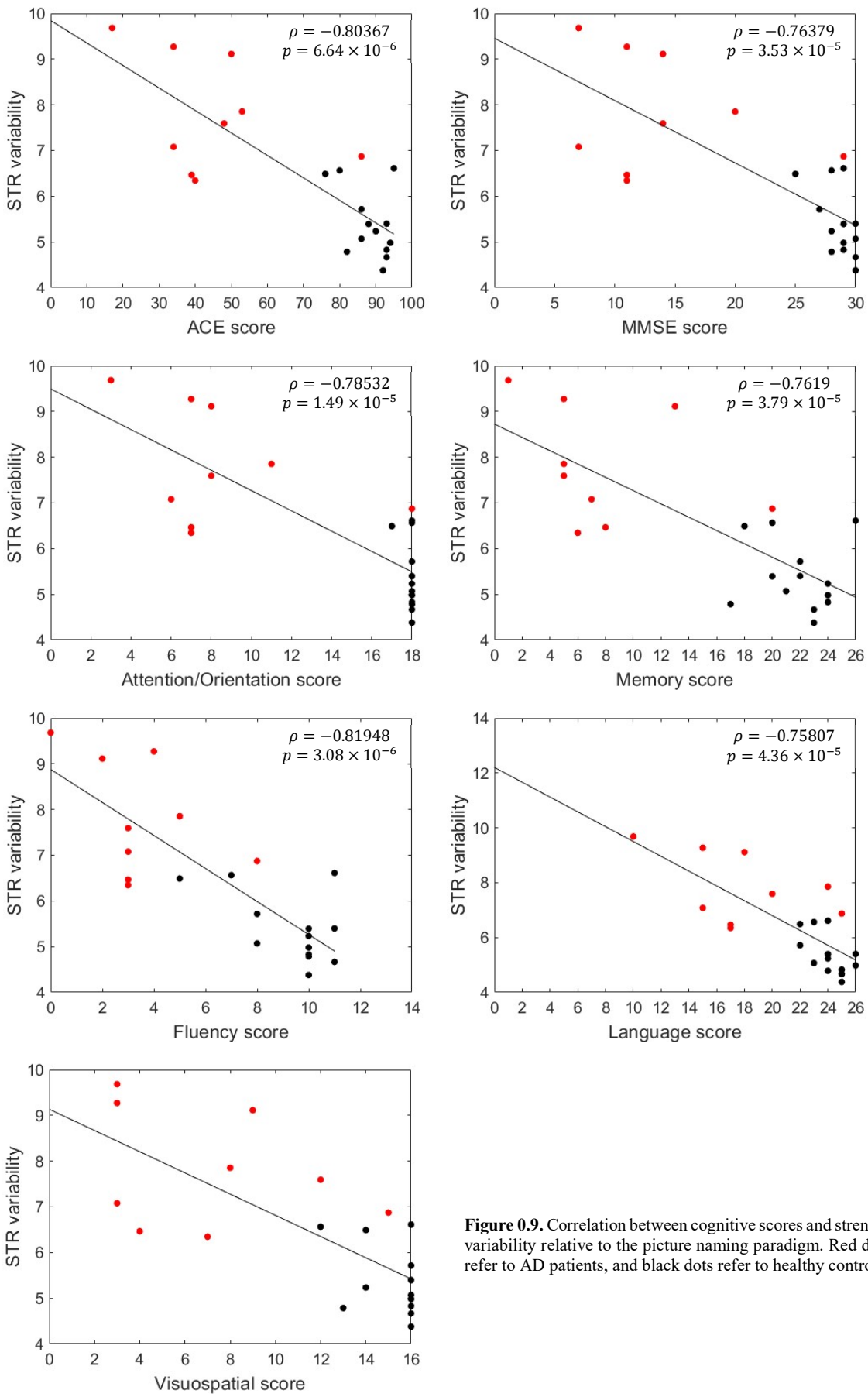


**Figure 0.9.** Correlation between cognitive scores and strength variability relative to the picture naming paradigm. Red dots refer to AD patients, and black dots refer to healthy controls.

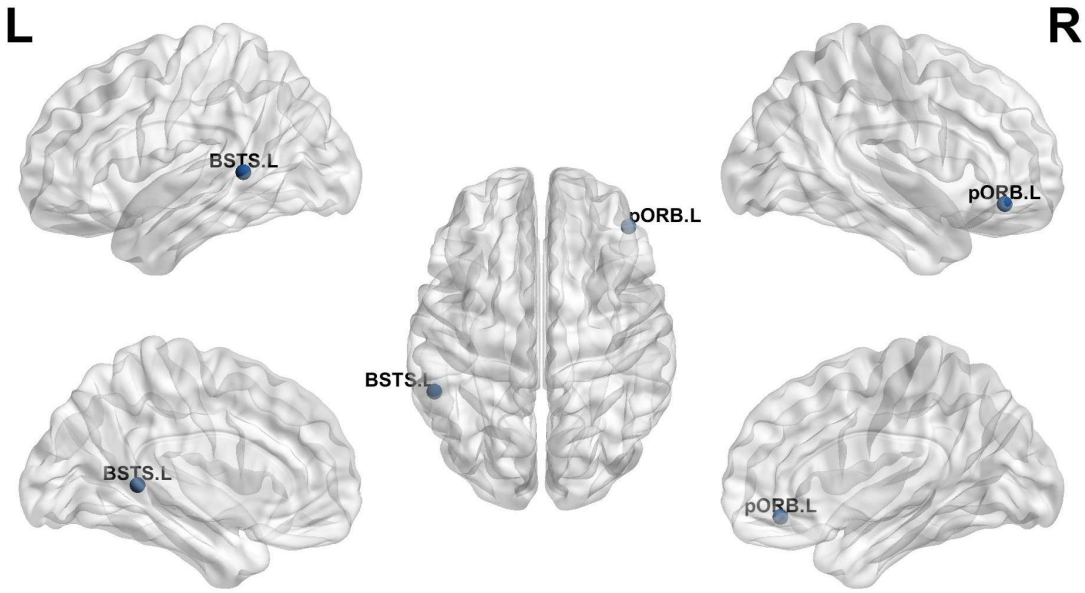


**Figure 0.10.** Seven nodes showing significant correlation between cognitive scores and strength variability in the button press task. Bonferroni correction ( $p_{\text{Bonferroni adjusted}} < \frac{0.05}{68}$ ) was applied.

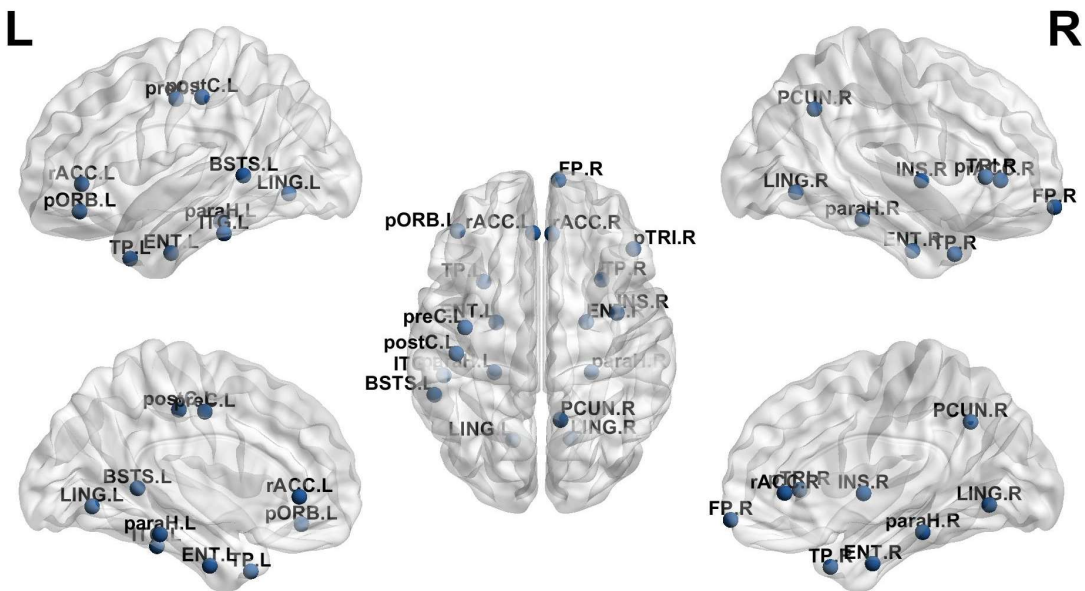


**Figure 0.11.** Seven nodes showing significant correlation between cognitive scores and strength variability in the button press task. Bonferroni correction ( $p_{\text{Bonferroni adjusted}} < \frac{0.05}{68}$ ) was applied.

## 5.9 Discussion:

The aim of this study is to characterize dynamic functional brain networks in AD patients and find a correlation between network derived index and cognitive impairment. Therefore, we

studied the strength variability of the network nodes. We performed both group and individual-level analysis.

Our study shows that the average strength variability is significantly decreased with a higher cognitive score in both task-related paradigms. These findings indicate that AD patients have excessive reconfiguration of functional brain networks leading to the loss of focus. In other words, a stable core network may be important to ensure good performance during cognitive tasks and to prevent unneeded fluctuations in the brain networks. One possible interpretation of the increased reconfiguration of brain networks in AD patients may be a possible compensatory mechanism ([Afshari & Jalili, 2017](#)), a way to adapt to the cognitive impairment and find alternative strategies ([Bullmore & Sporns, 2012](#)).

From another point of view, the lower strength variability in healthy controls, detected in both group and individual level analysis, may be interpreted as one of the brain network organization process aiming at minimizing running costs ([Bullmore & Sporns, 2012](#)).

In contrast to the motor task, the number of nodes that have shown a significant difference between group AD and controls was much greater in the picture naming task. In the group-level analysis, while no nodes were detected in the motor task, seven nodes showed a significant difference in the picture naming task. This number was much greater in the individual level analysis, 19 nodes in the picture naming task, and two nodes in the button press task.

In the motor task, the right parsorbitalis node revealed significant difference in the strength variability between AD and healthy controls. This node belongs to the right inferior frontal cortex (rIFC, also known as ventrolateral prefrontal cortex). It has been stated, for so long that rIFC is implicated in motor inhibitory responses (go/no-go task (GNG), the Stop Signal Task (SST), and their analogues ([Aron et al., 2004](#); [Logan & Cowan, 1984](#); [Menon et al., 2001](#); [Rubia et al., 2003](#)). However, rIFG is thought to be involved in attentional switching ([Cools et al., 2002](#); [Dove et al., 2000](#); [Hampshire & Owen, 2006](#)). ([Hampshire et al., 2010](#)) showed that rIFC is activated whenever a cue is detected, regardless of the following response, whether it includes an inhibition, a generation of motor response, or no response. Interestingly, in ([Eliasova et al., 2014](#)), a high frequency repetitive transcranial magnetic stimulation (rTMS) of the right inferior gyrus has led to a significant improvement of attention and psychomotor speed in patients with MCI/mild dementia due to AD. Other studies ([Corbetta & Shulman, 2002](#); [Pironti et al., 2014](#); [Raine et al., 2011](#)) also reported the involvement of the rIFC in processes such as attention and executive functions. Our findings are therefore in line with the previous studies.

The second node we detected in the button pressing task is the bankssts (banks of the superior temporal sulcus (STC)). ([Hein & Knight, 2008](#)) showed that different cognitive process may cause the activation of STC, having thus a multifunctional profile.

Overt picture naming involves several successive cognitive processes: visual feature extraction, visual information processing, object recognition, lexical retrieval and lemma selection, naming process, speech articulation ([Baldo et al., 2013](#); [Hassan et al., 2015](#); [Laaksonen et al., 2012](#); [Levelt et al., 2002](#); [Schuhmann et al., 2012](#)). All brain regions

(occipital, frontal, temporal, parietal, central) were shown to be involved, at different time periods, and with different participation percentage, in the picture naming paradigm (Hassan et al., 2015). This seems to be in line with our findings. Nodes showing significant difference were distributed all over the cortex.

## 5.10 Limitations

First, one of the main limitations of this study is the relatively low number of patients. As we are interested only in investigating the early stages of the disease (mild to moderate AD), we were limited by the number of participants to the study. In addition, our intent was to show differences between AD patients, healthy controls, and subjects at risk. However, since only two subjects at risk participated, we exclude them from the study.

Second, the EEG source connectivity was applied here to 32 scalp EEG channels. Although useful information can still be extracted from a low number of channels (Canuet et al., 2012; Hata et al., 2016; Vecchio et al., 2014), the accuracy of the obtained results is attenuated (Hassan et al., 2014).

Third, spurious connectivity values due to the volume conduction problem are reduced at the source level (Hassan et al., 2014), some “mixing-effect” may still occur (Brookes et al., 2014). All strategies proposed to solve this issue are based on ignoring zero-lag interactions among signals, by supposing that their contributions are only due to the source leakage (Brookes et al., 2012; Colclough et al., 2015). However, as reported in (Finger et al., 2016), true communications that occur at zero lag. In our study, we used the phase-locking value measure which showed robustness against spurious short connections in a previous study (Kabbara et al., 2017). Nevertheless, we believe that further methodological efforts are needed to completely solve the spatial leakage problem.

Fifth, the choice of the inverse solution/connectivity combination was supported by two comparative studies (Hassan et al., 2014, 2017), in which the combination wMNE/PLV, used in this paper, showed the highest similarity between reference (ground truth) and estimated networks. Nevertheless, other combinations or strategies that showed accurate construction of cortical networks from sensor level recordings could be also investigated (Brookes et al., 2012; Brookes et al., 2011; Colclough et al., 2015, 2016; O'Neill et al., 2017).

## 5.11 Conclusion

In this chapter, we investigated the functional brain networks alterations associated with Alzheimer’s disease. We reported an increased strength variability in AD patients compared to healthy controls. We showed that this network parameter is significantly correlated with the patients cognitive clinical scores. We believe that these findings, along with additional AD functional brain network characteristics, could contribute to the development of an EEG-based neuro-marker that could support clinical AD diagnosis.

# CONCLUSION

This research study is aimed at characterizing differences in brain activity between AD patients and healthy controls. Therefore, sclar voltage topographies were compared while performing a motor task. We highlighted the necessity of dynamic analysis and showed that static analysis does not provide a reliable representation of underlying neuronal activity since significant differences between the two groups were revealed by the dynamic analysis only. Then, we investigated functional alterations in AD brain networks. We used the “EEG source connectivity” approach and “sliding window” technique in order to conduct a dynamic analysis of the functional connectivity at reasonable spatial resolution. We characterized the network alterations in AD by assessing the strength variability of the network nodes. A significant negative correlation between the network-based index and the level of cognitive impairment was found.

A key factor characterizing this project is the analysis of AD brain activity during task-related paradigms in contrast to most previous researches limited to the study of resting state. In addition, we are benefiting from EEG being a non-invasive, low cost, and easy-to-use technique to track brain dynamics at a sub-second timescale.

The main difficulties we encountered during this project were in the data acquisition phase. Setting the appointments that were subject sometimes to both the doctor and the participant availability was a cumbersome procedure. In addition, due to the multitask task experimental paradigm, recording sessions were time-consuming relative to the project designated duration. Although no major difficulties were faced while dealing with the patients, however, it requires effort to manage the session and maintain the patient concentration, particularly during the neuropsychological test. In principle, cognitive screening must be done by a psychologist. Finally, equipment transportation between the research center and the clinic was needed before and after each and every appointment, which was bothersome and also time-consuming.

The results we obtained in this study are very encouraging. Further measures may be used in future work in order to assess additional differences between AD and healthy controls brain networks. In this project, we were limited to the analysis of the button press and picture naming paradigms. However, data collected from the resting state and one-back task are also to be studied. It would be interesting to test the ability of the obtained networks measures to predict AD using machine learning algorithm. In addition to the measures characterizing the network topology, we think that tracking the brain networks that form and dissolve to support ongoing cognitive function would reveal further differences between AD and healthy controls. Finally, an objective that we have mentioned previously is to increase the number of participants in order to validate the results we have obtained, and to recruit subjects presenting a risk of developing AD and include them in future work.

As researches continue, we hope to witness a successful development of an AD neuro-marker in the next few years.

# References

- Aalten, P., Verhey, F. R. ., Boziki, M., & Bullock, R. (2007). Neuropsychiatric Syndromes in Dementia. *Dement Geriatr Cogn Disord*, 24, 457–463. <https://doi.org/10.1159/000110738>
- Abásolo, D., Hornero, R., Gómez, C., García, M., & López, M. (2006). Analysis of EEG background activity in Alzheimer's disease patients with Lempel-Ziv complexity and central tendency measure. *Medical Engineering and Physics*, 28, 315–322. <https://doi.org/10.1016/j.medengphy.2005.07.004>
- Afshari, S., & Jalili, M. (2017). Directed Functional Networks in Alzheimer's Disease: Disruption of Global and Local Connectivity Measures. *IEEE Journal of Biomedical and Health Informatics*, 21(4), 949–955. <https://doi.org/10.1109/JBHI.2016.2578954>
- Al Salman, A. S. A. (2013). *The Saudi Arabian Adaptation of the Addenbrooke's Cognitive Examination – Revised (Arabic ACER)* (University of Glasgow). Retrieved from <http://theses.gla.ac.uk/4706/>
- Alario, F., & Ferrand, L. (1999). A set of 400 pictures standardized for French: Norms for name agreement, image agreement, .... *Behavior Research Methods, Instruments, and Computers*, 31(3), 531–552. Retrieved from <http://www.lpelab.org/userpage/ferrand/PDF/Alario-Ferrand99-BRMIC.pdf%0Apapers3://publication/uuid/FD101C0E-2F70-4468-B766-5DAE78D15364>
- Albers, M. W., Gilmore, G. C., Kaye, J., Murphy, C., Wingfield, A., Bennett, D. A., ... Zhang, L. I. (2015). At the interface of sensory and motor dysfunctions and Alzheimer's disease. *Alzheimer's and Dementia*, 11(1), 70–98. <https://doi.org/10.1016/j.jalz.2014.04.514>
- Allouch, S., Tabbal, J., Nasser, A., Hassan, M., Khalil, M., & Kabbara, A. (2019). Altered motor performance in Alzheimer ' s disease : a dynamic analysis using EEG. *Fifth International Conference on Advances in BioMedical Engineering IEEE, Lebanon*.
- Anderson, T. M., Sachdev, P. S., Brodaty, H., Trollor, J. N., & Andrews, G. (2007). Effects of Sociodemographic and Health Variables on Mini-Mental State Exam Scores in Older Australians. *American Journal of Geriatric Psychiatry*, 15(6), 467–476. <https://doi.org/10.1097/JGP.0b013e3180547053>
- Appell, J., Kertesz, A., & Fisman, M. (1982). A study of language functioning in Alzheimer patients. *Brain and Language*, 17, 73–91. [https://doi.org/10.1016/0093-934X\(82\)90006-2](https://doi.org/10.1016/0093-934X(82)90006-2)
- Aron, A. R., Robbins, T. W., & Poldrack, R. A. (2004). Inhibition and the right inferior frontal cortex. *Trends in Cognitive Sciences*, 8(4), 170–177. <https://doi.org/10.1016/j.tics.2004.02.010>
- Association, A. (2019). 2019 Alzheimer's Disease Facts and Figures. Retrieved from <https://www.alz.org/media/Documents/alzheimers-facts-and-figures-2019-r.pdf>
- Avena-Koenigsberger, A., Misic, B., & Sporns, O. (2018). Communication dynamics in complex brain networks. *Nature Reviews Neuroscience*, 19, 17–33. <https://doi.org/10.1038/nrn.2017.149>
- Baddeley, A. D. (1992). Working Memory. *Science*, 255, 556–559.

<https://doi.org/10.4249/scholarpedia.3015>

- Baillet, S. (2017). MEG for Brain Electrophysiology & Imaging. *Nature Neuroscience*, 327-. <https://doi.org/10.1038/nn.4504>
- Baillet, S., Mosher, J. C., & Leahy, R. M. (2001). Electromagnetic Brain Mapping. *IEEE Signal Processing Magazine*, (November), 14–30.
- Baldo, J. V., Arévalo, A., Patterson, J. P., & Dronkers, N. F. (2013). Grey and white matter correlates of picture naming: Evidence from a voxel-based lesion analysis of the Boston Naming Test. *Cortex*, 49, 658–667. <https://doi.org/10.1016/j.cortex.2012.03.001>
- Barrat, A., Barthélémy, M., Pastor-Satorras, R., & Vespignani, A. (2004). The architecture of complex weighted networks. *PNAS*, 101(11). <https://doi.org/10.1073/pnas.0400087101>
- Basser, P. J., Mattiello, J., & LeBihan, D. (1994). MR diffusion tensor spectroscopy and imaging. *Biophysical Journal*, 66, 259–267. [https://doi.org/10.1016/S0006-3495\(94\)80775-1](https://doi.org/10.1016/S0006-3495(94)80775-1)
- Bassett, D. S., & Sporns, O. (2017). Network neuroscience. *Nature Neuroscience*, 20(3), 353–364. <https://doi.org/10.1038/nn.4502>
- Bassett, D. S., Wymbs, N. F., Porter, M. A., Mucha, P. J., Carlson, J. M., & Grafton, S. T. (2011). Dynamic reconfiguration of human brain networks during learning. *PNAS*, 108(18), 7641–7646. <https://doi.org/10.1073/pnas.1018985108>
- Bateman, R. J., Xiong, C., Benzinger, T. L. S., Fagan, A. M., Goate, A., Fox, N. C., ... Dominantly Inherited Alzheimer Network. (2012). Clinical and biomarker changes in dominantly inherited Alzheimer's disease. *The New England Journal of Medicine*, 367(9), 795–804. <https://doi.org/10.1056/NEJMoa1202753>
- Bell, A. J., & Sejnowski, T. I. (1995). Communicated by An Information-Maximization Approach to Blind Separation and Blind Deconvolution. *Neural Computation (MIT)*, 7, 1129–1159. Retrieved from <https://www.mitpressjournals.org/doi/pdf/10.1162/neco.1995.7.6.1129>
- Bennys, K., Rondouin, G., Vergnes, C., & Touchon, J. (2001). Diagnostic value of quantitative EEG in Alzheimer's disease. *Neurophysiologie Clinique*, 31(3), 153–160. [https://doi.org/10.1016/S0987-7053\(01\)00254-4](https://doi.org/10.1016/S0987-7053(01)00254-4)
- Boersma, P. (2002). Praat, a system for doing phonetics by computer. *Glot International*, 5(9/10), 341–345.
- Braun, U., Schaefer, A., Betzel, R. F., Tost, H., Meyer-Lindenberg, A., & Bassett, D. S. (2018). From Maps to Multi-dimensional Network Mechanisms of Mental Disorders. *Neuron*, 97(1), 14–31. <https://doi.org/10.1016/j.neuron.2017.11.007>
- Brenner, R. P., Ulrich, R. F., Spiker, D. G., Sclabassi, R. J., Reynolds, C. F., Marin, R. S., & Boller, F. (1986). Computerized EEG spectral analysis in elderly normal, demented and depressed subjects. *Electroencephalography and Clinical Neurophysiology*, 64, 483–492. [https://doi.org/10.1016/0013-4694\(86\)90184-7](https://doi.org/10.1016/0013-4694(86)90184-7)
- Brookes, M. J., Woolrich, M. W., & Barnes, G. R. (2012). Measuring functional connectivity in MEG: A multivariate approach insensitive to linear source leakage. *NeuroImage*, 63, 910–920. <https://doi.org/10.1016/j.neuroimage.2012.03.048>

- Brookes, M., Woolrich, M., Luckhoo, H., Price, D., Hale, J., Stephenson, M., ... Morris, P. (2011). Investigating the elecctrophysiological basis of resting state networks using magnetoencephalography. *Proc Natl Acad Sci USA*, 108, 16783–16788.
- Brookes, Matthew J., Woolrich, M. W., & Price, D. (2014). An Introduction to MEG Connectivity Measurements. In *Magnetoencephalography*, S. Supek and C. J. Aine (eds.). <https://doi.org/10.1007/978-3-642-33045-2>
- Brunner, C., Billinger, M., Seeber, M., Mullen, T. R., & Makeig, S. (2016). Volume Conduction Influences Scalp-Based Connectivity Estimates. *Front. Comput. Neurosci.*, 10(121). <https://doi.org/10.3389/fncom.2016.00121>
- Brunns, A. (2004). Fourier-, Hilbert- and wavelet-based signal analysis: Are they really different approaches? *Journal of Neuroscience Methods*, 137, 321–332. <https://doi.org/10.1016/j.jneumeth.2004.03.002>
- Buchman, A. S., & Bennett, D. A. (2011). Loss of motor function in preclinical Alzheimer's disease. *Expert Rev Neurother*, 11(5), 665–676. <https://doi.org/10.1586/ern.11.57.Loss>
- Bullmore, E., & Sporns, O. (2009). Complex brain networks: graph theoretical analysis of structural and functional systems. *Nature Reviews Neuroscience*, 10(3), 186–198. <https://doi.org/10.1038/nrn2575>
- Bullmore, E., & Sporns, O. (2012). The economy of brain network organization. *Nature Reviews Neuroscience*, 13, 336–349. <https://doi.org/10.1038/nrn3214>
- Campion, D., Pottier, C., Nicolas, G., & Guennec, K. Le. (2016). Alzheimer disease : modeling an A  $\beta$  -centered biological network. *Molecular Psychiatry* (2016), 1–11. <https://doi.org/10.1038/mp.2016.38>
- Canuet, L., Tellado, I., Couceiro, V., Fraile, C., Fernandez-novoa, L., Ishii, R., ... Cacabelos, R. (2012). Resting-State Network Disruption and APOE Genotype in Alzheimer ' s Disease : A lagged Functional Connectivity Study. 7(9). <https://doi.org/10.1371/journal.pone.0046289>
- Chen, S., Ge, X., Chen, Y., Lv, Na., Liu, Z., & Yuan, W. (2013). Advances with RNA interference in Alzheimer ' s disease research. *Drug Design, Development and Therapy*, 7, 117–125.
- Coben, L. A., Danziger, W. L., & Berg, L. (1983). Frequency analysis of the resting awake EEG in mild senile dementia of Alzheimer type. *Electroencephalography and Clinical Neurophysiology*, 55(4), 372–380. [https://doi.org/10.1016/0013-4694\(83\)90124-4](https://doi.org/10.1016/0013-4694(83)90124-4)
- Coben, L. A., Danziger, W., & Storandt, M. (1985). A longitudinal EEG study of mild senile dementia of Alzheimer type: changes at 1 year and at 2.5 years. *Electroencephalography and Clinical Neurophysiology*, 61, 101–112. [https://doi.org/10.1016/0013-4694\(85\)91048-X](https://doi.org/10.1016/0013-4694(85)91048-X)
- Cohen, J. R., & D'Esposito, M. (2016). The Segregation and Integration of Distinct Brain Networks and Their Relationship to Cognition. *Journal of Neuroscience*, 36(48), 12083–12094. <https://doi.org/10.1523/JNEUROSCI.2965-15.2016>
- Colclough, G. L., Brookes, M. J., Smith, S. M., & Woolrich, M. W. (2015). A symmetric multivariate leakage correction for MEG connectomes. *NeuroImage*, 117, 439–448. <https://doi.org/10.1016/j.neuroimage.2015.03.071>

- Colclough, G. L., Woolrich, M. W., Tewarie, P. K., Brookes, M. J., Quinn, A. J., & Smith, S. M. (2016). How reliable are MEG resting-state connectivity metrics? *NeuroImage*, 138, 284–293. <https://doi.org/10.1016/j.neuroimage.2016.05.070>
- Comon, P. (1994). Independent component analysis, A new concept? *Signal Processing*, 36, 287–314. [https://doi.org/10.1016/0165-1684\(94\)90029-9](https://doi.org/10.1016/0165-1684(94)90029-9)
- Cools, R., Clark, L., Owen, A. M., & Robbins, T. W. (2002). Defining the neural mechanisms of probabilistic reversal learning using event-related functional magnetic resonance imaging. *The Journal of Neuroscience: The Official Journal of the Society for Neuroscience*, 22(11), 4563–7567. <https://doi.org/10.1026/0264-35>
- Corbetta, M., & Shulman, G. L. (2002). Control of goal-directed and stimulus-driven attention in the brain. *Nature Reviews. Neuroscience*, 3, 201–215. <https://doi.org/10.1038/nrn755>
- Croft, R. J., & Barry, R. J. (2000). Removal of ocular artifact from the EEG: a review. *Neurophysiol Clin*, 30, 5–19. [https://doi.org/10.1016/S0987-7053\(00\)00055-1](https://doi.org/10.1016/S0987-7053(00)00055-1)
- Crossley, N. A., Mechelli, A., Scott, J., Carletti, F., Fox, P. T., McGuire, P., & Bullmore, E. T. (2014). The hubs of the human connectome are generally implicated in the anatomy of brain disorders. *Brain*, 137(8), 2382–2395. <https://doi.org/10.1093/brain/awu132>
- Crous-bou, M., Mingüellón, C., Gramunt, N., & Molinuevo, J. L. (2017). *Alzheimer's disease prevention : from risk factors to early intervention*. 1–9. <https://doi.org/10.1186/s13195-017-0297-z>
- Cullen, B., O'Neill, B., Evans, J. J., Coen, R. F., & Lawlor, B. A. (2007). A review of screening tests for cognitive impairment. *Journal of Neurology, Neurosurgery and Psychiatry*, 78, 790–799. <https://doi.org/10.1136/jnnp.2006.095414>
- Cummings, J. L. (2000). Cognitive and behavioral heterogeneity in Alzheimer's disease: Seeking the neurobiological basis. *Neurobiology of Aging*, 21, 845–861. [https://doi.org/10.1016/S0197-4580\(00\)00183-4](https://doi.org/10.1016/S0197-4580(00)00183-4)
- Czigler, B., Csikós, D., Hidasi, Z., Anna Gaál, Z., Csibri, É., Kiss, É., ... Molnár, M. (2008). Quantitative EEG in early Alzheimer's disease patients - Power spectrum and complexity features. *International Journal of Psychophysiology*, 68, 75–80. <https://doi.org/10.1016/j.ijpsycho.2007.11.002>
- Desikan, R. S., Ségonne, F., Fischl, B., Quinn, B. T., Dickerson, B. C., Blacker, D., ... Killiany, R. J. (2006). An automated labeling system for subdividing the human cerebral cortex on MRI scans into gyral based regions of interest. *NeuroImage*, 31, 968–980. <https://doi.org/10.1016/j.neuroimage.2006.01.021>
- Dove, A., Pollmann, S., Schubert, T., Wiggins, C. J., & Yves Von Cramon, D. (2000). Prefrontal cortex activation in task switching: An event-related fMRI study. *Cognitive Brain Research*, 9, 103–109. [https://doi.org/10.1016/S0926-6410\(99\)00029-4](https://doi.org/10.1016/S0926-6410(99)00029-4)
- Eliasova, I., Anderkova, L., Marecek, R., & Rektorova, I. (2014). Non-invasive brain stimulation of the right inferior frontal gyrus may improve attention in early Alzheimer's disease: A pilot study. *Journal of the Neurological Sciences*, 346, 318–322. <https://doi.org/10.1016/j.jns.2014.08.036>
- Engel, A., Fries, P., & Singer, W. (2001). Dynamic predictions: Oscillations and synchrony in top-down processing. *Nat Rev Neu- Rosci*, 2, 704–716.

- Ewers, M., Sperling, R. A., Klunk, W. E., Weiner, M. W., & Hampel, H. (2011). Neuroimaging markers for the prediction and early diagnosis of Alzheimer's disease dementia. *Trends in Neurosciences*, 34(8), 430–442. <https://doi.org/10.1016/j.tins.2011.05.005>
- Ferreri, F., Pauri, F., Pasqualetti, P., Fini, R., Dal Forno, G., & Rossini, P. M. (2003). Motor cortex excitability in Alzheimer's disease: A transcranial magnetic stimulation study. *Annals of Neurology*, 53(1), 102–108. <https://doi.org/10.1002/ana.10416>
- Finger, H., Bönstrup, M., Cheng, B., Messé, A., Hilgetag, C., Thomalla, G., ... König, P. (2016). Modeling of Large-Scale Functional Brain Networks Based on Structural Connectivity from DTI: Comparison with EEG Derived Phase Coupling Networks and Evaluation of Alternative Methods along the Modeling Path. *PLoS Computational Biology*, 12(8), e1005025. <https://doi.org/10.1371/journal.pcbi.1005025>
- Fitzgibbon, S. P., Martin, D., Powers, W., Pope, K. J., & Clark, C. R. (2017). Removal of EEG Noise and Artifact Using Blind Source Separation. *Journal of Clinical Neurophysiology*, 24(3), 232–243. <https://doi.org/10.1097/WNP.0b013e3180556926>
- Fornito, A., Zalesky, A., & Breakspear, M. (2015). The connectomics of brain disorders. *Nature Reviews Neuroscience*, 16(3), 159–172. <https://doi.org/10.1038/nrn3901>
- Fornito, A., Zalesky, A., & Bullmore, E. T. (2016). *Fundamentals of Brain Network Analysis*.
- Fraschini, M., Hillebrand, A., Demuru, M., Didaci, L., & Marcialis, G. L. (2015). An EEG-Based Biometric System Using Eigenvector Centrality in Resting State Brain Networks. *666 IEEE SIGNAL PROCESSING LETTERS*, 22(6), 666–670.
- Friston, K. J. (2011). Functional and Effective Connectivity: A Review. *Brain Connectivity*, 1(1), 13–36. <https://doi.org/10.1089/brain.2011.0008>
- Gironell, A., García-Sánchez, C., Estévez-González, A., Boltes, A., & Kulisevsky, J. (2005). Usefulness of P300 in subjective memory complaints: A prospective study. *Journal of Clinical Neurophysiology*, 22(4), 279–284. <https://doi.org/10.1097/01.WNP.0000173559.60113.AB>
- González, G. F., Molen, M. J. W. Van der, G.Zaric, Bonte, M., Tijms, J., Blomert, L., ... Molen, M. W. Van der. (2016). Graph analysis of EEG resting state functional networks in dyslexic readers. *Clinical Neurophysiology Journal*, 127, 3165–3175. <https://doi.org/10.1016/j.clinph.2016.06.023>
- Gramfort, A., Papadopoulou, T., Olivi, E., & Clerc, M. (2010). OpenMEEG: opensource software for quasistatic bioelectromagnetics. *BioMedical Engineering OnLine*, 9(45). <https://doi.org/10.1186/1475-925X-8-1>
- Gratton, G., Coles, G. H. M., & Donchin, E. (1983). A new method for off-line removal of ocular artifact. *Electroencephalography and Clinical Neurophysiology*, 55, 468–484.
- Guiaquito, S., & Nolfe, G. (1986). THE EEG IN THE NORMAL ELDERLY: A CONTRIBUTION TO THE INTERPRETATION OF AGING AND DEMENTIA. *Electroencephalography and Clinical Neurophysiology*, 63, 540–546. <https://doi.org/10.1136/bmj.1.4662.1121-a>
- Gupta, D., Ossenblok, P., & Luijelaar, G. Van. (2011). Space – time network connectivity and cortical activations preceding spike wave discharges in human absence epilepsy : a MEG study. *Med Biol Eng Comput*, 49, 555–565. <https://doi.org/10.1007/s11517-011-0778-3>

- Haass, C., Kaether, C., Thinakaran, G., & Sisodia, S. (2012). Trafficking and Proteolytic Processing of APP. *Cold Spring Harb Perspect Med*, 2, 1–25. <https://doi.org/10.1101/cshperspect.a006270>
- Hafkemeijer, A., van der Grond, J., & Rombouts, S. A. R. B. (2012). Imaging the default mode network in aging and dementia. *Biochimica et Biophysica Acta*, 1822, 431–441. <https://doi.org/10.1016/j.bbadi.2011.07.008>
- Hämäläinen, M. S., & Ilmoniemi, R. J. (1994). Inetrpreting magnetic fields of the brain: minimum norm estimates. *Trends in Cognitive Sciences*, 32(1), 35–42.
- Hampshire, A., Chamberlain, S. R., Monti, M. M., Duncan, J., & Owen, A. M. (2010). The role of the right inferior frontal gyrus: inhibition and attentional control. *NeuroImage*, 50(3), 1313–1319. <https://doi.org/10.1016/j.neuroimage.2009.12.109>
- Hampshire, A., & Owen, A. M. (2006). Fractionating attentional control using event-related fMRI. *Cerebral Cortex*, 16, 1679–1689. <https://doi.org/10.1093/cercor/bhj116>
- Hassan, M., Benquet, P., Biraben, A., Berrou, C., Dufor, O., & Wendling, F. (2015). Dynamic reorganization of functional brain networks during picture naming. *Cortex*, 73, 276–288. <https://doi.org/10.1016/j.cortex.2015.08.019>
- Hassan, M., Dufor, O., Merlet, I., Berrou, C., & Wendling, F. (2014). EEG source connectivity analysis: From dense array recordings to brain networks. *PLoS ONE*, 9(8). <https://doi.org/10.1371/journal.pone.0105041>
- Hassan, M., Merlet, I., Mheich, A., Kabbara, A., Biraben, A., Nica, A., & Wendling, F. (2017). Identification of Interictal Epileptic Networks from Dense-EEG. *Brain Topography*, 30(1), 60–76. <https://doi.org/10.1007/s10548-016-0517-z>
- Hassan, M., & Wendling, F. (2018). Electroencephalography Source Connectivity. *IEEE Signal Processing Magazine*, (May), 81–96. <https://doi.org/10.1109/MSP.2017.2777518>
- Hata, M., Kazui, H., Tanaka, T., Ishii, R., Canuet, L., Pascual-Marqui, R. D., ... Takeda, M. (2016). Functional connectivity assessed by resting state EEG correlates with cognitive decline of Alzheimer's disease - An eLORETA study. *Clinical Neurophysiology*, 127, 1269–1278. <https://doi.org/10.1016/j.clinph.2015.10.030>
- Hein, G., & Knight, R. T. (2008). Superior temporal sulcus--It's my area: or is it? *Journal of Cognitive Neuroscience*, 2012(12), 2125–2136. <https://doi.org/10.1162/jocn.2008.20148>
- Hipp, J. F., Hawellek, D. J., Corbetta, M., Siegel, M., & Engel, A. K. (2012). Large-scale cortical correlation structure of spontaneous oscillatory activity. *Nature Neuroscience*, 15(6), 884–890. <https://doi.org/10.1038/nn.3101>
- Hogan, M. J., Swanwick, G. R. J., Kaiser, J., Rowan, M., & Lawlora, B. (2003). Memory-related EEG power and coherence reductions in mild Alzheimer's. *International Journal of Psychophysiology*, 49, 147–163. <https://doi.org/10.1016/S0167-8760>
- Hong, S. B., Zalesky, A., Cocchi, L., Fornito, A., Choi, E. J., Kim, H. H., ... Yi, S. H. (2013). Decreased Functional Brain Connectivity in Adolescents with Internet Addiction. *PLoS ONE*, 8(2). <https://doi.org/10.1371/journal.pone.0057831>
- Horvath, A., Szucs, A., Csukly, G., Sakovics, A., Stefanics, G., & Kamondi, A. (2018). EEG and ERP biomarkers of Alzheimer's disease: a critical review. *Frontiers in Bioscience (Landmark Edition)*, 23, 183–220. Retrieved from

<http://www.ncbi.nlm.nih.gov/pubmed/28930543>

- Huff, F. J., Corkin, S., & Growdon, J. H. (1986). Semantic impairment and anomia in Alzheimer's disease. *Brain and Language*, 28, 235–249. [https://doi.org/10.1016/0093-934X\(86\)90103-3](https://doi.org/10.1016/0093-934X(86)90103-3)
- Hyvärinen, A., & Oja, E. (1997). A Fast Fixed-Point Algorithm for Independent Component Analysis. *Neural Computation (MIT)*, 9, 1483–1492. <https://doi.org/10.1142/s0129065700000028>
- Ille, N., Berg, P., & Scherg, M. (2002). Artifact correction of the ongoing EEG using spatial filters based on artifact and brain signal topographies. *Journal of Clinical Neurophysiology*, 19(2), 113–124. <https://doi.org/10.1097/00004691-200203000-00002>
- Jack, C. R., Albert, M. S., Knopman, D. S., McKhann, G. M., Sperling, R. A., Carrillo, M. C., ... Phelps, C. H. (2011). Introduction to the recommendations from the National Institute on Aging-Alzheimer's Association workgroups on diagnostic guidelines for Alzheimer's disease. *Alzheimer's & Dementia*, 7(3), 257–262. <https://doi.org/10.1016/j.jalz.2011.03.004>
- Jacobs, D. (2015). Know your Brainwaves Hacking the Creative Brain - Web Directions 2015. Retrieved from [https://www.slideshare.net/denisejacobs/hacking-the-creative-brain-web-directions-2015/79-Know\\_your\\_Brainwaves](https://www.slideshare.net/denisejacobs/hacking-the-creative-brain-web-directions-2015/79-Know_your_Brainwaves)
- Jahn, H. (2013). *Clinical research*. 445–454.
- James, C. J., & Hesse, C. W. (2005). Independent component analysis for biomedical signals. *Physiological Measurement*, 26(1), R15–R39. <https://doi.org/10.1088/0967-3334/26/1/R02>
- Jelic, V., Johansson, S. E., Almkvist, O., Shigeta, M., Julin, P., Nordberg, A., ... Wahlund, L. O. (2000). Quantitative electroencephalography in mild cognitive impairment: Longitudinal changes and possible prediction of Alzheimer's disease. *Neurobiology of Aging*, 21, 533–540. [https://doi.org/10.1016/S0197-4580\(00\)00153-6](https://doi.org/10.1016/S0197-4580(00)00153-6)
- Jeong, J., Chae, J. H., Kim, S. Y., & Han, S. H. (2001). Nonlinear dynamic analysis of the EEG in patients with Alzheimer's disease and vascular dementia. *Journal of Clinical Neurophysiology*, 18(1), 58–67. <https://doi.org/10.1097/00004691-200101000-00010>
- Jeong, J., Gore, J. C., & Peterson, B. S. (2001). Mutual information analysis of the EEG in patients with Alzheimer's disease. *Clinical Neurophysiology*, 112, 827–835.
- Joyce, C. A., Gorodnitsky, I. F., & Kutas, M. (2004). Minor Planet Observations [H93 Berkeley Heights]. *Psychophysiology*, 41, 313–325. <https://doi.org/10.1046/j.1469-8986.2003.00141.x>
- Kabbara, A., El Falou, W., Khalil, M., Wendling, F., & Hassan, M. (2017). The dynamic functional core network of the human brain at rest. *Scientific Reports*, 7(1), 2936. <https://doi.org/10.1038/s41598-017-03420-6>
- Kabbara, A., Eid, H., Falou, W., El Khalil, M., & Wendling, F. (2018). Reduced integration and improved segregation of functional brain networks in Alzheimer's disease. *Journal of Neural Engineering*, 15. <https://doi.org/10.1088/1741-2552/aaaa76>
- Kabbara, Aya, Khalil, M., O'Neill, G., Dujardin, K., El Traboulsi, Y., Wendling, F., & Hassan, M. (2019). Detecting modular brain states in rest and task. *Network Neuroscience*.

*Advance Publication.* <https://doi.org/10.1162/NETN>

- Karantzoulis, S., & Galvin, J. E. (2014). *Expert Review of Neurotherapeutics major forms of dementia Distinguishing Alzheimer's disease from other major forms of dementia.* 7175. <https://doi.org/10.1586/ern.11.155>
- Karch, C. M., & Goate, A. M. (2015). Review Alzheimer's Disease Risk Genes and Mechanisms of Disease Pathogenesis. *Biological Psychiatry*, 77(1), 43–51. <https://doi.org/10.1016/j.biopsych.2014.05.006>
- Kirkove, M., François, C., & Verly, J. (2014). Comparative evaluation of existing and new methods for correcting ocular artifacts in electroencephalographic recordings. *Signal Processing*, 98, 102–120. <https://doi.org/10.1016/j.sigpro.2013.11.015>
- Klados, M. A., Papadelis, C., Braun, C., & Bamidis, P. D. (2011). REG-ICA: A hybrid methodology combining Blind Source Separation and regression techniques for the rejection of ocular artifacts. *Biomedical Signal Processing and Control*, 6, 291–300. <https://doi.org/10.1016/j.bspc.2011.02.001>
- Kumar, A., & Taso, J. (2018). Alzheimer Disease. *StatPearls. StatPearls Publishing.* Retrieved from <http://www.ncbi.nlm.nih.gov/pubmed/29763097>
- Kwak, Y. T. (2006). Quantitative EEG findings in different stages of Alzheimer's disease. *Journal of Clinical Neurophysiology*, 23(5), 457–462. <https://doi.org/10.1097/01.wnp.0000223453.47663.63>
- Laaksonen, H., Kujala, J., Hultén, A., Liljeström, M., & Salmelin, R. (2012). MEG evoked responses and rhythmic activity provide spatiotemporally complementary measures of neural activity in language production. *NeuroImage*, 60, 29–36. <https://doi.org/10.1016/j.neuroimage.2011.11.087>
- Lachaux, J.-P., Rodriguez, E., Le Van Quyen, M., Lutz, A., Martinerie, J., & Varela, F. J. (2000). Studying Single-Trials of Phase Synchronous Activity in the Brain. *International Journal of Bifurcation and Chaos*, 10(10), 2429–2439. <https://doi.org/10.1142/s0218127400001560>
- Lachaux, J.-P., Rodriguez, E., Martinerie, J., & Varela, F. J. (1999). Measuring Phase Synchrony in Brain Signals. *Human Brain Mapping*, 8(4), 194–208. <https://doi.org/10.1017/S0007680500048066>
- Lagerlund, T. D., Sharbrough, F. W., & Busacker, N. E. (1997). Spatial Filtering of Multichannel Electroencephalographic Recordings Through Principal Component Analysis by Singular Value Decomposition. *Journal of Clinical Neurophysiology*, 14(1), 73–82.
- Lanoiselee, H.-M., Nicolas G, W. D., A, R.-L., & Lacour M, R. S. (2017). APP , PSEN1 , and PSEN2 mutations in early- onset Alzheimer disease : A genetic screening study of familial and sporadic cases. *PloS Med*, 14(3), 1–16.
- Laureys, S., Peigneux, P., & Goldman, S. (2002). Brain imaging. *Biological Psychiatry*, 155–166.
- Levelt, W. J. M., Meyer, A. S., Salmelin, R., Praamstra, P., & Helenius, P. (2002). An MEG Study of Picture Naming. *Journal of Cognitive Neuroscience*, 10(5), 553–567. <https://doi.org/10.1162/089892998562960>

- Lin, F. H., Witzel, T., Ahlfors, S. P., Stufflebeam, S. M., Belliveau, J. W., & Hämäläinen, M. S. (2006). Assessing and improving the spatial accuracy in MEG source localization by depth-weighted minimum-norm estimates. *NeuroImage*, 31, 160–171. <https://doi.org/10.1016/j.neuroimage.2005.11.054>
- Lindau, M., Jelic, V., Johansson, S. E., Andersen, C., Wahlund, L. O., & Almkvist, O. (2003). Quantitative EEG abnormalities and cognitive dysfunctions in frontotemporal dementia and Alzheimer's disease. *Dementia and Geriatric Cognitive Disorders*, 15(2), 106–114. <https://doi.org/10.1159/000067973>
- Lipert, J., Bar, K. J., Meske, U., & Weiller, C. (2001). Motor cortex disinhibition in Alzheimer's disease. *Clin. Neurophysiol.*, 112, 1436–1441.
- Livingston, G., Sommerlad, A., Ortega, V., Costafreda, S. G., Huntley, J., Ames, D., ... Mukadam, N. (2017). *The Lancet Commissions Dementia prevention, intervention, and care*. 390. [https://doi.org/10.1016/S0140-6736\(17\)31363-6](https://doi.org/10.1016/S0140-6736(17)31363-6)
- Logan, G. ., & Cowan, W. . (1984). On the ability to inhibit though and action-atheory of an act of control. *Psychol. Rev.*, 295–327.
- Luck, S. J. (2014). *An Introduction to the Event-Related Potential Technique, Second Edition*.
- Lutz, A., Greischar, L., Rawlings, N., Ricard, M., & Davidson, R. (2004). Long-term meditators self-induce high-amplitude gamma synchrony during mental practice. *Proc Natl Acad Sci USA*, 101, 16369–16373.
- Marella, S. (2012). EEG artifacts. Retrieved from <https://www.slideshare.net/SudhakarMarella/eeg-artifacts-15175461>
- Masters, C. L., Bateman, R., Blennow, K., Rowe, C. C., Sperling, R. A., & Cummings, J. L. (2015). Alzheimer's disease. *Nature Reviews, Disease Primers*, 1(1), 1–18. <https://doi.org/10.1038/nrdp.2015.56>
- Mckhann, G. M., Knopman, D. S., Chertkow, H., Hyman, B. T., Jack, C. R., Kawas, C. H., ... Phelps, C. H. (2011). The diagnosis of dementia due to Alzheimer ' s disease: Recommendations from the National Institute on Aging-Alzheimer ' s Association workgroups on diagnostic guidelines for Alzheimer ' s disease. *Alzheimer's & Dementia*, 7(3), 263–269. <https://doi.org/10.1016/j.jalz.2011.03.005>
- Medaglia, J. D., Lynall, M.-E., & Bassett, D. S. (2015). Cognitive Network Neuroscience John. *Cognitive Network Neuroscience*. *J.Cogn.Neurosci.*, 27, 1471–1491.
- Mehrkanoon, S., Breakspear, M., Britz, J., & Boonstra, T. W. (2014). Intrinsic Coupling Modes in Source-Reconstructed Electroencephalography. *Brain Connectivity*, 4(10), 812–825. <https://doi.org/10.1089/brain.2014.0280>
- Menon, V., Adleman, N. E., White, C. D., Glover, G. H., & Reiss, A. L. (2001). Error-Related Brain Activation during a Go/NoGo Response Inhibition Task. *Human Brain Mapping*, 12, 131–143.
- Mioshi, E., Dawson, K., Mitchell, J., Arnold, R., & Hodges, J. R. (2006). The Addenbrooke's Cognitive Examination Revised (ACE-R): a brief cognitive test battery for dementia screening. *Int J Geriatr Psychiatry*, 21, 1078–1085. <https://doi.org/10.1002/gps>
- Mizuno, T., Takahashi, T., Cho, R. Y., Kikuchi, M., Murata, T., Takahashi, K., & Wada, Y. (2010). Assessment of EEG dynamical complexity in Alzheimer's disease using

- multiscale entropy. *Clinical Neurophysiology*, 121, 1438–1446. <https://doi.org/10.1016/j.clinph.2010.03.025>
- Morgan, C. D., & Murphy, C. (2002). Olfactory Function and Event-Related Potentials in Alzheimer's Disease. *Journal Of the International Neuropsychological Society*, 8, 753–763.
- Mucke, L. (2009). *Q & A Alzheimer's disease*. 461(October), 895–897.
- Myers, R. H., Schaefer, E. J., Wilson, P. W. F., Agostino, R. D., Ordovas, J. M., Espino, A., ... Wolf, P. A. (1996). *Apolipoprotein E ε 4 association with dementia in a population-based study : The Framingham Study*. 673–678.
- Nunez, P., Srinivasan, R., Westdorp, A., Wijesinghe, R., Tucker, D., Silberstein, R., & Cadusch, P. (1997). EEG coherency I: statistics, reference electrode, volume conduction, Laplacians, cortical imaging, and interpretation at multiple scales. *Electroencephalography and Clinical Neurophysiology*, 103, 499–515. [https://doi.org/10.1016/S0013-4694\(97\)00066-7](https://doi.org/10.1016/S0013-4694(97)00066-7)
- O'Brien, J. T., Firbank, M. J., Davison, C., Barnett, N., Bamford, C., Donaldson, C., ... Lloyd, J. (2014). 18F-FDG PET and Perfusion SPECT in the Diagnosis of Alzheimer and Lewy Body Dementias. *Journal of Nuclear Medicine*, 55, 1959–1965. <https://doi.org/10.2967/jnumed.114.143347>
- O'Neill, G. C., Tewarie, P. K., Colclough, G. L., Gascoyne, L. E., Hunt, B. A. E., Morris, P. G., ... Brookes, M. J. (2017). Measurement of dynamic task related functional networks using MEG. *NeuroImage*, 146, 667–678. <https://doi.org/10.1016/j.neuroimage.2016.08.061>
- Olejniczak, P. (2006). Neurophysiologic Basis of EEG. *J Clin Neurophysiol*, 23, 186–189. Retrieved from <http://norwalk.braincoretherapy.com/wp-content/uploads/2014/01/Neurophysiologic-Basis-of-EEG.pdf>
- Olichney, J. M., Morris, S. K., Ochoa, C., Salmon, D. P., Thal, L. J., Kutas, M., & Iragui, V. J. (2002). Abnormal verbal event related potentials in mild cognitive impairment and incipient Alzheimer's disease. *Journal of Neurology Neurosurgery and Psychiatry*, 73, 377–384. <https://doi.org/10.1136/jnnp.73.4.377>
- Olichney, John M., Iragui, V. J., Salmon, D. P., Riggins, B. R., Morris, S. K., & Kutas, M. (2006). Absent event-related potential (ERP) word repetition effects in mild Alzheimer's disease. *Clinical Neurophysiology*, 117, 1319–1330. <https://doi.org/10.1016/j.clinph.2006.02.022>
- Oostenveld, R., Fries, P., Maris, E., & Schoffelen, J.-M. (2011). FieldTrip : Open Source Software for Advanced Analysis of MEG , EEG , and Invasive Electrophysiological Data. *Computational Intelligence and Neuroscience*. <https://doi.org/10.1155/2011/156869>
- Park, H. J., & Friston, K. (2013). Structural and functional brain networks: From connections to cognition. *Science*, 342(6158). <https://doi.org/10.1126/science.1238411>
- Pasquale, F. De, Della, S., Snyder, A. Z., Lewis, C., & Mantini, D. (2010). Temporal dynamics of spontaneous MEG activity in brain networks. *Proc. Natl Acad. Sci. USA*. <https://doi.org/10.1073/pnas.0913863107>
- Penttila, M., Partanen, J. V., Soininen, H., & Riekkinen, P. . (1985). QUANTITATIVE ANALYSIS OF OCCIPITAL EEG IN DIFFERENT STAGES OF ALZHEIMER'S

- DISEASE. *Electroencephalography and Clinical Neurophysiology*, 60, 1–6.
- Pepin, J. L., Bogacz, D., De Pasqua, V., & Delwaide, P. J. (1999). Motor cortex inhibition is not impaired with Alzheimer disease: evidence from paired transcranial magnetic stimulation. *J. Neurol. Sci.*, 170, 119–123.
- Perl, D. P. (2010). Neuropathology of Alzheimer's Disease. *Mount Sinai Journal of Medicine*, 77, 32–42.
- Petit, D., Montplaisir, J., Lorrain, D., & Gauthier, S. (1992). Spectral analysis of the rapid eye movement sleep electroencephalogram in right and left temporal regions: A biological marker of Alzheimer's disease. *Annals of Neurology*, 32(2), 172–176. <https://doi.org/10.1002/ana.410320208>
- Petrovic, M., Hurt, C., Collins, D., Burns, A., Camus, V., Liperoti, R., ... Byrne, E. J. (2007). Clustering of behavioural and psychological symptoms in dementia ( bpsd ): a european alzheimer ' s disease consortium ( eadc ) study. *Acta Clinica Belgica*, 62(6), 426–432. <https://doi.org/10.1179/acb.2007.062>
- Pettersson, A. F., Olsson, E., & Wahlund, L. O. (2005). Motor function in subjects with mild cognitive impairment and early Alzheimer's disease. *Dement Geriatr Cogn Disord*, 19, 299–304. <https://doi.org/10.1159/000084555>
- Pironti, V. A., Lai, M. C., Müller, U., Dodds, C. M., Suckling, J., Bullmore, E. T., & Sahakian, B. J. (2014). Neuroanatomical abnormalities and cognitive impairments are shared by adults with attention-deficit/hyperactivity disorder and their unaffected first-degree relatives. *Biological Psychiatry*, 76, 639–647. <https://doi.org/10.1016/j.biopsych.2013.09.025>
- Pokryszko-dragan, A., Słotwiński, K., & Podemski, R. (2003). Modality-specific changes in P300 parameters in patients with dementia of the Alzheimer type. *Med Sci Monit*, 9(4), 182–187.
- Ponten, S. C., Douw, L., Bartolomei, F., Reijneveld, J. C., & Stam, C. J. (2009). Indications for network regularization during absence seizures : Weighted and unweighted graph theoretical analyses. *Experimental Neurology*, 217, 197–204. <https://doi.org/10.1016/j.expneurol.2009.02.001>
- Raine, A., Laufer, W. S., Yang, Y., Narr, K. L., Thompson, P., & Toga, A. W. (2011). Increased executive functioning, attention, and cortical thickness in white-collar criminals. *Human Brain Mapping*, 33. <https://doi.org/10.1002/hbm.21415>
- Reitz, C., & Mayeux, R. (2014). Alzheimer disease : Epidemiology , diagnostic criteria , risk factors and biomarkers. *Biochemical Pharmacology*, 88(4), 640–651. <https://doi.org/10.1016/j.bcp.2013.12.024>
- Report, W. A. (2018). No Title. Retrieved from <https://www.alz.co.uk/research/WorldAlzheimerReport2018.pdf>
- Rowe, C. C., Ackerman, U., Browne, W., Mulligan, R., Pike, K. L., O'Keefe, G., ... Villemagne, V. L. (2008). Imaging of amyloid  $\beta$  in Alzheimer's disease with 18F-BAY94-9172, a novel PET tracer: proof of mechanism. *The Lancet Neurology*, 7, 129–135. [https://doi.org/10.1016/S1474-4422\(08\)70001-2](https://doi.org/10.1016/S1474-4422(08)70001-2)
- Rubia, K., Smith, A. B., Brammer, M. J., & Taylor, E. (2003). Right inferior prefrontal cortex mediates response inhibition while mesial prefrontal cortex is responsible for error

- detection. *NeuroImage*, 20(1), 351–358. [https://doi.org/10.1016/S1053-8119\(03\)00275-1](https://doi.org/10.1016/S1053-8119(03)00275-1)
- Scazufca, M., Almeida, A. E. O. P., Vallada, A. E. H. P., Tasse, A. E. W. A., Menezes, A. E. P. R., Ageing, P., ... Almeida, O. P. (2009). Limitations of the Mini-Mental State Examination for screening dementia in a community with low socioeconomic status. *Eur Arch Psychiatry Clin Neurosci*, 259, 8–15. <https://doi.org/10.1007/s00406-008-0827-6>
- Schneider, W., Eschman, A., Zuccolotto, A., Burgess, S., Cernicky, B., Gilkey, D., ... James, J. S. (2002). *Eprime - USER 'S GUIDE*.
- Schoffelen, J., & Gross, J. (2009). Source Connectivity Analysis With MEG and EEG. *Human Brain Mapping*, 30, 1857–1865. <https://doi.org/10.1002/hbm.20745>
- Schreiter-gasser, U., Gasser, T., & Ziegler, P. (1994). Quantitative EEG analysis in early onset Alzheimer's disease : correlations with severity , clinical characteristics , visual EEG and CCT. *Electroencephalography and Clinical Neurophysiology*, 90, 267–272.
- Schuhmann, T., Schiller, N. O., Goebel, R., & Sack, A. T. (2012). Speaking of which: Dissecting the neurocognitive network of language production in picture naming. *Cerebral Cortex*, 22(3), 701–709. <https://doi.org/10.1093/cercor/bhr155>
- Serrano-pozo, A., Frosch, M. P., Masliah, E., & Hyman, B. T. (2011). *Neuropathological Alterations in Alzheimer Disease*. 1–24.
- Seshadri, S., Fitzpatrick, L., Ikram, M. A., DeStefano, A. L., Gudnason, V., Boada, M., ... Lorca, R. R.-. (2010). Genome-wide Analysis of Genetic Loci. *JAMA*, 303(18), 1832–1840.
- Singh, K. D. (2012). NeuroImage Which “ neural activity ” do you mean ? fMRI , MEG , oscillations and neurotransmitters. *NeuroImage*, 62, 1121–1130. <https://doi.org/10.1016/j.neuroimage.2012.01.028>
- Sporns, O. (2014). Contributions and challenges for network models in cognitive neuroscience. *Nature Neuroscience, Advanced Online Publications*. <https://doi.org/10.1038/nn.3690>
- Sporns, O., Chialvo, D. R., Kaiser, M., & Hilgetag, C. C. (2004). Organization, development and function of complex brain networks. *Trends in Cognitive Sciences*, 8(9), 418–425. <https://doi.org/10.1016/j.tics.2004.07.008>
- Sporns, O., Tononi, G., & Kötter, R. (2005). The human connectome: A structural description of the human brain. *PLoS Computational Biology*, 1(4), 0245–0251. <https://doi.org/10.1371/journal.pcbi.0010042>
- Stam, C. J., Jones, B. F., Nolte, G., Breakspear, M., & Scheltens, P. (2006). Small-world networks and functional connectivity in Alzheimer's disease. *Cerebral Cortex*, 17, 92–99. <https://doi.org/10.1093/cercor/bhj127>
- Supekar, K., Menon, V., Rubin, D., Musen, M., & Greicius, M. D. (2008). Network analysis of intrinsic functional brain connectivity in Alzheimer's disease. *PLoS Computational Biology*, 4(6). <https://doi.org/10.1371/journal.pcbi.1000100>
- Tadel, F., Baillet, S., Mosher, J., Pantazis, D., & Leahy, R. (2011). Brainstorm. Retrieved from <http://neuroimage.usc.edu/brainstorm>
- Thomson, H. (2018). Wave therapy. *Nature*, 555, 20–22.
- Tsiaras, V., Simos, P. G., Rezaie, R., Sheth, B. R., Garyfallidis, E., Castillo, E. M., &

- Papanicolaou, A. C. (2011). Extracting biomarkers of autism from MEG resting-state functional connectivity networks. *Computers in Biology and Medicine*, 41, 1166–1177. <https://doi.org/10.1016/j.combiomed.2011.04.004>
- Uhlhaas, P. J., & Singer, W. (2006). Neural Synchrony in Brain Disorders : Relevance for Cognitive Dysfunctions and Pathophysiology. *Neuron*, 52, 155–168. <https://doi.org/10.1016/j.neuron.2006.09.020>
- Urigüen, J. A., & Garcia-Zapirain, B. (2015). EEG artifact removal - State-of-the-art and guidelines. *Journal of Neural Engineering*, 12, 1–23. <https://doi.org/10.1088/1741-2560/12/3/031001>
- Valk, P. E., Delbeke, D., Bailey, D. L., Townsend, D. W., & Maisey, M. N. (2006). *Positron Emission Tomography*.
- van de Steen, F., Faes, L., Karahan, E., Songsiri, J., Valdes-Sosa, P. A., & Marinazzo, D. (2016). Critical Comments on EEG Sensor Space Dynamical Connectivity Analysis. *Brain Topogr*, 1–12. <https://doi.org/10.1007/s10548-016-0538-7>
- van Deursen, J. A., Vuurman, E. F. P. M., Smits, L. L., Verhey, F. R. J., & Riedel, W. J. (2009). Response speed, contingent negative variation and P300 in Alzheimer's disease and MCI. *Brain and Cognition*, 69, 592–599. <https://doi.org/10.1016/j.bandc.2008.12.007>
- Varela, F., Lachaux, J., Rodriguez, E., & Martinerie, J. (2001). The brainweb: phase synchronization and large-scale integration. *Nature Reviews Neuroscience*, 2, 229–239. <https://doi.org/10.1038/35067550>
- Vecchio, F., Miraglia, F., Marra, C., Quaranta, D., Vita, M. G., Bramanti, P., & Rossini, P. M. (2014). Human brain networks in cognitive decline: A graph theoretical analysis of cortical connectivity from EEG data. *Journal of Alzheimer's Disease*, 41, 113–127. <https://doi.org/10.3233/JAD-132087>
- Verma, M., Wills, Z., & Chu, C. T. (2018). *Excitatory Dendritic Mitochondrial Calcium Toxicity: Implications for Parkinson ' s and Other Neurodegenerative Diseases*. 12(August), 1–12. <https://doi.org/10.3389/fnins.2018.00523>
- Vidoni, E. D., Thomas, G. P., Honea, R. A., Loskutova, N., & Burns, J. M. (2012). Evidence of Altered Corticomotor System Connectivity in Early- Stage Alzheimer's Disease. *J Neurol Phys Ther.*, 36(1), 8–16. <https://doi.org/10.1097/NPT.0b013e3182462ea6>
- Vourkas, M., Karakonstantaki, E., Simos, P. G., Tsirka, V., Antonakakis, M., Vamvoukas, M., ... Dimitriadis, S. (2014). Simple and difficult mathematics in children : A minimum spanning tree EEG network analysis. *Neuroscience Letters*. Retrieved from <http://dx.doi.org/10.1016/j.neulet.2014.05.048>
- Wallace, L., Theou, O., Rockwood, K., & Andrew, M. K. (2018). Relationship between frailty and Alzheimer ' s disease biomarkers : A scoping review. *Alzheimer's & Dementia: Diagnosis, Assessment & Disease Monitoring*, 10, 394–401. <https://doi.org/10.1016/j.jad.2018.05.002>
- Weller, J., & Budson, A. (2018). *Current understanding of Alzheimer ' s disease diagnosis and treatment [ version 1 ; referees : 2 approved ] Referee Status : 7(0) , 1–9*. <https://doi.org/10.12688/f1000research.14506.1>
- WHO. (2019). No Title. Retrieved from <https://www.who.int/news-room/fact-sheets/detail/dementia>

- Wu, X., Yu, X., Yao, L., & Li, R. (2014). Bayesian network analysis revealed the connectivity difference of the default mode network from the resting-state to task-state. *Frontiers in Computational Neuroscience*, 8(118). <https://doi.org/10.3389/fncom.2014.00118>
- Zhao, Q., Tan, L., Wang, H., Tan, M., Tan, L., Xu, W., ... Lai, T. (2016). The Prevalence of Neuropsychiatric Symptoms in Alzheimer's Disease: Systematic Review and Meta-analysis. *Journal of Affective Disorders*, 190, 264–271. <https://doi.org/10.1016/j.jad.2015.09.069>

## Appendix A.

### عنوان المشروع:

استخراج العلامات البيولوجية لمرض الألزهايمر عن طريق الاشارات الدماغية.

### دعوة:

أنت مدعو للمشاركة في دراسة بحثية حول مرض الألزهايمر.

مشاركتكم ستساعدنا في فهم أسباب المرض، والتغيرات الدماغية التي تطرأ على شبكة الدماغ.

سيتم القيام بالمشروع في المركز الطبي "Vita Nova" من قبل الطالبة جودي طبال والطالبة سحر علوش، تحت اشراف الدكتور عاصف ناصر، الدكتور محمود حسن، الدكتورة آية كباره، و الدكتور محمد خليل.

### ماذا سيحدث:

سوف نسعى إلى تقييم مرحلة المرض عند كل مشارك عن طريق القيام ب Neuropsychological Tests . و بعد ذلك يخضع للمراحل التالية:

المرحلة الأولى: بعد وضع اللاقطات على الدماغ، سوف يطلب منه الجلوس في وضع مريح دون القيام بأي أمر.

المرحلة الثانية: سوف يطلب منه الجلوس في وضع مريح ثم التركيز على شاشة الكمبيوتر. ثم سيتم عرض مجموعة من الصور بشكل تسلسلي، المطلوب منه هو أن يسمى الصورة التي يراها على الشاشة. وسيتم خلال هذه المرحلة تسجيل تخطيط الدماغ. و ذلك من أجل تحليل الشبكة الدماغية المسؤولة عن الذاكرة و المنطق.

المرحلة الثالثة: سوف يطلب منه الجلوس في وضع مريح ثم التركيز على شاشة الكمبيوتر. ثم سيتم عرض مجموعة من الأرقام بشكل تسلسلي، المطلوب منه هو أن يضغط في كل مرة على الرقم الذي ظهر في المحاولة السابقة.

المرحلة الرابعة: سوف يطلب منه الجلوس في وضع مريح و القيام بحركة بسيطة باصبعه. وسيتم خلال هذه المرحلة تسجيل تخطيط الدماغ. و ذلك من أجل تحليل الشبكة الدماغية المسؤولة عن الحركة.

يرجى محاولة عدم التحرك أثناء الجلسات.

### الالتزام بالوقت:

التقييم: 30 د.

التحضير: 10 د. المرحلة الاولى: 5 د. المرحلة الثانية: 15 د. المرحلة الثالثة: 10 د. المرحلة الرابعة: 10 د.

### حقوق المشاركين:

لديك الحق في أن تطلب أن يتم سحب أي بيانات خاصة بك.

لديك الحق في حذف أو رفض الإجابة أو الرد على أي سؤال خاص.

إذا كان لديك أي أسئلة نتيجة لقراءة هذه الورقة المعلومات، بإمكانك أن تسأل الباحث قبل أن تبدأ الدراسة.

### فوائد ومخاطر:

لا يوجد أي فوائد أو مخاطر لك في هذه الدراسة.

### تكلفة، بالاسترداد والتعويض:

مشاركتك في هذا البحث تطوعية.

### السرية / عدم الكشف عن هويته:

البيانات التي نجمعها لا تحتوي على أي معلومات شخصية عنك.

### لمزيد من المعلومات:

سيكون فريق البحث سعيدا بالإجابة على أسئلتكم حول هذه الدراسة في أي وقت.

تستطيع الاتصال على رقم الهاتف أو إرسال رسالة على البريد الإلكتروني:

جودي طبال: 76789524      [judy\\_tab95@hotmail.com](mailto:judy_tab95@hotmail.com)

سحر علوش: 76575058      [saharallouch@gmail.com](mailto:saharallouch@gmail.com)

رقم المشترك:

اسم المشترك:

**استماراة الموافقة**

أؤكد أنني قد قرأت وفهمت ورقة المعلومات للدراسة المذكورة أعلاه. وقد أتيحت لي الفرصة للنظر في المعلومات، وطرح الأسئلة، وكانت الإجابة مرضية.

أؤكد أن مشاركتي طوعية وأنها حر في الانسحاب في أي وقت، دون إبداء أي سبب.

أعلم أن المعلومات التي قدمتها يمكن أن تستخدم في التقارير المقبلة، المقالات أو العروض التي سيقدمها فريق البحث.

أؤكد أنه لن يظهر اسمي في أي تقارير، مقالات أو عروض.

أنا أوافق على المشاركة في الدراسة المذكورة أعلاه.

---

إمضاء المشارك أو ولائي أمره

---

اسم المشارك أو ولائي أمره

---

التاريخ

---

إمضاء الباحث

---

اسم الباحث

## Appendix B.

اختبار أنابروكس المعرفي النسخة المنقحة ج (2012)														
الذكاء والتوظيف	رقم الملف الطبي: ..... تاريخ الميلاد: ..... هل الشخص يعتمد على اليد اليمنى أو اليسرى في العمل؟ ..... <b>التوجه</b> <table border="1" style="width: 100%; border-collapse: collapse;"> <tr> <td style="width: 15%;">[الدرجة 5-0] <input type="text"/></td> <td style="width: 15%;">الفصل ..... الدولة ..... [الدرجة 5-0] <input type="text"/></td> <td style="width: 15%;">السنة ..... المنطقة ..... [الدرجة 3-0] <input type="text"/></td> <td style="width: 15%;">الشهر ..... مدينة ..... [الدرجة 5-0] <input type="text"/></td> <td style="width: 15%;">التاريخ ..... طابق ..... [الدرجة 5-0] <input type="text"/></td> <td style="width: 15%;">اليوم ..... مبني ..... [الدرجة 5-0] <input type="text"/></td> <td style="width: 15%;">اسأل: ما هو ..... اسأل: أي ..... [الدرجة 5-0] <input type="text"/></td> </tr> </table>							[الدرجة 5-0] <input type="text"/>	الفصل ..... الدولة ..... [الدرجة 5-0] <input type="text"/>	السنة ..... المنطقة ..... [الدرجة 3-0] <input type="text"/>	الشهر ..... مدينة ..... [الدرجة 5-0] <input type="text"/>	التاريخ ..... طابق ..... [الدرجة 5-0] <input type="text"/>	اليوم ..... مبني ..... [الدرجة 5-0] <input type="text"/>	اسأل: ما هو ..... اسأل: أي ..... [الدرجة 5-0] <input type="text"/>
	[الدرجة 5-0] <input type="text"/>	الفصل ..... الدولة ..... [الدرجة 5-0] <input type="text"/>	السنة ..... المنطقة ..... [الدرجة 3-0] <input type="text"/>	الشهر ..... مدينة ..... [الدرجة 5-0] <input type="text"/>	التاريخ ..... طابق ..... [الدرجة 5-0] <input type="text"/>	اليوم ..... مبني ..... [الدرجة 5-0] <input type="text"/>	اسأل: ما هو ..... اسأل: أي ..... [الدرجة 5-0] <input type="text"/>							
<b>التسجيل</b> قل: "سأقوم بإلقاء ثلاثة كلمات عليك وأود أن تقوم بتكرارها ورائي: ليمون - مفتاح - كرة". وبعد أن يقوم المفحوص بتكرار، قل: "حاول تذكر الكلمات لأنني سأطرح عليك الأسئلة فيما بعد". سجل فقط درجات المحاولة الأولى (كرر ثلاثة مرات عند الضرورة). سجل عدد المحاولات ..... <b>الانتباه والتركيز</b> اطلب من المفحوص: هل يمكنك طرح 7 من 100؟ وبعد أن يجب اطلب من المفحوص طرح 7 من إجمالي خمس عمليات طرح. وإذا قام المفحوص بأي خطأ قم بالمواصلة ثمتحقق من عدد الإجابات الصحيحة. مثلاً لو كانت إجابات المفحوص على التحدي التالي ..... اسأل: "هل يمكنك أن تهجي كلمة مدرسة؟" ثم اطلب من المفحوص القيام بتهجيهها بالمقlobe. <b>الذاكرة - الاسترجاع</b> اسأل: "أي ثلاثة كلمات طلبت منك القيام بتكرارها وتذكرها؟" 														
الذاكرة	<b>الذاكرة - ذاكرة تقدمية</b> سأقوم بذكر اسم وعنوان عليك، وأود منك تكرارها ورائي - سنقوم بذلك ثلاثة مرات لذا فإنه لديك الفرصة لتنكرها. وسأقوم بطرح أسئلة عليك فيما بعد. سجل فقط درجات المحاولة الثالثة ..... <table border="1" style="width: 100%; border-collapse: collapse;"> <tr> <td style="width: 25%;">[الدرجة 7-0] <input type="text"/></td> <td style="width: 25%;">المحاولات ..... المحاولات ..... المحاولات ..... [الدرجة 7-0] <input type="text"/></td> <td style="width: 25%;">المحاولات ..... المحاولات ..... المحاولات ..... [الدرجة 7-0] <input type="text"/></td> <td style="width: 25%;">المحاولات ..... المحاولات ..... المحاولات ..... [الدرجة 7-0] <input type="text"/></td> </tr> </table>							[الدرجة 7-0] <input type="text"/>	المحاولات ..... المحاولات ..... المحاولات ..... [الدرجة 7-0] <input type="text"/>	المحاولات ..... المحاولات ..... المحاولات ..... [الدرجة 7-0] <input type="text"/>	المحاولات ..... المحاولات ..... المحاولات ..... [الدرجة 7-0] <input type="text"/>			
	[الدرجة 7-0] <input type="text"/>	المحاولات ..... المحاولات ..... المحاولات ..... [الدرجة 7-0] <input type="text"/>	المحاولات ..... المحاولات ..... المحاولات ..... [الدرجة 7-0] <input type="text"/>	المحاولات ..... المحاولات ..... المحاولات ..... [الدرجة 7-0] <input type="text"/>										
<b>الذاكرة - الذكرة الرجعية</b> ما هي عاصمة الدولة التي تقيم فيها ..... ما هو اسم الحاكم السابق لبلدك ..... اسم رئيس الولايات المتحدة الأمريكية ..... اسم الحاكم الحالي لبلدك ..... 														

**الطلقة – حرف "م" والحيوانات**

**الحرف**

قل: سأقوم بإعطائكم حرف من الحروف الأبجدية وأود منك ذكر أكبر عدد من الكلمات التي يمكنك إعدادها والتي تبدأ بهذا الحرف، ولكن تذكر أنها ليست أسماء أشخاص أو أماكن. هل أنت جاهز؟ لديك دقة وحرف هو "م"

[الدرجة 7-0]

**الطلقة الفنية**

[الدرجة 7-0]

**الحيوانات**

قل: "هل يمكنك ذكر أكبر عدد من أسماء الحيوانات بقدر الإمكان؟ (يمكنك أن تبدأ بأي حرف تشاء)". (لديك دقة واحدة فقط)

[الدرجة 7-0]

**اللغة**

[الدرجة 1-0]

أظهر التعليمات المكتوبة:

**أغلق عينيك**

[الدرجة 3-0]

أمر مكون من ثلاثة مراحل:

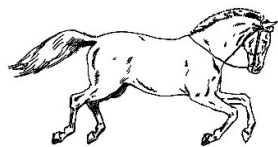
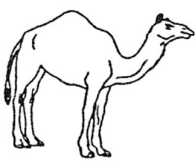
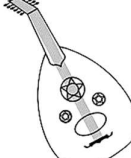
خذ الورقة بيديك اليمنى. قم بطريق الورقة نصفين. وضع الورقة على الأرض.

**اللغة – الكتابة**

[الدرجة 1-0]

اطلب من المفحوص إعداد جملة وكتابتها في الفراغ أدناه:

قم بتسجيل 1 إذا كانت الجملة تحتوي على بناء صحيح (انظر الدليل للأمثلة)

اللغة	<input type="text"/> [الدرجة 2-0]	<b>اللغة - التكرار</b> اطلب من المفحوص تكرار الكلمات التالية (فسيفكفيكم، أتزر مكموها، فأسقيناكموه، ليستخلفنهم) قم بتسجيل نتيجة كلمتين إذا كانت جميعها صحيحة وكلمة واحدة إذا كانت ثلاث كلمات صحيحة، ولا تقم بتسجيل أي نتيجة إذا كانت الكلمات الصحيحة اثنتين أو أقل.	
	<input type="text"/> [الدرجة 1-0]	اطلب من المفحوص تكرار ما يلي: "فوق، إلى ما بعد، وأسفل"	
	<input type="text"/> [الدرجة 1-0]	اطلب من المفحوص تكرار "لا إذا أو لكن و"	
<b>اللغة - التسمية</b>		اطلب من المفحوص تسمية الصور التالية:	
<input type="text"/> [الدرجة 2-0] + قلم مرسم ساعة		 <hr/>  <hr/>  <hr/>	
<input type="text"/> [الدرجة 10-0]		 <hr/>  <hr/>  <hr/>	
<b>اللغة</b>		 <hr/>  <hr/>  <hr/>	
 <hr/>  <hr/>  <hr/>			
<b>اللغة - الفهم</b>		باستخدام الصور المذكورة أعلاه اطلب من المفحوص: • أشر إلى الصورة المرتبطة بالحدي وسائل الحرب القديمة • أشر إلى الصورة المرتبطة بالحيوان الصحراوي • أشر إلى الصورة المرتبطة باداة تستخدم المصيد • أشر إلى الصورة المرتبطة بالشئ الذي يستخدم لنقل الماء	
<b>اللغة - القراءة</b>		اطلب من المفحوص تكرار الكلمات التالية [قم بتسجيل درجة واحدة فقط إذا كانت جميعها صحيحة]	
<input type="text"/> [الدرجة 1-0]			

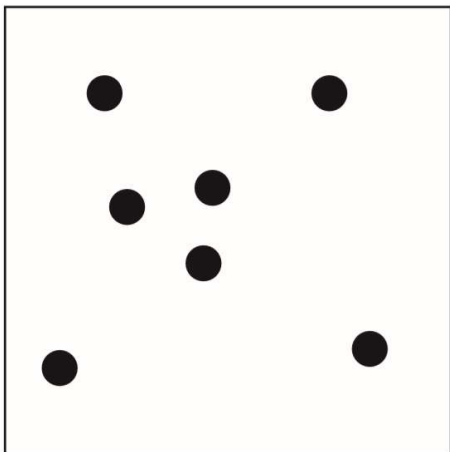
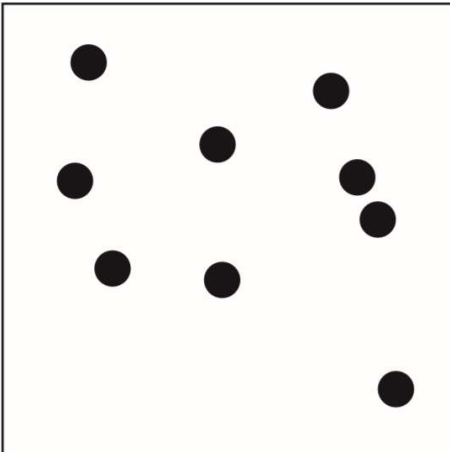
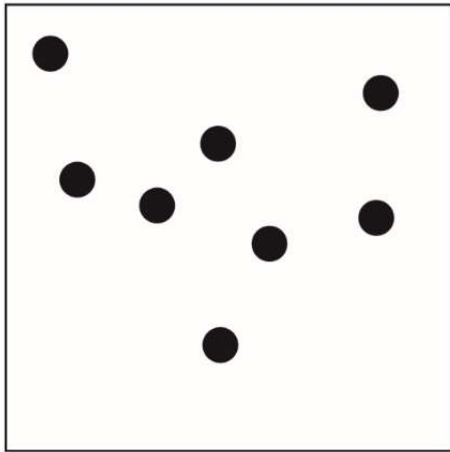
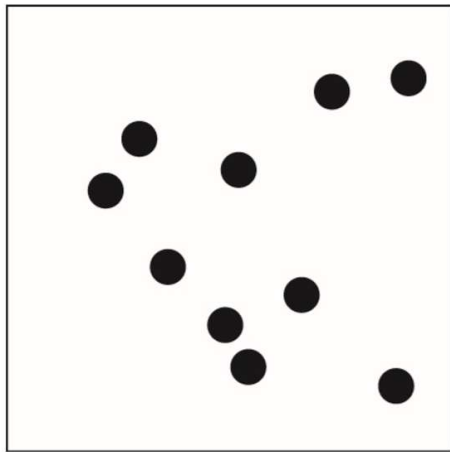
		<p><b>خياطة</b>  <b>طول</b>  <b>دخان</b>  <b>عجينة</b>  <b>هرّة</b></p>
<b>القدرات الإبصارية الفراغية</b>		
	[الدرجة 1-0] <input type="text"/>	شكلين خماسيي متداخلة: اطلب من المفحوص نسخ هذا الرسم
	[الدرجة 2-0] <input type="text"/>	مكعب سلكي: اطلب من المفحوص نسخ هذا الرسم (التسجيل الدرجات، انظر دليل التعليمات)
<b>إبصاري فراغي</b>	[الدرجة 5-0] <input type="text"/>	الساعة: اطلب من المفحوص رسم وجه ساعة بها أرقام وتوجد العقارب على الساعة الخامسة وعشرين دقيقة. (التسجيل الدرجات انظر دليل التعليمات: الدائرة = 1، الأرقام = 2، العقارب = 2 إذا كانت جميعها صحيحة)

**القدرات الإدراكية**

[الدرجة ٤-٠]

اطلب من المفحوص عد النقاط دون الإشارة إليها:

بصاري فراغي



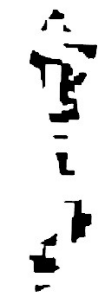
**القدرات الإدراكية**

اطلب من المفحوص التعرف على الأحرف:

[الدرجة 4-0]

بصري فراغي


 
**الاسترجاع**

اسأل: والآن أخبرني ما الذي تذكره عن ذلك الاسم وعنوان الذين كانوا يكررها في البداية

مصطفى شاهين

طابق 6

بنابة غلابيني

طريق الملا

طرابلس

الإدراك

[الدرجة 7-0]

.....

.....

.....

.....

الذاكرة

يجب إجراء هذا الاختبار إذا أخفق المفحوص في تذكر عنصرين أو أكثر. وإذا تم تذكر جميع العناصر تخطي هذا الاختبار وقم بتسجيل 5. وإذا تم تذكر فقط جزءاً إبدأ بوضع العناصر التي تذكرها في الخانة المطللة على الجانب الأيمن. ثم قم بإجراء اختبار حول العناصر التي لم يتم تذكرها بقولك "حسناً سوف أعطيك بعض التلميحات: هل كان الاسم أكشن أو واي أو زد؟ وما إلى ذلك. وتكون نتيجة كل عنصر تذكره (1) والتي يتم إضافتها للنقطة التي تم الحصول عليها بالذكر.

[الدرجة 5-0]

الذكر	سعد المصري	مصطفى شاهين	أحمد يافى
الذكر	طابق 4	طابق 5	طابق 5
الذكر	بنابة التوم	بنابة الكرى	بنابة الكرى
الذكر	طريق الميناء	شارع المتنين	طريق الملا
الذكر	صيدا	طرابلس	جبيل

**الدرجات العامة لمجموعة المتعلمين:****الدرجات العامة**

	/100	اختبار أدنبروكس المعرفي (المنقح)
		الدرجات الفرعية
/18		الانتباه والتوجيه
/26		الذاكرة
/14		الطلقة
/26		اللغة
/16		القدرات الإبصارية الفراغية

## Appendix C.

BSTS L	bankssts L		paraH L	parahippocampal L
BSTS R	bankssts R		paraH R	parahippocampal R
cACC L	caudalanteriorcingulate L		pOPER L	parsopercularis L
cACC R	caudalanteriorcingulate R		pOPER R	parsopercularis R
cMFG L	caudalmiddlefrontal L		pORB L	parsorbitalis L
cMFG R	caudalmiddlefrontal R		pORB R	parsorbitalis R
CUN L	cuneus L		pTRI L	parstriangularis L
CUN R	cuneus R		pTRI R	parstriangularis R
ENT L	entorhinal L		periCAL L	pericalcarine L
ENT R	entorhinal R		periCAL R	pericalcarine R
FP L	frontalpole L		postC L	postcentral L
FP R	frontalpole R		postC R	postcentral R
FUS L	fusiform L		PCC L	posteriorcingulate L
FUS R	fusiform R		PCC R	posteriorcingulate R
IPL L	inferiorparietal L		preC L	precentral L
IPL R	inferiorparietal R		preC R	precentral R
ITG L	inferiortemporal L		PCUN L	precuneus L
ITG R	inferiortemporal R		PCUN R	precuneus R
INS L	insula L		rACC L	rostralanteriorcingulate L
INS R	insula R		rACC R	rostralanteriorcingulate R
iCC L	isthmuscingulate L		rMFG L	rostralmiddlefrontal L
iCC R	isthmuscingulate R		rMFG R	rostralmiddlefrontal R
LOG L	lateraloccipital L		sFG L	superiorfrontal L
LOG R	lateraloccipital R		sFG R	superiorfrontal R
LOF L	lateralorbitofrontal L		SPL L	superiorparietal L
LOF R	lateralorbitofrontal R		SPL R	superiorparietal R
LIN L	lingual L		STG L	superiortemporal L
LIN R	lingual R		STG R	superiortemporal R
MOF L	medialorbitofrontal L		SMAR L	supramarginal L
MOF R	medialorbitofrontal R		SMAR R	supramarginal R
MTG L	middletemporal L		TP L	temporalpole L
MTG R	middletemporal R		TP R	temporalpole R
paraC L	paracentral L		TT L	transversetemporal L
paraC R	paracentral R		TT R	transversetemporal R

Anatomic regions of interest (ROIs) as derived from the Desikan Killiany atlas.